# *IASI Level 2: Product Generation Specification*

Doc.No. : EPS.SYS.SPE.990013
Issue : v8E e-signed
Date : 10 July 2017
WBS :

EUMETSAT
Eumetsat-Allee 1, D-64295 Darmstadt, Germany
Tel: +49 6151 807-7
Fax: +49 6151 807 555
http://www.eumetsat.int

# *Document Change Record*

***Note***: Only the last version changes pertaining to the PPF version 6 and subsequent incremental updates are listed here. A complete summary of historical document changes is in Appendix A.

| *Issue/Revision* | *DCN No.* | *Changed Pages / Paragraphs* |
|---|---|---|
| V8 | | Reorganised the document structure and content in line with the IASI L2 PPF version 6 |
| V8A | | Editing and changes to signature list. Added text to Section 5.5 |
| V8B | | Updated signature table<br>Moved historical Document Change Records to the Appendix A<br>Updated section 5.4 in line with PPF v6.2 and in the introduction of the PWLR[3]<br>Updated Figure 2 and §5.6.2: surface emissivity is retrieved with PWLR[3].<br>Updated 8.3 with different OEM configuration for land and sea |
| V8C | | Editorial refinements for publication |
| V8D | | Update for version 6.3<br>• SO2<br>• Dust Index<br>• Data QC and selection of SST L2Pcore |
| V8E | | Completion of updates for version 6.3. Corrections to reference links. |

# *Table of Contents*

# *Table of Figures*

# *Table of Tables*

# 1 INTRODUCTION

## 1.1 Purpose and Scope of Document

The purpose of this specification is to present all requirements specific to the Metop IASI Level 2 product generation function (PF) which are not already covered in the CGSRD (Core Ground Segment Requirements Document) and the other applicable documents. This specification encompasses not only the required algorithm functions but also the identified supporting functions pertaining to the product generation function.

The document covers all the functions encompassed by the corresponding PF, the interrelations between these functions and the relation to the other functions of the EPS Core Ground Segment (CGS).

## 1.2 Relations to EPS Core Ground Segment

This document addresses all the requirements pertaining to the corresponding instrument PF of the EPSCGS. The product generation function encompasses all the functions (algorithmic, scientific and supporting functions) required for the generation of the products.

The instrument product generation function is a constituent of the CGS. Therefore, unless otherwise specified, all the requirements of the Core Ground Segment Requirements Document (CGSRD) in [CGSRD] shall apply to this product generation function. In particular, the PF shall comply with all the requirements of the generic PGE services.

## 1.3 Requirements Hierarchy and Precedence

In the case of conflict between these product generation function requirements and Core Ground Segment Requirements Document requirements, the latter shall take precedence.

Any conflicts shall be brought to the attention of EUMETSAT, in order to resolve such conflicts with the participation of EUMETSAT.

## 1.4 Structure of the Document

| | |
|---|---|
| Chapter 1 | this introduction |
| Chapter 2 | a description of the instrument |
| Chapter 3 | the overall processor structure |
| Chapter 4 | the specifications of the output products and input measurement and configuration data |
| Chapter 5 | the processing sequence specifications |
| Chapter 6 | the specifications of generic functions |
| Chapter 7 | listing and description of all the processing flags |
| Chapter 8 | description of the static auxiliary data |

## 1.5 Conventions

Where a deviation from or limitation to the use of the convention is required it will be explicitly defined within this document. In particular, in the case of a conflict between definitions in other documents and this document, the conventions in this document shall take precedence.

## 1.6 Reference Frames Definition and Use

The usage of reference frames shall comply with the definitions expressed in this document:
*EPS Mission Conventions Document EUMETSAT* [EPSconv]
DM Number [EUM/EPS/GGS/SPE/990002.]

The numbering of IFOVs within an EFOV shall comply with this document:
*IASI L1C processing specifications: « Dossier de definition des algorithmes » [*IASIL1spe]
EUMETSAT Document Number [IA-DF-0000-2006-CNE]

## 1.7 Acronyms used in this document

| *Acronym* | *Meaning* |
|---|---|
| AC SAF | Atmospheric Composition Monitoring SAF |
| AMSU-A | Advanced Microwave Sounding Unit A (part of ATOVS) |
| API | Application Programming Interface |
| ANN | Artificial Neural Network |
| ATBD | Algorithm Theoretical Basis Document |
| ATOVS | Advanced TIROS Operational Vertical Sounder |
| AVHRR | Advanced Very High Resolution Radiometer |
| CGS | Core Ground Segment |
| CGSRD | Core Ground Segment Requirements Document |
| ECMWF | European Centre for Medium-Range Weather Forecasts |
| EFOV | Elementary Field of View |
| EOF | Empirical Orthogonal Function |
| EPS | EUMETSAT Polar System |
| FG | First Guess |

| *Acronym* | *Meaning* |
|---|---|
| FOV | Field of View |
| FRTM | Fast Radiative Transfer Model |
| FTS | Fourier Transform Spectrometer |
| GIADR | Global Internal Auxiliary Data Record |
| G/S | Ground Segment |
| GHG | Green-house gases |
| GHRSST | Group for High Resolution SST |
| HIRS | High-resolution Infrared Radiation Sounder (part of ATOVS) |
| IASI | Infrared Atmospheric Sounder Interferometer |
| IFOV | Instantaneous Field of View |
| IIS | Integrated Imaging System (of IASI) |
| IPSF | Instrument Point Spread Function |
| ISRF | Instrument Spectral Response Function |
| L1C | Level 1C |
| LST | Land Surface Temperature |
| MHS | Microwave Humidity Sounder (part of ATOVS) |
| NRT | Near-real time |
| OSI SAF | Ocean and Sea-Ice SAF |
| PCC | Principal Component Compression |
| PCR | Principal Component Residuals |
| PF | Product generation Function |
| PGE | Product Generation Environment |
| PSF | Point Spread Function |
| SAD | Static Auxiliary Data |
| SAF | Satellite Applications Facility |
| SCC | Super Channel Cluster |
| SST | Sea surface temperature |
| TRG | Trace Gases |

## 1.8 Reference Documents

| *No.* | *Document Title* | *EUMETSAT Reference* |
|---|---|---|
| EURD | EPS End Users Requirements Document | EUM.EPS.MIS.REQ.93.001 |
| AVHL1PGS | AVHRR Level 1 Product Generation Specification | EUM/EPS/SYS/SPE/990004 |
| IASIL1spe | IASI L1C processing specifications: « Dossier de definition des algorithmes » | IA-DF-0000-2006-CNE |
| IASISpe] | IASI Instrument Specification | IA-SP-1000-201-CNE |

| *No.* | *Document Title* | *EUMETSAT Reference* |
|---|---|---|
| IASIPsfSpe | IASI PSF format description | IASI-TN-0000-3312-CNE 01/00, 03/06/2009 |
| GPFS] | EPS Generic Product Format Specification | EPS/GGS/SPE/96167 |
| AMSUL1PFS | AMSU-A Level 1 Product Format Specification | EPS/MIS/SPE/97228 |
| MHSL1PFS | MHS Level 1 Product Format Specification Document | EPS/MIS/SPE/97229 |
| IASIL2PFS | IASI Level 2 Product Format Specification | EPS/MIS/SPE/980760 |
| EPSconv | EPS Mission Conventions Document | EUM/EPS/GGS/SPE/990002 |
| CGSRD | Core Ground Segment Requirements Documents | EUM/EPS/GGS/REQ/95327 |
| BUFRcodes | World Meteorological Organisation manual on Codes Volume 1, International Codes, | ISBN: 92-63-1506-X |
| IASIL1PFS | IASI Level 1 Product Format Specification | EPS/SYS/SPE/990003 |
| PCCPFS | EPS IASI L1 PCC Product format specification | EUM/OPS-EPS/SPE/08/0195 |
| Menzel83 | W.P. Menzel, W.L. Smith, T.R. Stewart, *Improved cloud motion wind vector and altitude assignment using VAS3* | Journal of Climate and Applied Meteorology, 22, 377-384, 1983 |
| Smith90 | W.L. Smith, R. Frey, *On cloud altitude determination from high resolution interferometer sounder (HIS) observations* | Journal of Applied Metreorology, 29, 658-662, 1990 |
| Grody | Microwave Surface and Precipitation Products System Algorithms | http://www.star.nesdis.noaa.gov/corp/scsb/mspps/algorithms.html |
| Rodgers | C.Rodgers, *Inverse methods for atmospheric sounding* | Series on Atmposheric, Oceanic and Planetray Physics, Vol.2. World Scientific, 2004 |
| FORLI | D. Hurtmans et al, *FORLI radiative transfer and retrieval code for IASI* | J. Quant. Spectrosc. Radiat. Transfer , 113, 1391-1408, |
| FORLIatbd | Fast Optimal Retrieval on Layers for IASI, Algorithm Theoretical Basis Document<br>FORLI-CO, Complement to FORLI ATBD: Descriptions of the inputs to FORLI-CO v20100815 | SAF/O3M/ULB/ForlíATBDv01<br>SAF/O3M/ULB/FORLICO_CATBD |
| Stub99 | C. Stubenrauch et al, *Clouds as Seen by satellite Sounders (3I) and Imagers (UISCCP). Part II: A New Approach for Cloud Parameter Determination in the 3I Algorithms* | J. Climate, 1999, 12, pp 2214-2223. |
| Eyre89 | J. Eyre and W. P. Menzel, 1989: *Retrieval of Cloud Parameters from Satellite Sounder Data: A simulation Study*. | J. Appl. Met. 28, 267-275 |
| GTOPO | Global 30 Arc-Second Elevation (GTOPO30) | https://lta.cr.usgs.gov/GTOPO30 |
| [LSM | Description of Land/sea and Coastline Data Bases for AAPP upgrade | EUM/EPS/SYS/TEN/00/018 |
| UWIREMS | Global Infrared Land Surface Emissivity Database | cimss.ssec.wisc.edu/iremis/ |
| AAPP | Pre-processing of ATMS and CrIS | NWPSAF-MO-UD-027 |
| GRIBAPI | ECMWF GRIB API User Manual | https://software.ecmwf.int/wiki/display/GRIB/Releases |
| RTTOVguide | RTTOV v11 Users Guide | NWPSAF-MO-UD-028 |

| *No.* | *Document Title* | *EUMETSAT Reference* |
|---|---|---|
| RTTOVval | RTTOV-11 Science and Validation Report | NWPSAF-MO-TV-032 |
| SmithMet | R.J. List, 1958: *Smithsonian Meteorological Table* | 6th Edition, Smithsonian, Institution Press, Washington D.C., |
| GHRSSTspe | The Recommended GHRSST Data Specification Revision 2.0 | www.ghrsst.org/modules/documents/documents/GDS2.0_TechnicalSpecifications_v2.0 |
| BresciaATBD | IASI Brescia SO2: Algorithm Theoretical Basis Document | SAF/O3M/ULB/BresciaSO2_ATBD |

## 1.9 Background Documents

These documents give background information and are meant as supplemental reading to aid the understanding of scientific or technical details. Algorithms adopted from some scientific papers have undergone evolution, so the information given in the following documents may be outdated. In such cases, the specifications given in this document take precedence.

| *No.* | *Document Title* | *Reference* |
|---|---|---|
| BD 1 | Hyperspectral earth observation from IASI: Five years of accomplishments. | Hilton et al. 2012, Bulletin of the American Meteorological Society, 93, 347–370, DOI: 10.1175/BAMS-D-11-00027.1. |
| BD 2 | IASI on Metop-A: Operational Level 2 retrievals after five years in orbit | T. August et al, JQSRT, 113 (11), 1340-1371, doi:10.1016/j.jqsrt.2012.02.028, 2012. |
| BD 3 | Global land surface emissivity retrieved from satellite ultraspectral IR measurements | D. Zhou et al, IEEE Trans. Geosci. Remote Sens., 49, 1277--1290, doi:10.1109/TGRS.2010.2051036, 2011 |
| BD 4 | Technical Note: An assessment of the accuracy of the RTTOV fast radiative transfer model using IASI data | Matricardi, Atmos. Chem. Phys., 9, 6899-6913, 2009 |
| BD 5 | Assessing the impact of radiometric noise on IASI performances | U. Amato, V. Cuomo and C. Serio *Int. J. Remote Sensing*, vol. 16, N°15, 2927-2938, |
| BD 6 | The information content of clear sky IASI radiance and their potential for numerical weather prediction | P. Prunet, J.-N. Thepaut, V. Casse *QJRMS*, 124, pp 211-241, 1998 |
| BD 7 | The GEISA system in 1996 : toward an operational tool for the second generation vertical sounders radiance simulation | N. Jacquinet-Husson et al. *JSQRT*, 59, N°3-5, 511-527, 1998 |
| BD 8 | The effects of nonlinearity on analysis and retrieval errors | J.R. Eyre *UKMO Forecasting Research Technical Report* N°252 |
| BD 9 | Assimilation of carbon monoxide measured from satellite in a three-dimensional chemistry-transport model | C. Clerbaux, J. Hadji-Lazaro, D. Hauglustaine, G. Mégie, B. Khattatov and J.F. Lamarque J. *Geophys. Res*., 106, D14,15, 385-394, 2001 |
| BD 10 | Channel selection methods for Infrared Atmospheric Sounding Interferometer radiances | F. Rabier, N. Fourrié, D. Chafaï and P. Prunet Q.*J. R. Meteorol. Soc*., 128,1011-1027, 2002 |
| BD 11 | Balloon-borne calibrated spectroradiometer for atmospheric nadir sounding | Y. Té, P. Jeseck, C. Camy Peyret, S. Payan, G. Perron and G. Aubertin *Applied Optics*, Vol 41, N°30, 6431-6441, 2002 |
| BD 12 | Retrieval of CO from nadir remote-sensing measurements in the infrared by use of four different inversion algorithms | C. Clerbaux, J. Hadji-Lazaro, S. Payan, C. Camy-Peyret, J. Wang, D.P. Edwards and M. Lo *Applied Optics*, Vol. 41,N° 33, 7068-7078, 2002 |
| BD 13 | First satellite ozone distributions retrieved from nadir high-resolution infrared spectra | S. Turquety, J. Hadji-Lazaro and C. Clerbaux Geophys. Res. Lett., Vol.29,N°24,2198, 2002 |

| No. | Document Title | Reference |
|---|---|---|
| BD 14 | Simulation of uplooking and downlooking high-resolution radiance spectra with two different radiative transfer model | R. Rizzi, M. Matricardi and F. Miskolczi Applied Optics,41,6, 940-956, 2002 |
| BD 15 | The feasibility of monitoring CO2 from high resolution infrared sounders | A. Chédin, R. Saunders, A. Hollingworth, N. Scott, M. Matricardi, J. Etcheto, C. Clerbaux, R. Armante, C. Crevoisier *J. Geophysical. Research*, Vol. 108, N° D2, 4064-4083, 2003 |
| BD 16 | Spectroscopic measurements of halocarbons and hydrohalocarbons by satellite-borne remote sensors | P.F. Coheur, C. Clerbaux and R. Rolin *J. Geophysical Research*., Vol. 108,N° D4,4130, 2003 |
| BD 17 | Classification of IASI inhomogeneous scenes using co-located AVHRR data | Phillips, P., P. Schlüssel Proc. SPIE, 5979, 29-41, 2005 |
| BD 18 | Technical note: Analytical estimation of the optimal parameters for EOF retrievals of the IASI Level 2 Product Processing Facility and its application using AIRS and ECMWF data | Calbet, X., P. Schlüssel *Atmos. Chem. Phys*., 6, 831-846, 2006 |
| BD 19 | An introduction to the EUMETSAT Polar System | Klaes, K.D., M. Cohen, Y. Buhler, P. Schlüssel, R. Munro, J.-P. Luntama, A. Von Engeln, E. Ó. Clerigh, H. Bonekamp, J. Ackermann, J. Schmetz *Bulletin of the American Meteorological Society*, 88, 1085-1096, doi:10.1175/BAMS.88.7.1085, |
| BD 20 | Sensitivity of analysis error covariance to the mis-specification of background error covariance | Eyre and Hilton, Q. J. R. Meteorol. Soc., 139, 524-533, doi: 10.1002/qj.1979, 2013 |
| BD 21 | Toward improved validation of satellite sea surface skin temperature measurements for climate research | Donlon, C.J., P.J. Minnett, C. Gentemann, T.J. Nightingale, I.J.Barton, B. Ward, and M.J. Murray *J. Climate,* 15**,** 353–369, 2002 |
| BD 22 | Diurnal signals in satellite sea surface temperature measurements | Gentemann, C.L., C.J. Donlon, A. Stuart-Menteth, and F.J. Wentz *Geophys. Res. Let.*, 30, 3, 1140 |
| BD 23 | Diurnal warm-layer events in the western Mediterranean and European shelf seas | Merchant C. J., M.J. Filipiak, P. Le Borgne, H. Roquet, Autret Emmanuelle, J-F. Piolle, S. Lavender *Geophys. Res. Let.*, 2008, 35 |
| BD 24 | Observations of the oceanic thermal skin in the Atlantic Ocean | Donlon, C.J. and I.S. Robinson, *Journ. Geophys. Res.*, 102, C8, 1997 |
| BD 25 | Operational SST retrieval from METOP/AVHRR validation report | Le Borgne, P., G. Legendre, A. Marsouin, and S. Pere, *Ocean and Sea-Ice SAF CDOP report*, Version 2.0, July 2008 |
| BD 26 | FORLI radiative transfer and retrieval code for IAS | Hurmtans et al, JQSRT, 113, 1391-1408, doi:10.1016/j.jqsrt.2012.02.036, 2012 |
| BD 27 | Monitoring of atmospheric composition using the thermal infrared IASI/MetOp sounder | Clerbaux et al, *Atmos. Chem. Phys*., 9, 6041-6054, 2009. |
| BD 28 | Measurements of total and tropospheric ozone from IASI: comparison with correlative satellite, ground-based and ozonesonde observations | Boynard et al, *Atmos. Chem. Phys*., 9, 6255-6271, 2009. |
| BD 29 | Carbon monoxide distributions from the IASI/METOP mission: evaluation with other space-borne remote sensors | George et al, *Atmos. Chem. Phys*., 9, 8317-8330, 2009 |
| BD 30 | A unified approach to aerosol remote sensing and type specification in the infrared | Clarisse et al, *Atmos. Chem. Phys*., 13, 2195-2221, doi:10.5194/acp-13-2195-2013, 2013 |
| BD 31 | The MACC reanalysis: an 8-year data set of atmospheric composition | Atmos. Chem. Phys., 13, 4073-4109, doi:10.5194/acp-13-4073-2013, 2013 |
| BD 32 | The 2007-2011 evolution of tropical methane in the mid-troposphere as seen from space by MetOp-A/IAS | Crevoisier et al, *Atmos. Chem. Phys*., 13, 4279-4289, doi:10.5194/acp-13-4279-2013, 2013. |

| *No.* | *Document Title* | *Reference* |
|---|---|---|
| BD 33 | The Concordiasi field experiment over Antarctica: first results from innovative atmospheric measurements | Rabier et al, Bull. Amer. Meteor. Soc., 94, ES17-ES20, doi http://dx.doi.org/10.1175/ BAMS-D-12-00005.1, 2013 |
| BD 34 | Equatorial total column of nitrous oxide as measured by IASI on MetOp-A: implications for transport processes | Ricaud et al, Atmos. Chem. Phys., 9, 3947-3956, 2009 |
| BD 35 | Retrieval of desert dust aerosol vertical profiles from IASI measurements in the TIR atmospheric window | Vandenbusche et al, Atmos. Meas. Tech., 6(10), 2577-2591, doi:10.5194/amt-6-2577-2013, 2013. |
| BD 36 | Tracking and quantifying volcanic SO2 with IASI, the September 2007 eruption at Jebel at Tair | Clarisse et al., ACP 2008, doi:10.5194/acp-8-7723-2008 |
| BD 37 | Retrieval of sulphur dioxide from the infrared atmospheric sounding interferometer (IASI) | Clarisse et al., Atmos. Meas. Tech., 5, 581-594, doi:10.5194/amt-5-581-2012, 2012. |
| BD 38 | The 2011 Nabro eruption, a SO2 plume height analysis using IASI measurements | Clarisse et al., Atmos. Chem. Phys., 14, 3095-3111, doi:10.5194/acp-14-3095-2014, 2014. |
| BD 39 | Retrieval of near-surface sulfur dioxide (SO2) concentrations at a global scale using IASI satellite observations | Baudouin et al, AMT 2016, doi:10.5194/amt-9-721-2016 |
| BD 40 | A unified approach to infrared aerosol remote sensing and type specification | Clarisse et al., 2013, doi:10.5194/acp-13-2195-2013, 2013 |

# 2 INSTRUMENT DESCRIPTION

The Infrared Atmospheric Sounding Interferometer (IASI) is a multi-purpose sounding Instrument on-board Metop, used for global measurement of temperature, water vapour, trace-gases such as ozone, nitrous oxide, carbon dioxide, and methane, as well as surface temperature, surface emissivity, and cloud characteristics. IASI has 8461 spectral channels, aligned in three bands between 3.62 µm and 15.5 µm, with a spectral resolution of 0.5 $cm^{-1}$, after apodisation. The spectral sampling interval is 0.25 $cm^{-1}$. The full specification of the IASI Instrument is given in IASIL1spe.

## 2.1 Spectral Characteristics of IASI

Table 1 summarises the spectral characteristics of IASI IASIL1spe. A satellite altitude of 819 km is assumed.

| *Band* | *Wavenumbers ($cm^{-1}$)* | *Wavelength (µm)* |
|---|---|---|
| 1 | 645 – 1210 | 8.26 – 15.50 |
| 2 | 1210 – 2000 | 5.00 – 8.26 |
| 3 | 2000 – 2760 | 3.62 – 5.00 |

*Table 1: Spectral characteristics of IASI.*

The channel numbers *k* of the IASI Level 1c data are defined by the positions of the channel centres in the wave number domain:

$$\nu_k = 645.00 + (k - 1) \times 0.25\, cm^{-1}, k = 1,\ldots,8461 \qquad \textit{Equation 1}$$

where:

| | |
|---|---|
| $\nu_k$ | is the centre wave number of channel k |

## 2.2 Sampling Characteristics of IASI

IASI is an across-track scanning system with a scan range of ±48°20′, symmetrically with respect to the Nadir direction. Each line covers 30 scan positions and 2 calibration views (one internal black body and one deep space view). The scan starts on the Sunward side. The elementary field of view (EFOV) is the useful field of view at each scan position. Each EFOV is covered by a 2 × 2 matrix of circular samples. Each sample has an Instantaneous Field of View (IFOV) with a diameter of 14.65 mrad, corresponding to 12 km nadir ground resolution at a satellite altitude of 819 km. The 2 × 2 matrix of IFOVs (IFOV quadruples) is centred on the current viewing direction. The instrument's point spread function (PSF), defined as the horizontal sensitivity within an IFOV is uniform within 80 % of the IFOV, the non-uniformity is less than 5 %. Included in the sounding instrument is an Integrated Imaging System (IIS). It consists of a broadband radiometer measuring between 10 µm and 12 µm with high spatial resolution to obtain detailed analysis of cloud properties inside the IASI sounder IFOVs. The IIS IFOV is defined by a squared area of 59.63 mrad × 59.63 mrad, covering 64 × 64 pixels. However, the information of the IIS is only used during Level 1 processing for co-registration with AVHRR and is not used for level 2 processing. Henceforth, the term IASI refers to the IASI sounder alone if not explicitly stated otherwise.

The instrument scans in a step and stare modus. Each interferogram is acquired within 151 milliseconds. The 30 × 120 Earth interferograms per scan line are taken in equally spaced time intervals every 8/37 seconds so that a synchronisation with AMSU is reached. The calibration of IASI is done by one space view, and a view to a hot calibration target.

In addition to the nominal scan sequence, the IASI Instrument can be operated in an "external calibration mode", in which a specific target—any of the Earth views, the blackbody, or one of two space views—is viewed instead of the 30 different Earth views during the nominal scan. Table 2 summarizes the scanning characteristics:

| *Characteristics* | *Value* | *Unit* |
|---|---|---|
| Scan type | Step and stare | |
| Scan rate | 8 | second |
| Stare interval | 151 | ms |
| Step interval | 8/37 | |
| EFOV/scan | 30 | |
| Swath | ± 48.333 | degrees |
| Swath width | ± 1100 | km |
| IFOV | 14.65 | mrad |
| IFOV shape | circular | |
| IFOV size (nadir) | 12 | km |
| IFOV size (edge) – across track | 39 | km |
| IFOV size (edge) – along track | 20 | km |
| IFOV separation within EFOV - along-track at nadir | 19 | km |

*Table 2: Scanning characteristics of IASI*

# 3 PROCESSOR STRUCTURE OVERVIEW

The retrieval sequence and generated products are summarised in the following figures. The blue trapezoids are output products for dissemination and archive (solid lines) and for internal processing and in-house monitoring on MPSTAR (PRP files, with dashed lines). Input files are represented by parallelograms: measurements are in blue, model data is in green and static configurable datasets are in orange.

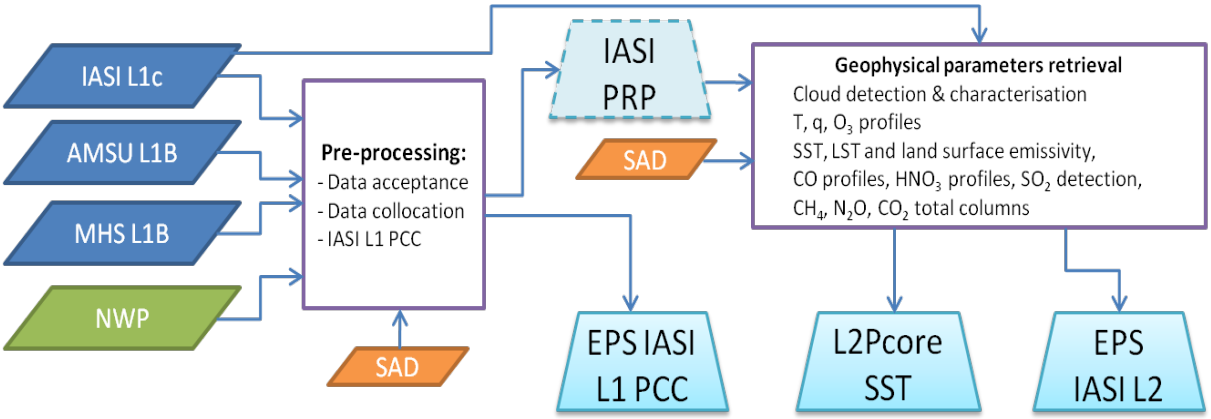


*Figure 1: High level overview of the IASI L1 PCC, L2P and L2 processing.*

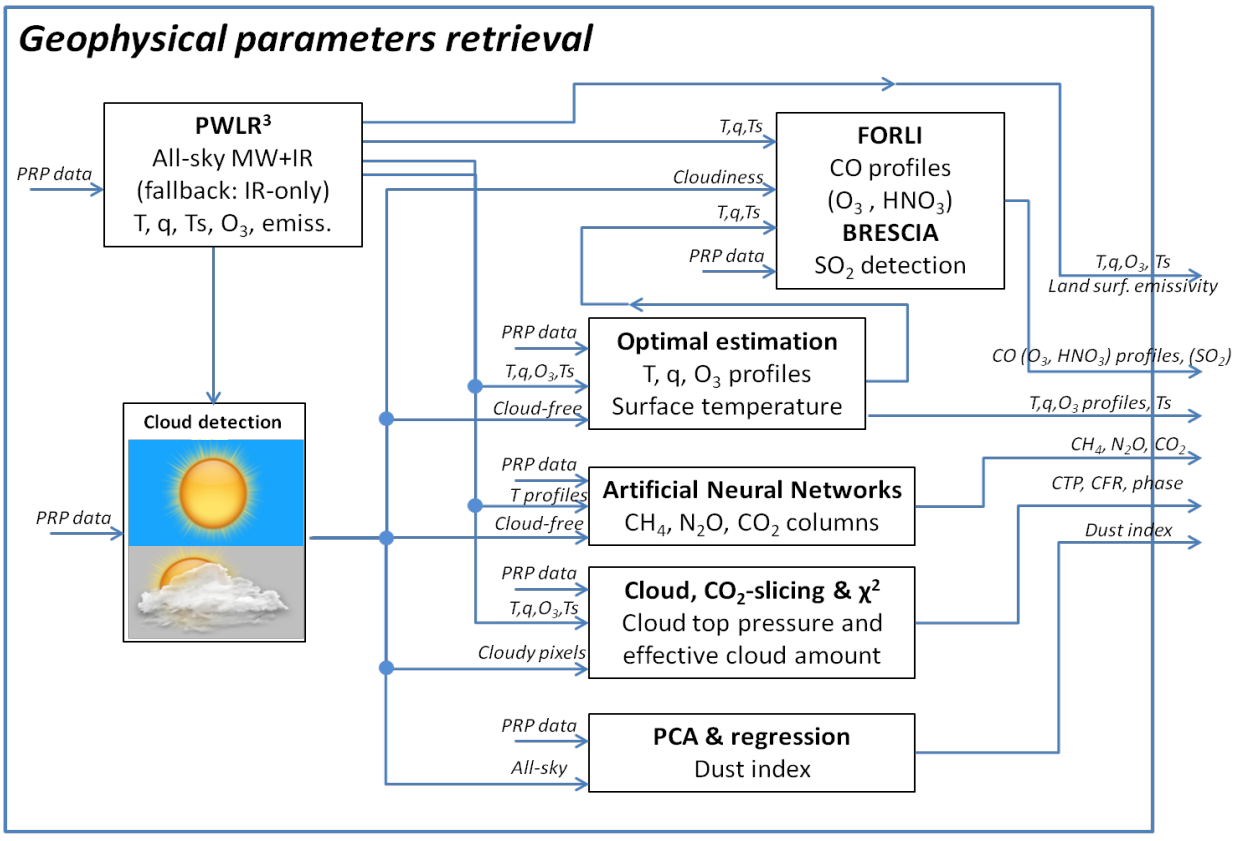


*Figure 2: Overview of the geophysical parameters retrieval modules and sequence.*

# 4 PROCESSOR INPUT/OUTPUT

## 4.1 Generated products

The tables that follow list the measurement and geophysical products to be generated from the IASI L2 PPF. The L2 products shall be output as specified in [IASIL2PFS] and the principal components products as per [PCCPFS].

| *Name* | *Content of L2 products* | *Purpose* |
|---|---|---|
| T | Temperature profile | NRT dissemination and archive |
| q | Specific humidity profile | NRT dissemination and archive |
| CLDNES | Cloud detection | NRT dissemination and archive |
| DUSTCLD | Dust detection | NRT dissemination and archive |
| CFR | Cloud fractional coverage | NRT dissemination and archive |
| TCWV | Water vapour total column | NRT dissemination and archive |
| CLDPHI | Cloud top phase | NRT dissemination and archive |
| CTP | Cloud top height /pressure | NRT dissemination and archive |
| SST | Sea surface temperature | NRT dissemination and archive |
| LST | Land and ice surface temperature | NRT dissemination and archive |
| LSE | Land and ice surface emissivity | NRT dissemination and archive |
| CO | Carbon monoxide profile | NRT dissemination and archive |
| COTC | Carbon monoxide total column | NRT dissemination and archive |
| $CH_4$ | Methane total column | NRT dissemination and archive |
| $HNO_3$ | Nitric acid profiles | NRT dissemination and archive *(Under development)* |
| $N_2O$ | Nitrous oxide total column | NRT dissemination and archive |
| $O_3$ | Ozone profile | NRT dissemination and archive |
| $O_3TC$ | Ozone total column | NRT dissemination and archive |
| $SO_2$ | Sulphur dioxide total column | NRT dissemination and archive |

*Table 3: List of IASI L2 products to be generated.*

| *Product* | *Content of L1 PCC products* | *Purpose* |
|---|---|---|
| PCS | Principal component scores and reconstruction skills | NRT dissemination and archive |
| PCR | Radiance residuals after reconstruction from the PCS and quality control | Archive |
| IPO | Identification of outliers: spectra that are not correctly represented by the leading PCS | Archive and monitoring |

*Table **4**: List of IASI L1 PCC products to be generated*

## 4.2 Algorithm Input

This section specifies the dynamic inputs and static atlases used to process the IASI L2 products.

### 4.2.1 Primary Sensor Data

#### *4.2.1.1 IASI L1C spectra*

The instrument characteristics are explained in Section 2.

The primary input to the IASI L2 processing algorithms are the spectra and quality information contained in the IASI L1C products specified in IASIPsfSpe. In the IASI L1C processing, the effects of the instrument function are corrected for, such that the measurements from each of the four detectors may be processed with the same configuration for higher level products.

The spectra are contained in the field `GS1cSpect`. The Boolean flags **DEGRADED_FIGURE_MDR** and **DEGRADED_PROC_MDR** give general quality information with respect to degradation due to Instrument and/or processing. These variables are the generic quality indicators. Additional quality flags and Instrument noise indicators are generated during the Level 1 processing based on information gained during on-board and Level 1 processing, which shall be inspected for processing the IASI L2 products. The Boolean quality flag **GQisFlagQual** indicates the quality of each of the three IASI spectral bands for every IASI spectrum. See Table 1 for specifications. **GQisFlagQual** is established by evaluating the formerly derived quality flags and quality information from on-board and Level 1 processing, e.g. quality of the internal calibration black body temperature measurement.

#### *4.2.1.2 Acquisition geometry and product numbering*

The following three figures illustrate the acquisition geometry and numbering of the IASI EFOV in the successive 30 scan positions (SP) and the identification of the four pixels (IFOVs) in each scan position.

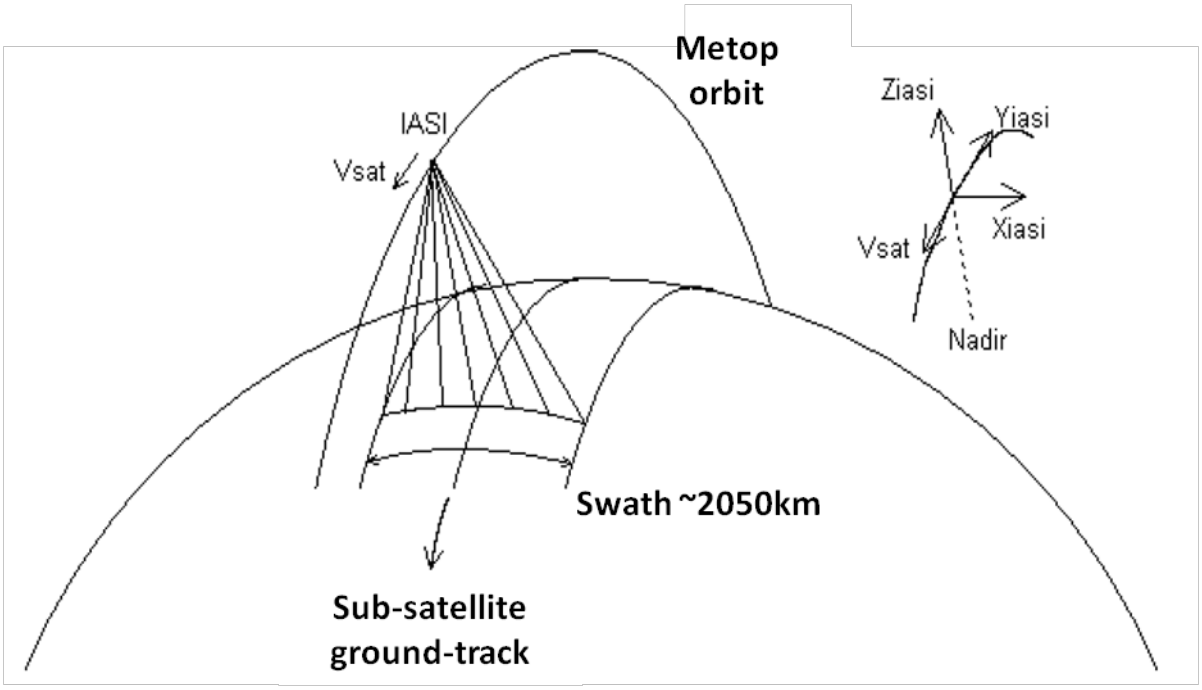


*Figure 3: IASI scanning geometry, adapted from **IASISpe]***

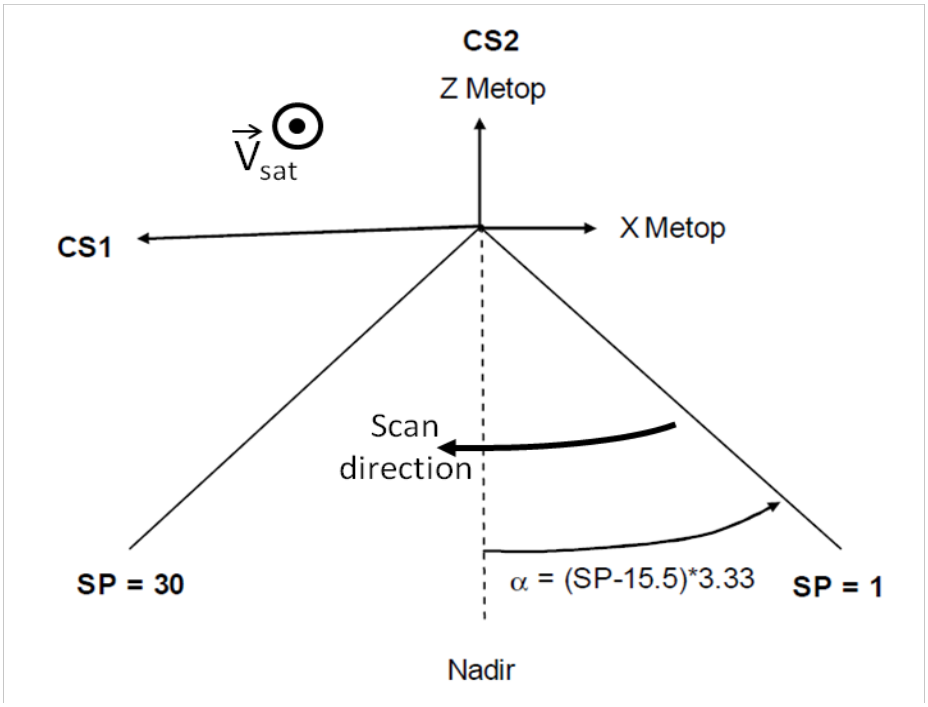


*Figure 4: Scan position (SP) numbering and viewing angle computation (α, in degrees), adapted from [*IASIPsfSpe*].*

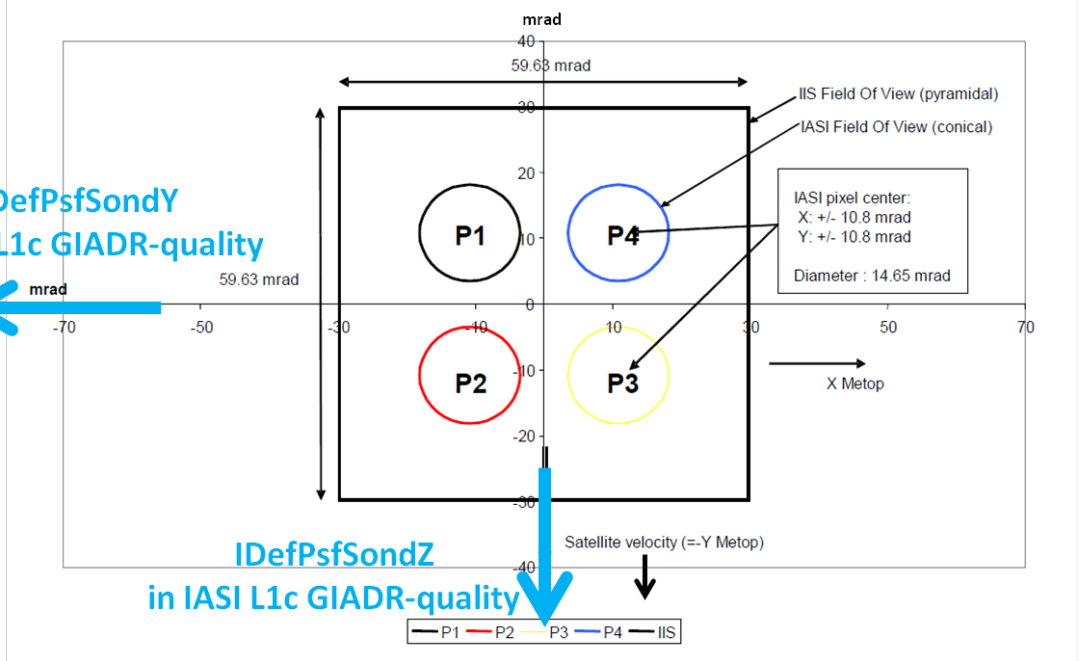


*Figure 5: IASI pixels identification and PSF pixels ordering projected on ground, adapted from* [IASIPsfSpe]

A line of data, or measurement data record (MDR) consists of 30 successive acquisitions of four simultaneous fields of view. The pixel numbering in a line goes from 1 to 120 as follows:

$$ifovNumber = 4 * scanPosition + pixelNumber \quad \text{Equation 2}$$

The line or MDR number in a product is incremented along the satellite velocity.

### 4.2.2 Auxiliary sensor data

#### *4.2.2.1 AMSU L1B measurements*

The AMSU-A is a fifteen-channel microwave radiometer that is used for measuring global atmospheric temperature profiles and providing information on atmospheric water in all its forms. AMSU-A measures in 15 spectral bands, whereas temperature sounding mainly exploits one band, the oxygen band at 50 GHz. These spectral bands are summarised in Table 5 below:

| *Channel* | *Channel frequency (GHz)* | *Passes per band* | *Nominal bandwidth (MHz)* | *Calibration accuracy (K)* |
|---|---|---|---|---|
| **AMSU-A2** | | | | |
| 1 | 23.8 | 1 | 270 | < 2.0 |
| 2 | 31.4 | 1 | 180 | < 2.0 |
| **AMSU-A1** | | | | |
| 3 | 50.3 | 1 | 180 | < 1.5 |
| 4 | 52.8 | 1 | 400 | < 1.5 |
| 5 | 53.59 ± 0.115 | 2 | 170 | < 1.5 |
| 6 | 54.40 | 1 | 400 | < 1.5 |
| 7 | 54.94 | 1 | 400 | < 1.5 |
| 8 | 55.50 | 1 | 330 | < 1.5 |
| 9 | $F_{LO}$ = 57.290344 | 1 | 330 | < 1.5 |
| 10 | $F_{LO}$ ± 0.217 | 2 | 78 | < 1.5 |
| 11 | $F_{LO}$ ± 0.3222 ± 0.048 | 4 | 36 | < 1.5 |
| 12 | $F_{LO}$ ± 0.3222 ± 0.022 | 4 | 16 | < 1.5 |
| 13 | $F_{LO}$ ± 0.3222 ± 0.010 | 4 | 8 | < 1.5 |
| 14 | $F_{LO}$ ± 0.3222 ± 0.0045 | 4 | 3 | < 1.5 |
| 15 | 89.0 | 1 | <6000 | < 2.0 |

*Table 5: Spectral characteristics of AMSU-A*

Hardware for the two lowest frequencies is located in the AMSU-A2 module. Hardware for the remaining thirteen frequencies is in the AMSU-A1 module.

AMSU-A is an across-track scanning system with a scan range of ± 48.33° with respect to the Nadir direction. The instantaneous field of view (IFOV) of each channel is approximately 57.6 milliradians (3.3°) leading to a IFOV size close to 47.63 km at nadir and a swath width of ± 1026.31 km (with sampling time of 200.0 ms) for a nominal altitude of 833 km. The sampling angular interval is closer to 58.18 milliradians (3.3333°). The distance between two consecutive scans is approximately equal to 52.69 km.

There are 30 Earth views, two views of the internal warm target, and two views of cold space per scan line for each channel. Each scan takes 8.0 seconds to complete and is synchronised with IASI scanning. Table 6 summarises the scanning characteristics of the AMSU-A.

| *Criteria* | *Value* | *Unit* |
|---|---|---|
| Scan direction | west to east (northbound) | - |
| Scan type | step | - |
| Scan rate | 8 | second |
| Sampling interval (duration) | 200 | ms |
| Sampling interval | 3.3333 | degree |
| Pixels/scan | 30 | - |
| Swath | ± 48.33 | degree |
| Swath width | ± 1026.31 | km |
| IFOV | 3.3 | degree |
| IFOV type | circular | - |
| IFOV size (nadir) | 47.63 | km |
| IFOV size (edge): across-track | 146.89 | km |
| IFOV size (edge): along-track | 78.79 | km |
| Scan separation (adjacent scan lines) | 52.69 | km |

*Table 6: Scanning characteristics of AMSU-A.*

#### *4.2.2.2 Microwave Humidity Sounder (MHS) L1B measurements*

The Microwave Humidity Sounder (MHS) is the follow-on Instrument to the Advanced Microwave Sounding Unit-B (AMSU-B) which flew as a part of ATOVS on the NOAA-KLM satellite series. It is procured by EUMETSAT for the Metop and NOAA satellites. MHS is a five-channel microwave radiometer, which complements the AMSU-A channels. In some MHS descriptions documents, MHS channels may be numbered as a continuation of the AMSU-A channels: 16, 17, 18, 19 and 20.

These frequencies carry information about humidity profiles and cloud liquid water content. Additionally, the Instrument's sensitivity to large water droplets in precipitating clouds can provide a qualitative estimate of precipitation rates. Table 7 summarises the spectral characteristics of the MHS.

| *Channel* | *Central frequency (GHz)* | *Bandwidth (MHz)* | *Calibration accuracy (K)* |
|---|---|---|---|
| H1 | 89.0 | ± 1400 | 1.0 |
| H2 | 157.0 | ± 1400 | 1.0 |
| H3 | 183.311 ± 1.00 | ± 250 | 1.0 |
| H4 | 183.311 ± 1.00 | ± 500 | 1.0 |
| H5 | 190.311 | ± 1100 | 1.0 |

*Table 7: Spectral characteristics of MHS.*

MHS is an across-track scanning system with a scan range of ±49.44° with respect to the Nadir direction. The IFOV of each channel is approximately 19.2 milliradians (1.1°) producing a circular IFOV size close to 15.88 km at nadir for a nominal altitude of 833 km. Each scan takes 2.667 seconds to complete. The scan of the MHS Instrument is synchronised with the AMSU-A scan. There are three scans of MHS for each scan of AMSU-A.

There are 90 Earth samples per scan and per channel for a swath width of ± 1077.68 km with a sampling time of 19.0 ms. Calibration is performed using a cold-space view and an on-board black body target. The sampling angular interval is close to 19.39 milliradians (1.1111°). The distance

between two consecutive scans is approximately equal to 17.56 km. Table 8 below summarises the scanning characteristics.

| *Criteria* | *Value* | *Unit* |
|---|---|---|
| Scan direction | west to east (northbound) | - |
| Scan type | continuous | - |
| Scan rate | 2.667 | second |
| Sampling interval (duration) | 18.52 | ms |
| Sampling interval | 1.1111 | degree |
| Pixels per scan | 90 | - |
| Swath | ±49.44 | degree |
| Swath width | ±1077.68 | km |
| IFOV | 1.1 | degree |
| IFOV type | circular | - |
| IFOV size (nadir) | 15.88 | km |
| IFOV size (edge): across-track | 52.83 | km |
| IFOV size (edge): along-track | 27.10 | km |
| Scan separation (adjacent scan lines) | 17.56 | km |

*Table 8: Scanning characteristics of MHS*

#### *4.2.2.3 AVHRR radiance clusters and cloud analyses*

The Advanced Very High Resolution Radiometer (AVHRR) is a multipurpose imaging Instrument used for global monitoring of cloud cover, sea surface temperature, ice, snow and vegetation cover characteristics. The Instrument model flying together with IASI on the Metop satellites is AVHRR/3.

The AVHRR/3 is a six-channel scanning radiometer providing three solar channels in the visible/near-infrared region and three thermal infrared channels. It has two one-micrometre wide channels between 10.3 and 12.5 micrometres. AVHRR/3 is an across-track scanning system with a scan range of ± 55.37° with respect to the Nadir direction. The field of view (IFOV) of each channel is approximately 1.3 milliradians (0.0745°) leading to a square instantaneous field of view size of 1.08 km at nadir for a nominal altitude of 833 km. The scanning rate of 360 scans per minute is continuous with one scan every 1/6 second. There are 2048 Earth views per scan and per channel for a swath width of approximately ± 1447 km, with a sampling time of 0.025 ms. The sampling angular interval is close to 0.944 milliradians (0.0541°). The distance between two consecutive scans is approximately equal to 1.1 km.

Although AVHRR/3 is a six-channel radiometer, only five channels are transmitted to the ground at any given time. Channels 3a and 3b cannot operate simultaneously. For Metop, channel 3a is operated during the daytime portion of the orbit and channel 3b during the night-time portion.

The spectral characteristics of AVHRR/3 are summarized in Table 9.

| *Channel* | *Central wavelength (µm)* | *Half power points (µm)* | *Channel noise specifications* | |
|---|---|---|---|---|
| | | | *Surface/ Noise @ 0.5% reflectance* | *NEdT @ 300K* |
| 1 | 0.630 | 0.580 - 0.680 | 9:1 | - |
| 2 | 0.865 | 0.725 - 1.000 | 9:1 | - |
| 3a | 1.610 | 1.580 - 1.640 | 20:1 | - |
| 3b | 3.740 | 3.550 - 3.930 | - | < 0.12 K, 0.0031 mW/(m$^2$ sr cm$^{-1}$ ) |
| 4 | 10.800 | 10.300 - 11.300 | - | < 0.12 K, 0.20 mW/(m$^2$ sr cm$^{-1}$ ) |
| 5 | 12.000 | 11.500 - 12.500 | - | < 0.12 K, 0.21 mW/(m$^2$ sr cm$^{-1}$ ) |

*Table 9: Spectral characteristics of AVHRR/3.*

The AVHRR measurements are already collocated to the IASI IFOVs as part of the IASI L1C processing. The AVHRR information required as input to the IASI L2 algorithms is extracted from the following fields of the IASI L1C products. See also IASIPsfSpe:

| *IASI L1C fields* | *Description* |
|---|---|
| **IDefCcsChannelId** | Radiance Analysis: Identification of the AVHRR channel or pseudo-channels used for Radiance Analysis. |
| **GCcsRadAnalNbClass** | Radiance Analysis: Number of identified classes in the sounder FOV |
| **GCcsRadAnalWgt** | Radiance Analysis: sounder FOV Radiance Analysis (per cent covered by each class) |
| **GCcsRadAnalY** | Radiance Analysis: Y Angular position of the centre of gravity. |
| **GCcsRadAnalZ** | Radiance Analysis: Z Angular position of the centre of gravity. |
| **GCcsRadAnalMean** | Radiance Analysis: Mean AVHRR radiances (all channels) of the sounder FOV classes. |
| **GCcsRadAnalStd** | Radiance Analysis: Standard deviation AVHRR radiances (all channels) of the sounder FOV classes. |
| **GEUMAvhrr1BCldFrac** | Cloud fraction in IASI FOV from AVHRR 1B in IASI FOV. |
| **GEUMAvhrr1BLandFrac** | Land and Coast fraction in IASI FOV from AVHRR 1B. |
| **GEUMAvhrr1BQual** | Quality indicator. If the quality is good, it gives the coverage of snow/ice. |

*Table 10: AVHRR input data within IASI L1C products.*

#### *4.2.2.4 Acquisition geometry and collocation with IASI*

The acquisition geometry and collocation of IASI with the microwave sounding Instruments and image on-board Metop is illustrated in Figure 6.

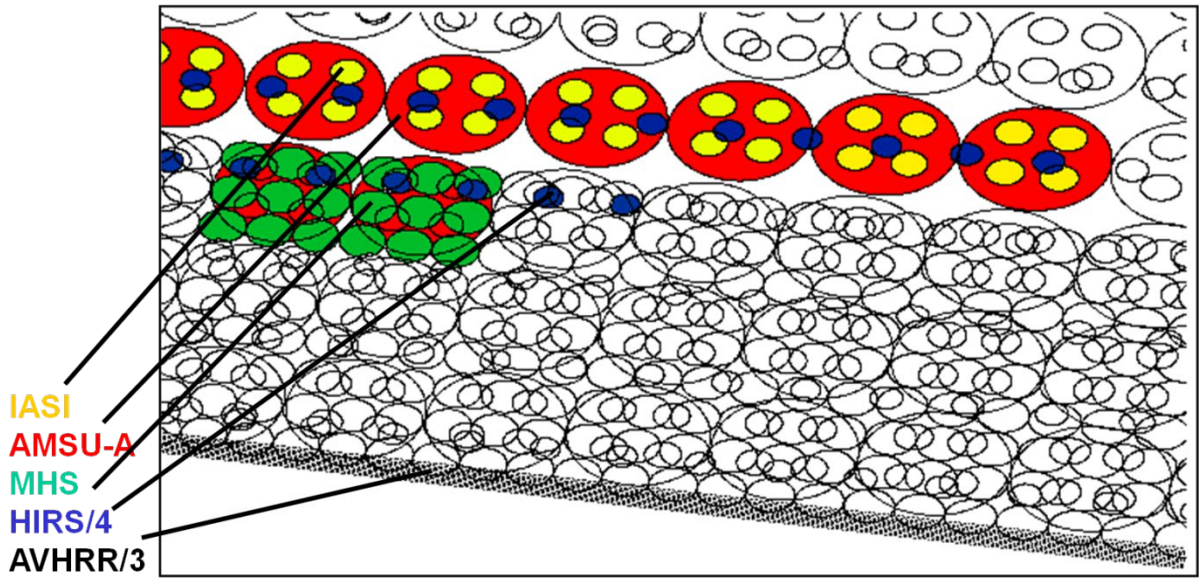


*Figure 6: IASI footprint geometry with the AMSU, MHS and AVHRR instruments providing auxiliary measurements to the IASI L2 processing.*

### 4.2.3 Static Auxiliary Atlases

The static auxiliary atlases described in this section are part of the data package which is installed directly on the IASI L2 PPF nodes.

#### *4.2.3.1 Digital Elevation Model*

The digital elevation model consists of a single file `GlobalGtopo2.DEM` which has been compiled from the tile files constituting the GTOPO30 global digital elevation model. This is fully detailed in GTOPO The file is composed by 58320000 16-bit binary signed little-endian integers. These integers correspond to altitudes on a regular latitude/longitude grid with 30 by 30 grid points per 1 degree by 1 degree box. The GTOPO30 has a resolution of 120 pixels per degree in longitude and 120 pixels in latitude. An average of four by four grid points has been used for the lower resolution `GlobalGtopo2.DEM` file. The altitudes are stored from north to south and from west to east, with longitude varying the fastest, such that the position $p$ in the file of a point at longitude $\lambda$ (from –180 to 180) and latitude $\phi$ (from –90 to 90) is given by this expression:

$$p = 10800 * [30 * (90 - \phi)] + [30 * (180 + \lambda)] \qquad \textit{Equation 3}$$

where:

| | |
|---|---|
| [ ] | denotes rounding to nearest integer ( [12.3] = 12 and [12.9] = 13). |

#### *4.2.3.2 Land/Sea mask*

The land sea mask consists of a single file `clo.10.00.prd` which contains a land/sea mask and coastline mask. Both masks are stored as quad trees based on the principle of recursive decomposition of space with a latitude/longitude resolution of 0.01 degree. For a given geo-location, the value of both masks is looked up. This results in one of four possibilities:

0) Sea and not coast,
1) Land and not coast,
2) Coastline and sea,
3) Coastline and land.

For the computation of the land fraction within a IASI IFOV any coastline is considered as being land. Only the value 0 is considered as being sea. The detailed description of the data organisation and access is provided in [LSM].

#### *4.2.3.3 Land surface emissivity atlas*

The land surface emissivity atlas consists of 12 files, one for each month of the year structured as follows `UWirbfemis _V2.1_0.1deg_2007??_mask_nc4.nc`, These files come from the UW/CIMSS Global IR Land Surface Emissivity Database as part of RTTOV. They have been converted to netcdf-4 so they are readable with the hdf-5 software library. For a given month of the year, the corresponding file holds the emissivity at ten wave numbers at a latitude/longitude resolution of 0.1 degree. To save space, the file only includes `2250931` grid points with emissivity values, in the NCDF fields `/emis1../emis10`. A separate table `/emis_flag` is used to look up any geo-location. The result of this look-up is a flag indicating whether an emissivity is available for that grid point. From this flag, the index number in the emissivity dataset can be derived. Usually, emissivities are not available because the location is over sea. The ten emissivity values are transformed to an emissivity spectrum at IASI channel wave number resolution as follows:

1) Transform the 10 emissivities, $E_j$, to 6 PC scores $s$,

$$s_i = \sum_{j=1}^{10} D_{ij}\left(E_j - \bar{E}_j\right); i = 1..6 \qquad \textit{Equation 4}$$

2) Transform the 6 PC scores to emissivity spectra on $N_k$ configurable wavenumbers $\nu_k^{UW}$.

$$e_k = \bar{e}_k + \sum_{i=1}^{6} P_{ki} s_i \,; k = 1..N_k \qquad \textit{Equation 5}$$

3) Interpolate linearly (as defined in Section 6.5) the emissivity spectra $e_k$ defined at the 417 wavenumber $\nu_k^{UW}$ to the wavenumbers of the IASI channels defined in Equation 1.

The eigenvectors $\boldsymbol{P}$ are stored in the file `UWiremis_labeigvects_nc4.nc` in the table `/PC_scores` and the coefficients $D$, $\bar{E}$ and $\bar{e}$ are configurable.

### 4.2.4 Dynamic Auxiliary Data

#### *4.2.4.1 NWP forecast*

The NWP fields of temperature, humidity, ozone, surface temperature and surface pressure provided by ECMWF are input to the IASI L2 processing. They give initial description of the atmospheric and surface state which can be used for cloud detection and as alternative or complementary inputs to some of the retrieval functions of the IASI L2 processing chain.

The data come in the GRIB format and are read with the GRIB API maintained and released by ECMWF. See [*GRIBAPI*] for specifications on the GRIB API. The vertical profiles are stored on a $N_{lev}$ level grid, where the pressures at each level depend on the actual pressure at the surface. The pressure $p_k$ at level k is computed as follows:

$$p_k = \frac{A_{k-\frac{1}{2}} + A_{k+\frac{1}{2}}}{2} + P_S . \frac{B_{k-\frac{1}{2}} + B_{k+\frac{1}{2}}}{2}; 1 \leq k \leq N_{lev}$$

*Equation 6*

where:

| | |
|---|---|
| $N_{lev}$ | is the number of levels of the profiles |
| $A_n$ | are coefficients defined at half-levels |
| $B_n$ | are coefficients defined at half-levels |
| $N_{lev}$, $A_n$ and $B_n$ | are stored in the header of each GRIB file |

# 5 PROCESSING SEQUENCE SPECIFICATIONS

## 5.1 Input Data Preparation

The purpose of the input data preparation is to gather IASI L1C measurements and relevant collocated data in a common `IASI_PRP` file, which serves as input for the further processing. The format of the IASI_PRP files is HDF5 and the IASI L1C spectra are represented as PC scores in order to limit their size and noise filter the radiances. The collocated data includes AVHRR cluster radiance mean and standard deviations (already included in the IASI L1C files), AMSU and MHS radiances, ECMWF forecast data as well as land fraction and surface elevation mean and standard deviation within each IASI field of view. The IASI principal component compression products IASI_PCS and IASI_PCR are also generated as part of the input data preparation.

The datasets which are copied or derived directly from the input IASI L1C file are found in the HDF5 group /L1C. The collocated data are organised in four additional HDF5 groups:

- `/Maps`,
- `/Amsu`,
- `/Mhs`
- `/Nwp`

according to the origin of the data. Table 11 below provides an initial overview of the contents of the `IASI_PRP` files, further details are provided in subsections that follow the table.

| ID | Data Type | DIM 1 | DIM 2 | DIM 3 | DIM 4 | Units | Description |
|---|---|---|---|---|---|---|---|
| **/L1C/** | | | | | | | |
| CloudFraction | uint8 | LINE | PIX | | | % | Cloud fraction in IASI FOV from AVHRR 1B in IASI FOV (from GEUMAvhrr1BCldFrac) |
| EUMQflag | uint8 | LINE | PIX | | | | Quality indicator. If the quality is good, it gives the coverage of snow / ice (from GEUMAvhrr1BQual) |
| EarthSatDistance | uint32 | LINE | | | | | Distance of satellite from Earth center |
| FLG_SATMAN | uint8 | LINE | | | | | Satellite manoeuvre flag (0 = normal, 1 = manoeuvre) |
| InstrumentMode | uint8 | LINE | | | | | 161=normal |
| LandFraction | uint8 | LINE | PIX | | | % | Land and coast fraction in IASI FOV from AVHRR 1B (from GEUMAvhrr1BLandFrac) |
| Latitude | float | LINE | PIX | | | degrees_north | Latitude of IFOV |
| LineNumber | int32 | LINE | | | | | Scanline number in file |
| Longitude | float | LINE | PIX | | | degrees_east | Longitude of centre of IFOV |
| QFlag | uint8 | LINE | PIX | | | | Quality flag.<br>Bit1: Band 1 L1C, Bit2: Band 2 L1C, Bit3: Band 3 L1C,<br>Bit4: Band 1 PCC, Bit5: Band 2 PCC, Bit6: Band 3 PCC |
| SatAzimuth | float | LINE | PIX | | | degrees | Satellite azimuth angle |
| SatZenith | float | LINE | PIX | | | degrees | Satellite zenith angle |
| SensingEndTime_day | uint16 | LINE | | | | days | UTC-based scanline stop time. Days since 1 January 2000 |
| SensingEndTime_msec | uint32 | LINE | | | | msec | UTC-based scanline stop time. Milliseconds in day |
| SensingTime_day | uint16 | LINE | | | | days | UTC-based scanline start time. Days since 1 January 2000 |
| SensingTime_msec | uint32 | LINE | | | | msec | UTC-based scanline start time. Milliseconds in day |
| SunAzimuth | float | LINE | PIX | | | degrees | Sun azimuth angle |
| SunZenith | float | LINE | PIX | | | degrees | Sun zenith angle |

| *ID* | *Data Type* | *DIM 1* | *DIM 2* | *DIM 3* | *DIM 4* | *Units* | *Description* |
|---|---|---|---|---|---|---|---|
| **/L1C/Avhrr/** | | | | | | | |
| RadAnalMean | float | LINE | PIX | CLUSTER | AVH_CH | W/(m² × sr) and W/(m² × m$^{-1}$) | Mean AVHRR radiance within the three main radiance analysis clusters |
| RadAnalStd | float | LINE | PIX | CLUSTER | AVH_CH | W/(m² × sr) and W/(m² × sr · m$^{-1}$) | Standard deviation of AVHRR radiance within the three main radiance analysis clusters |
| RadAnalWgt | float | LINE | PIX | CLUSTER | | | Fraction of IASI FOV covered by main AVHRR radiance analysis clusters |
| T4_mean | float | LINE | PIX | | | W/(m² × sr × m$^{-1}$) | Overall mean value of AVHRR channel 4 |
| T4_std | float | LINE | PIX | | | W/(m² · × sr × m$^{-1}$) | Standard deviation of AVHRR channel 4 |
| T5_mean | float | LINE | PIX | | | W/(m² × sr × m$^{-1}$) | Overall mean value of AVHRR channel 5 |
| T5_std | float | LINE | PIX | | | W/(m² × sr × m$^{-1}$) | Standard deviation of AVHRR channel 5 |
| **/L1C/PCscores/** | | | | | | | |
| Band1/P1 | int32 | LINE | PIX | B1P1 | | | Band 1 PCScores coded with 4 bytes |
| Band1/P2 | int16 | LINE | PIX | B1P2 | | | Band 1 PCScores coded with 2 bytes |
| Band1/P3 | int8 | LINE | PIX | B1P3 | | | Band 1 PCScores coded with 1 byte |
| Band2/P1 | int32 | LINE | PIX | B2P1 | | | Band 2 PCScores coded with 4 bytes |
| Band2/P2 | int16 | LINE | PIX | B2P2 | | | Band 2 PCScores coded with 2 bytes |
| Band2/P3 | int8 | LINE | PIX | B2P3 | | | Band 2 PCScores coded with 1 byte |
| Band3/P1 | int32 | LINE | PIX | B3P1 | | | Band 3 PCScores coded with 4 bytes |
| Band3/P2 | int16 | LINE | PIX | B3P2 | | | Band 3 PCScores coded with 2 bytes |
| Band3/P3 | int8 | LINE | PIX | B3P3 | | | Band 3 PCScores coded with 1 byte |
| RadianceSum | float | LINE | PIX | BND | | W/(m² × sr × m$^{-1}$) | Sum of reconstructed radiances in each band |
| ResidualRms | float | LINE | PIX | BND | | | Noise normalized residual RMS in each band |
| **/Maps/** | | | | | | | |
| Height | float | LINE | PIX | | | meter | Average Height (from GTOPO30) |
| HeightStd | float | LINE | PIX | | | meter | Standard deviation of height |
| LandFraction | uint8 | LINE | PIX | | | % | Map based land fraction (quad tree map) |

| *ID* | *Data Type* | *DIM 1* | *DIM 2* | *DIM 3* | *DIM 4* | *Units* | *Description* |
|---|---|---|---|---|---|---|---|
| **/Amsu/** | | | | | | | |
| Radiance | float | LINE | EFV | AMS_CH | | W/(m² × sr × m$^{-1}$) | AMSU Radiance |
| Latitude | float | LINE | EFV | | | degree | AMSU latitude |
| Longitude | float | LINE | EFV | | | degree | AMSU longitude |
| FLG_AMSUBAD | uint8 | LINE | EFV | | | | AMSU availability/quality flag |
| **/Mhs/** | | | | | | | |
| Radiance | float | LINE | PIX | MHS_CH | | W/(m² × sr × m$^{-1}$) | MHS radiance co-located to IASI IFOV |
| FLG_MHSBAD | uint8 | LINE | PIX | | | | MHS availability/quality flag |
| **/Nwp/** | | | | | | | |
| Latitude | int16 | GRID | | | | degrees_north | Latitude of NWP grid point (scaling factor = 0.5) |
| Longitude | int16 | GRID | | | | degrees_east | Longitude of NWP grid point (scaling factor = 0.5) |
| O | float | GRID | LEV | | | kg/kg | Ozone volume mixing ratio |
| Sp | float | GRID | | | | hPa | Surface pressure |
| T | float | GRID | LEV | | | K | Air temperature |
| Ta | float | GRID | | | | K | Air temperature (2m) |
| Ts | float | GRID | | | | K | Surface temperature |
| U | float | GRID | | | | m/s | Windspeed (zonal) |
| V | float | GRID | | | | m/s | Windspeed (meridional) |
| W | float | GRID | LEV | | | kg/kg | Water vapour volume mixing ratio |
| Wa | float | GRID | | | | K | Dew point temperature (2m) |
| Index | uint16 | LINE | PIX | DLO | DLA | | Index to match grid points to IFOVs |
| PV_a | double | LEV+1 | | | | Pa | ECMWF model level definitions, vector A of Equation 6. |
| PV_b | double | LEV+1 | | | | | ECMWF model level definitions, vector B of Equation 6. |

*Table 11: Structure and content of the PRP files.*

As can be seen in the table, most of the data are organised according to IASI scan line (LINE) and pixel number (PIX). The collocated ECMWF forecast data are a major exception, here the fields are kept at the original ECMWF grid points, but only grid points surrounding IASI IFOVs are retained. The data set `/Nwp/index` indentifies the four surrounding grid points of each IASI IFOV. See Section 5.1.5 for further details of the collocation. Furthermore, the AMSU measurements are kept at their original resolution with 30 fields of view per scan line. See Section 5.1.8 for further details of this collocation.

The dimensions used in the table above are summarised in Table 12. The values are configurable and given as indication of the implementation in version 6.0. For example, both the total number of PC scores in each band and the number of these that are stored with 4 bytes, 2 bytes, and 1 byte is configurable and could change in future versions.

| *ID* | *Value* | *Description* |
|---|---|---|
| LINE | variable | IASI scan lines |
| PIX | 120 | IASI IFOV number within scan line |
| CLUSTER | 3 | AVHRR cluster (3 main clusters) |
| AVH_CH | 6 | AVHRR channel number |
| B1P1 | 1 | Band 1 PC score, stored with 4 bytes |
| B1P2 | 41 | Band 1 PC score, stored with 2 bytes |
| B1P3 | 48 | Band 1 PC score, stored with 1 bytes |
| B2P1 | 2 | Band 2 PC score, stored with 4 bytes |
| B2P2 | 61 | Band 2 PC score, stored with 2 bytes |
| B2P3 | 57 | Band 2 PC score, stored with 1 bytes |
| B3P1 | 1 | Band 3 PC score, stored with 4 bytes |
| B3P2 | 44 | Band 3 PC score, stored with 2 bytes |
| B3P3 | 45 | Band 3 PC score, stored with 1 bytes |
| AMS_CH | 15 | AMSU channel number |
| MHS_CH | 5 | MHS channel number |
| GRID | variable | ECMWF grid point |
| LEV | 137 | ECMWF model “full” level. The current ECMWF model uses 137 levels; but this can change. |
| DLO | 2 | Longitude direction of 4 surrounding ECMWF grid points |
| DLA | 2 | Latitude direction of 4 surrounding ECMWF grid points |

*Table 12: Configurable parameters and dimensions of the data stored in the PRP files.*

### 5.1.1 IASI L1C Principal Components Compression

Two output products are generated by the IASI L1C Principal Component Compression (PCC) function, namely the product types PCS (Principal Component Scores) and PCR (Principal Component Residuals) respectively. In both Instances, the `INSTRUMENT_ID = IASI` and `PROCESSING_LEVEL = 1C`.

1. ***Product type PCS***: This product contains a copy of a subset of the MDR fields identified in the L1 PCS product format specification [PCCPFS]:
   - geolocation,
   - L1C quality flags,
   - satellite
   - sun angles

   These are taken from the input IASI_xxx_1C product as well as the PC scores from which noise-reduced radiances can be reconstructed.
2. ***Product type PCR***: This product contains the noise-normalised difference between the original radiances in the IASI_xxx_1C product and the noise-reduced radiances reconstructed from the IASI_PCS_1C product. The format is specified in this document [PCCPFS].

The principal component scores as well as the radiance sum and residual RMS in each IASI band are also written to the IASI_PRP file. The purpose of the IASI L1C PCC is to apply Principal Component Compression (PCC) to IASI L1C radiance spectra. PCC works by representing multidimensional data, like IASI spectra, in a lower dimensional space, which accounts for most of the variance seen in the data. This space is spanned by a truncated set of the eigenvectors of the data covariance matrix. By noise-normalising the spectra prior to the application of the compression technique, the ability to fit the data is enhanced by avoiding giving too much weight to variance caused by noise.

The PCC is applied individually to each of the three IASI spectral bands.

One eigenvector file for each of the spectral bands is needed for the application of the PCC. The file names of the eigenvector files used for the compression are included in the PCS (and PCR) products— the same files must be used to reconstruct noise-reduced radiances from the PC scores. The eigenvector files are static auxiliary data files are as follows:

- `IASI_EV1`
- `IASI_EV2`
- `IASI_EV3`

The format of the eigenvector files is specified in Section 5.1 and the reconstruction steps are shown in Section 5.8.4. The sequence of operations for compression and encoding the PCS and PCR products is described in Section 5.1.1.1 to Section 5.1.1.6. Besides the eigenvectors, a number of parameters configure these algorithms; these are detailed in the XML configuration file described in Section 8.4.

#### *5.1.1.1 Decoding of Level 1C spectra*

Before compression, the L1C radiances shall be decoded using the information provided in the IASI `GIADR-SCALEFACTORS` record [IASIL1PFS].

```
Input sets:
P  = [0 .. IDefScaleSondNbScale [
K  = [1 .. 8461]
KP(K,P) = [IdefScaleSondNsFirst(P) - IdefNsfirst ..
           IdefScaleSondNsLast(P)  - IdefNsfirst] * P

Input data:
GS1cSpect(K) (mixed units)     // from IASI L1C MDR
IdefSondScaleFactor(P)         // from IASI GIADR-SCALEFACTORS

Output:
R(K)   (unit: W/m2/sr/m-1)

Algorithm:
R(K) = sum(KP(K,P), GS1cSpect(K)*pow(10, -IdefSondScaleFactor(P)
```

*Figure 7: Pseudo code I. (decoding of radiances).*

#### *5.1.1.2 Computation of PC Scores*

`NBSxP1 + NBSxP2 + NBSxP3` PC scores shall be computed for band x, corresponding to the `NBSxP1 + NBSxP2 + NBSxP3` first eigenvectors in band x as shown in the pseudo code in Figure 8. NBSxP1, 2, 3 refer to the number of scores to be encoded in 4, 2 and 1 bytes, respectively. See also Table 12 and Section 5.1.1.3.

```
Input sets:
K  = [FirstChannel .. FirstChannel+NbrChannels [
P  = [1 .. NBSxP1 + NBSxP2 + NBSxP3]

Input data:
R(K) [unit: W/m2/sr/m-1]           // decoded radiance as per section
5.2
Noise(K) [unit: W/m2/sr/m-1]       // from eigenvector file
Eigenvectors(K,P)                  // from eigenvector file

Output:
PcScoresBx(P)                      // PC scores in band x

Algorithm:
PcScoresBx(P) = sum(K, (R(K)/Noise(K) - Mean(K))*Eigenvectors(K,P))
```

*Figure 8: Pseudo code II (compression of radiances in band x) .*

#### *5.1.1.3 PFS Encoding of PC Scores*

Before the PC scores enter the product they must be quantised; they must be divided by the quantisation factor and rounded to the nearest integer.

Within each band, three different types are used for encoding the PC scores in the IASI_PCS_1C product:

- signed 4-byte Integer,
- signed 2-byte Integer
- signed byte

This is because the range of the PC scores decreases rapidly with PC rank and therefore a higher number of bytes are required to encode the leading PC scores than the subsequent PC scores.

If a quantised PC score falls outside the range of its type, the *undefined* value as specified in GPFS] shall be used for this particular score as well as for the corresponding `ResidualRMS`. Furthermore, this event will be flagged in the `DEGRADED_PROC_MDR` field. See the pseudo code in Figure 9.

***Note***: It is expected that the number of fields of each type will be configured such that this will not happen.

```
Input sets:
P1 = [1 .. NBSxP1]
P2 = [NBSxP1 + 1 .. NBSxP1 + NBSxP2]
P3 = [NBSxP1 + NBSxP2 + 1 .. NBSxP1 + NBSxP2 + NBSxP3]
P  = [1 .. NBSxP1 + NBSxP2 + NBSxP3]

Input data:
PcScoresBx(P)                        // output from pseudo-code II
SQ = ScoreQuantisationFactor(x)      // from config file

Output:
PcScoresBxP1(P1)                      // for MDR-PCS
PcScoresBxP2(P2)                      // for MDR-PCS
PcScoresBxP3(P3)                      // for MDR-PCS

Algorithm:
PcScoresBxP1(P1) = round(PcScoresBx(P1)/SQ)
PcScoresBxP2(P2) = round(PcScoresBx(P2)/SQ)
PcScoresBxP3(P3) = round(PcScoresBx(P3)/SQ)
```

*Figure 9: Pseudo code III (encoding of PC scores in band x).*

#### *5.1.1.4 Residual and Residual RMS*

The residual is computed as the noise-normalised difference between the decoded L1C radiances and the reconstructed radiances based on the quantised PC scores as shown in the pseudo code in Figure 10. If the compression failed in a band—this is indicated by having a quantised PC score falling outside the range of its type—the residual in the band shall be set to zero and the `ResidualRMS` to *undefined* value specified in GPFS].

```
Input sets:
K  = [FirstChannel .. FirstChannel+NbrChannels[
P1 = [1 .. NBSxP1]
P2 = [NBSxP1 + 1 .. NBSxP1 + NBSxP2]
P3 = [NBSxP1 + NBSxP2 + 1 .. NBSxP1 + NBSxP2 + NBSxP3]
P  = [1 .. NBSxP1 + NBSxP2 + NBSxP3]

Input data:
R(K) [unit: W/m2/sr/m-1]           // decoded radiance as per section 5.2
Noise(K) [unit: W/m2/sr/m-1]       // from eigenvector file
Mean(K)                            // from eigenvector file
PcScoresBxP1(P1)                   // from MDR-PCS
PcScoresBxP2(P2)                   // from MDR-PCS
PcScoresBxP3(P3)                   // from MDR-PCS
Eigenvectors(K,P)                  // from eigenvector file
SQ = ScoreQuantisationFactor(x)    // from config file

Output:
Residual(K)     // noise normalised residual before quantisation
ResidualRMS     // ResidualRMS in band x

Algorithm:
Residual(K) = R(K)/Noise(K) -
               ( Mean(K)
                 + SQ*sum(P1, PcScoresBxP1(P1)*Eigenvectors(K,P1))
                 + SQ*sum(P2, PcScoresBxP2(P2)*Eigenvectors(K,P2))
                 + SQ*sum(P3, PcScoresBxP3(P3)*Eigenvectors(K,P2)) )
ResidualRMS = sqrt(sum(K, Residual(K)*Residual(K))/NbrChannels)
```

*Figure 10: Pseudo code IV (Residual and ResidualRMS in band x)*

#### *5.1.1.5 Detection of outlier spectra*

For detection of outliers, the residual RMS is adjusted by subtracting the sum of all individual radiances multiplied by a configurable scalar, `outlierSlope`. The result is compared to a pixel - (detector) dependent threshold as detailed in the pseudo-code in Figure 11.

***Note:*** A spectrum is considered an outlier if `isOutlier` is true for at least one of the three IASI bands.

```
Input sets:
K  = [FirstChannel .. FirstChannel+NbrChannels [
Detector  = [1 .. 4]

Input data:
R(K) [unit: W/m2/sr/m-1]          // decoded radiance as per section
5.2
ResidualRMS                        // ResidualRMS in band x
OutlierThreshold(Detector)         // Detector dependent threshold
value
                                   // from config file
OutlierSlope                       // Slope from config file
D                                  // Pixel number

Output:
isOutlier                          // Boolean indicator of outlier
spectra

Algorithm:
isOutlier = (ResidualRMS - OutlierSlope*sum(K, R(K))) > OutlierThreshold(D)
```

*Figure 11: Pseudo-code V (detection of outlier spectra, band x).*

#### *5.1.1.6 PFS Encoding of PC Residuals*

Before the PC residuals enter the PCR product they must be quantised. Quantised means divided by the quantisation factor and rounded to the nearest integer.

If a quantised residual falls outside the range of its type (–127 to 127), it shall be set to the *undefined* value defined in document GPFS].

```
Input sets:
K = [1 .. 8461]

Input data:
Residual(K)                          // output from pseudo-code IV
RQ = ResidualQuantisationFactor(x)   // from config file

Output:
PccResidual(K)                       // for MDR-PCR

Algorithm:
PccResidual(K) = round(Residual(K)/RQ)
```

*Figure 12: Pseudo code VI (encoding of PC residuals).*

### 5.1.2 Acceptance and collocation of AVHRR scenes analysis

As part of the IASI level 1 processing, the AVHRR pixels within each IASI field of view are identified and divided in up to seven distinct clusters IASIL1spe. For each of these clusters, the standard deviation and mean of the radiances of each AVHRR channel is provided in the IASI L1C files together with the fractional coverage and centre of gravity.

The flag **FLG_AVHRRBAD** indicates whether the AVHRR radiance analyses is available and reflects the quality and readiness of collocated AVHRR radiances for processing:

- It is set to 1 if the IASI L1C flag $GEUMAvhrr1BQual\ bit\ 8$ is on.
- It is set to 2 if no radiance clusters have been analysed.

***Note***: In IASI L1C product, $GCcsRadAnalNbClass\ = 0$) **FLG_AVHRRBAD** is otherwise set to 0, reflecting the availability of good AVHRR information which is the condition for further use in subsequent functions of the IASI L2 processor.

For the PRP files, the clusters are sorted in order of decreasing fractional coverage and only the first three clusters are kept.

For the two infrared AVHRR channels 4 and 5, the overall radiance mean and standard deviation within each IASI IFOV is computed from the individual cluster mean and standard deviations as well as their fractional coverage. For each of the channels, let $W_i$, $M_i$ and $S_i$ be the fractional coverage, mean and standard deviation radiance in cluster $i$ (i = 1..7). The corresponding IASI IFOV mean radiance MI is computed as follows:

$$MI = \sum_{i=1..7} W_i M_i$$ *Equation 7*

and the corresponding IASI IFOV radiance standard deviation SI is computed as follows:

$$SI = \sqrt{\sum_{i=1..7} W_i(S_i^2 + (M_i - MI)^2)}$$ *Equation 8*

### 5.1.3 Topography information within the IFOV

In each IASI IFOV, the PSF-weighted mean $\bar{z}$ and the standard deviation $\sigma_z$ of the surface altitude within the footprint is computed after Equation 9 then Equation 10. The footprint is represented by a grid of variable dimensions $N_Y$ and $N_Z$. A grid cell (i;j), $i = 1..N_Y$ and $j = 1..N_Z$, is associated to the value of the point spread function $\Psi_{i,j}$. The computation of the geolocation of each PSF grid cell is detailed in Section 6.2. The height of each of these grid cells, $z_{i,j}$, is looked up in the Gtopo30 database.

$$\bar{z} = \frac{\sum_{j=1}^{N_Z}\sum_{i=1}^{N_Y}\Psi_{i,j}\cdot z_{i,j}}{\sum_{j=1}^{N_Z}\sum_{i=1}^{N_Y}\Psi_{i,j}}$$ *Equation 9*

$$\sigma_z = \sqrt{\frac{\sum_{j=1}^{N_Z}\sum_{i=1}^{N_Y}\Psi_{i,j}\,.\,(z_{i,j}-\bar{z}_p)^2}{\sum_{j=1}^{N_Z}\sum_{i=1}^{N_Y}\Psi_{i,j}}}$$

*Equation 10*

It is expected that the PSF is normalised and hence that this equation is true:

$$\sum_{j=1}^{N_Z}\sum_{i=1}^{N_Y}\Psi_{i,j} = 1.$$

This can be computed once for all when processing a product file.

### 5.1.4 Land-sea mask within the IFOV

The PSF-weighted fractional land coverage within each IASI IFOV $\bar{\Lambda}$ is computed by looking up the land/sea mask $\lambda_{i,j}$ for each PSF grid cell (i;j) whose geolocation is detailed in Section 6.2. The land/sea mask database is organised as a quad tree and distinguishes between land, sea and coast See [LSM . In this context, we treat coast as land and weight their contribution to the fractional land coverage by the PSF value $\Psi_{i,j}$.

$$\bar{\Lambda} = \frac{\sum_{j=1}^{N_Z}\sum_{i=1}^{N_Y}\Psi_{i,j}\,.\,\lambda_{i,j}}{\sum_{j=1}^{N_Z}\sum_{i=1}^{N_Y}\Psi_{i,j}}$$

$$\lambda_{i,j} = \begin{cases} 1\ if\ land \\ 1\ if\ coast \\ 0\ is\ ocean \end{cases}$$

*Equation 11*

The PSF should be normalised; therefore it is in denominator in Equation 11.

$\sum_{j=1}^{N_Z}\sum_{i=1}^{N_Y}\Psi_{i,j} = 1$ is true.

This can be computed one time for all values when processing a product file.

### 5.1.5 Acceptance of IASI L1C data

The quality indicator ***GQisFlagQual*** in the IASI L1c products shall be inspected.

**Procedure:**

| *Condition...* | *action* |
|---|---|
| bad measurements are reported | the processing flag **FLG_IASIBAD** is set to 1 and no processing is performed. |
| the IASI L1C flag ***GQisFlagQual*** indicates good measurements but:<br>• Latitude is outside [90°S ; 90°N] or longitude is outside [180°W ; 180°E]<br>• The satellite zenith angle is outside [0° ; 60°]<br>• The reconstruction score exceeds a configurable threshold. (See `ResidualRMS` in Section 5.1.1.4.) | the flag **FLG_IASIBAD** is set to 2. |
| If the satellite is undergoing a manoeuvre as indicated in IASI L1C flags | no processing can take place this is reflected in the L2 flag **FLG_SATMAN** |

### 5.1.6 Acceptance and Collocation of AMSU L1B

The AMSU Instrument is synchronised with IASI and the collocation is based simply on the sensing time of the two measurements. An AMSU line is collocated with a IASI line if the absolute difference between the record start times of the two measurement scan lines is less than two seconds. One AMSU FOV is used for the four IASI IFOVs it covers, so IASI pixel, *p*, is paired with AMSU pixel, *p div 4*. This is illustrated in Figure 6.

The status and availability of collocated AMSU measurements to each IASI pixel are recorded in the flag **FLG_AMSUBAD**.

## Procedure:

| *Condition...* | *action* |
|---|---|
| no corresponding AMSU measurement is available | **FLG_AMSUBAD** is set to 2. |
| if any of the radiances are outside of the valid interval defined for each channel in Table 13. Only channels with value one the static auxiliary dataset COF_MWCHAN are considered for this test. | **FLG_AMSUBAD** is set to 1. |
| collocated AMSU measurements are only used for further processing if available and of good quality | **FLG_AMSUBAD** is set to 0. |

| *Channel* | *1* | *2* | *3* | *4* | *5* | *6* | *7* |
|---|---|---|---|---|---|---|---|
| Minimum | 0.0005 | 0.0008 | 0.0033 | 0.0044 | 0.0049 | 0.0052 | 0.0052 |
| Maximum | 0.0018 | 0.0032 | 0.0075 | 0.0077 | 0.0074 | 0.0070 | 0.0068 |
| *8* | *9* | *10* | *11* | *12* | *13* | *14* | *15* |
| 0.0051 | 0.0052 | 0.0052 | 0.0053 | 0.0054 | 0.0057 | 0.0060 | 0.0081 |
| 0.0069 | 0.0075 | 0.0076 | 0.0080 | 0.0083 | 0.0086 | 0.0089 | 0.0244 |

*Table 13: Valid intervals for AMSU radiances (W/(m² . sr . m-1) ).*

### 5.1.7 Acceptance and Collocation of MHS L1B

The MHS measurements are collocated with IASI by bilinear interpolation to the geo-location of centre of the IASI field of view. See specification in Section 6.8 The bilinear interpolation is performed in the coordinate system defined by MHS line and pixel numbers and the location of the IASI field of view within this coordinate system must be computed first. For this, the same method as was used to co-locate ATMS to CrIS is used. This method is described in Section 4 of [AAPP].

**Procedure:**

| *Step* | *Action* |
|---|---|
| 1 | Let P denote the point corresponding to the IASI IFOV centre for which we want to find the coordinates in the MHS grid. |
| 2 | Let O denote the point corresponding to the MHS FOV centre for which the scan time is closest to the IASI scan time and where the scan angle is closest to the IASI scan angle. |
| 3 | Let A and B be points corresponding to the MHS FOVs in the same scan position as O, but in the previous and next scan lines respectively. Let C and D be points corresponding to the MHS FOVs in the same scan line as O, but in the previous and next scan position respectively. |
| 4 | Convert all latitude/longitude values of relevant MHS and IASI geolocations to Cartesian X/Y/Z co-ordinates. See Section 6.12. Taking the point O as the origin, the coordinates of point P, in units of the MHS grid $(x, y)$ is given by Equation 12 and Equation 13: |

$$x = 2\frac{\left(\overrightarrow{OP} \times \overrightarrow{CD}\right) \cdot \left(\overrightarrow{AB} \times \overrightarrow{CD}\right)}{\left\|\overrightarrow{AB} \times \overrightarrow{CD}\right\|^2} \qquad \textit{Equation 12}$$

$$y = -2\frac{\left(\overrightarrow{OP} \times \overrightarrow{AB}\right) \cdot \left(\overrightarrow{AB} \times \overrightarrow{CD}\right)}{\left\|\overrightarrow{AB} \times \overrightarrow{CD}\right\|^2} \qquad \textit{Equation 13}$$

where:

| | |
|---|---|
| $\overrightarrow{OP}$ | is a vector in Cartesian coordinates |
| $\overrightarrow{AB}$ | is a vector in Cartesian coordinates |
| $\overrightarrow{CD}$ | is a vector in Cartesian coordinates |
| $\times$ | denotes vector product (See Section 6.11.1.) |
| dot $\cdot$ | denotes scalar product (See Section 6.11.) |
| $\|\|$ $\|\|$ | denotes Euclidean norm (See Section 6.10.) |

The status of collocated MHS data is recorded in the flag **FLG_MHSBAD**.

**Procedure:**

| *Condition...* | *action* |
|---|---|
| no collocated MHS data is available | **FLG_MHSBAD** is set to 2. |
| any of the four MHS pixels used for the interpolation has any radiance value outside of the valid interval for each channel as specified in Table 14, or if the measurements are of bad quality according to MHS L1B quality flags as formulated in Equation 14. | **FLG_MHSBAD** is set to 1. |
| MHS radiances are used for further processing when available and are of good quality in all four pixels surrounding the IASI IFOV | **FLG_MHSBAD** is set to 0. |

$$FLG\_MHSBAD = 1 \quad if \quad \begin{cases} MHS\ rad_i < t_{1,i}\ , & or \\ MHS\ rad_i > t_{2,i} \end{cases} \qquad \textit{Equation 14}$$

| *Channel* | *1* | *2* | *3* | *4* | *5* |
|---|---|---|---|---|---|
| Minimum | 0.0080 | 0.0218 | 0.0431 | 0.0364 | 0.0335 |
| Maximum | 0.0243 | 0.0762 | 0.0891 | 0.0928 | 0.1054 |

*Table 14: Valid intervals for MHS radiances (W/(m² . sr . m-1) ).*

### 5.1.8 Acceptance and Collocation of NWP forecasts

The NWP fields provided in the HDF5 group NWP in the PRP files originates from the ECMWF forecasts received operationally in the EPS ground segment. All NWP information is retained at the original horizontal and vertical grids used in the input GRIB files, but has been time-interpolated linearly from the two closest forecast times, which are available at three-hour intervals. See also Section 6.5.

For each IASI FOV, the indices of the four NWP grid points that surround it geographically are stored in `/Nwp/index`. This allows for easy bilinear interpolation of the NWP fields. The geo-location of the NWP grid points included in the PRP files are given in `/Nwp/Longitude` and `/Nwp/Latitude`. Currently, the forecasts are provided at 137 model levels, of which 91 levels are provided in the GRIB files received in the EPS ground segment. In the profile fields of `PRP` files, space is reserved for all forecast model levels and the value for the levels which are not received is set to zero.

## 5.2 Status flags setting

After the pre-processing step is completed, a number of status and processing flags need to be set. They will be used in the subsequent processing functions or stored in the final L2 products as additional information to the users.

### 5.2.1 FLG_AVHRRBAD

The flag **FLG_AVHRRBAD** indicates whether the AVHRR radiance analyses is available and reflects the quality and readiness of collocated AVHRR radiances for processing:

- It is set to 1 if the IASI L1C flag $GEUMAvhrr1BQual\ bit\ 8$ is on.
- It is set to 2 if no radiance clusters have been analysed.

***Note***: In IASI L1C product, $GCcsRadAnalNbClass = 0$. **FLG_AVHRRBAD** is otherwise set to 0, reflecting the availability of good AVHRR information which is the condition for further use in subsequent functions of the IASI L2 processor.

### 5.2.2 FLG_LANSEA

The flag **FLG_LANSEA** summarises the surface type from the topography values found in Equation 9 and Equation 10 and the land fraction (taken from Equation 11) information as follows:

| **FLG_LANSEA** | |
|---|---|
| ***Value*** | ***Reasons for setting*** |
| 0 | Land fraction $\overline{\Lambda} < \tau_W$ |
| 1 | Land fraction $\overline{\Lambda} > \tau_L$<br>Topography variability $\sigma_z < \tau_{DEM}$ |
| 2 | Land fraction $\overline{\Lambda} > \tau_L$<br>Topography variability $\sigma_z > \tau_{DEM}$ |
| 3 | Land fraction $\tau_W \leq \overline{\Lambda} \leq \tau_L$<br>Topography variability $\sigma_z < \tau_{DEM}$ |
| 4 | Land fraction $\tau_W \leq \overline{\Lambda} \leq \tau_L$<br>Topography variability $\sigma_z > \tau_{DEM}$ |

where:

| | |
|---|---|
| $\tau_W$ | is a configurable threshold |
| $\tau_L$ | is a configurable threshold |
| $\tau_{DEM}$ | is a configurable threshold |

### 5.2.3 FLG_NWPBAD

Values for this flag are outlined below.

| ***Condition...*** | ***action*** |
|---|---|
| good collocated NWP data is available | **FLG_NWPBAD** is set to 0. |

| | |
|---|---|
| the collocated NWP data contain some values exceeding predefined and configurable bounds | **FLG_NWPBAD** is set to 1. |
| no NWP data is available for collocation with the IASI IFOV | **FLG_NWPBAD** is set to 2. |

## 5.3 Characterisation of the illumination conditions

The configuration and quality of some retrieval algorithms described in the following sections varies with the solar illumination conditions, which must be flagged for processing within the IASI L2 PPF and for information to the users. The flag **FLG_DAYNIT** summarises if the scene is observed during daytime, twilight, or night-time based on the solar zenith angle $\hat{z}_{sun}$ read from IASI L1C files as follows:

$$\mathbf{FLG\_DAYNIT} = \begin{cases} 0 \; if \; \hat{z}_{sun} < \tau_{day} \\ 1 \; if \; \hat{z}_{sun} > \tau_{night} \\ 2 \; if \; \tau_{day} \leq \hat{z}_{sun} \leq \tau_{night} \end{cases} \qquad \textit{Equation 15}$$

where: $\tau_{day}$ and $\tau_{night}$ are configurable thresholds.

Under certain sensing configurations, the IASI observations are contaminated by the specular reflection of the solar radiations on high reflective surfaces like plain water. This affects channels in the band 3. Because this contribution is poorly represented in the forward model, channels containing Solar contributions should be avoided for retrievals and the presence of Sun Glint flagged in **FLG_SUNGLNT** for L2 processing and information to the users. A sun glint is detected if:

$$\mu_n \geq 0.9999 \qquad \textit{Equation 16}$$

Or if:

$$0.9 \leq \mu_n < 0.9999 \;\; \mathbf{AND} \;\; \frac{1}{4 \cos\theta \cos\theta_0 \left|\mu_n^2 - \mu_n^4\right|} \qquad \textit{Equation 17}$$

with:

$$\mu_n : \frac{\cos\theta + \cos\theta_0}{\sqrt{2(1+\cos\theta_r)}} \qquad \textit{Equation 18}$$

and:

$$\cos\theta_r = \sin\theta \,.\, \sin\theta_0 \,.\, \cos\varphi + \cos\theta \,.\, \cos\theta_0 \qquad \textit{Equation 19}$$

where:

| | |
|---|---|
| $\theta$ | is the satellite zenith angle (positive). |
| $\theta_0$ | is the Solar zenith angle (positive). |
| $\varphi = \lvert\varphi_{sat} - \varphi_{sun}\rvert$ | is the relative satellite-solar azimuth angle. Positive between 0 and 180°. |

## 5.4 All-sky statistical geophysical state estimate

### 5.4.1 Piece-wise linear retrieval principle

Piece-wise Linear Regression (PWLR) is a fast, statistical all-sky retrieval scheme, which has been developed for version 6 of EUMETSAT's operational IASI L2 processor. The retrieval uses IASI as well as co-located AMSU and MHS radiances as inputs and serves two purposes in the IASI L2 processing:

- to provide a high quality all-sky temperature and water vapour profile product
- to provide a-priori information used in the clear sky optimal estimation retrievals.

The retrieval is based on linear regression, but to capture non-linear relationships between the inputs and the outputs better, the input space is divided into several intervals. For each of these intervals, a separate set of linear regression coefficients is computed from the corresponding subset of the training set. Overall, a piecewise linear function from the input space into the output space is obtained. The piecewise linear regression retrieval errors are substantially smaller than the corresponding retrieval errors from linear regression. When MHS or AMSU data (or both) are not available, a IASI-only version of the PWLR is used. The origin of the measurements used in this first guess retrieval shall be reflected in the processing flag **FLG_INITIA** by setting its bits according to the availability and use of the respective measurements.

A further improvement of the scheme called PWLR[3], which exploits horizontal correlation by using measurements from all four IFOVs within each EFOV as predictors, has been developed for version 6.2 and is described in this section.

### 5.4.2 Retrieved parameters

The retrieved parameters consist of the following parameters:

- surface pressure
- surface air temperature
- surface air dew point temperature
- surface skin temperature and emissivity
- atmospheric profiles of temperature, humidity and ozone

For the regression step, we have chosen to keep the profiles at the 137 (surface pressure dependent) model levels found in the ECMWF analysis files forming the training base. The water-vapour mixing ratios at each profile level, $w$, have been converted to dew point temperature as we expect to find a better linear relationship with the predictors using this unit. See Section 6.13. Also, the ozone profile mixing ratios have been converted to “dew point temperature” using the same formula as for water-vapour. The retrieved surface pressure is used to assign pressures to the model levels such that the profiles can be interpolated to a fixed pressure grid after the regression retrieval on model levels. Each regression retrieves the atmospheric state and associated quality indicators (estimates of absolute errors) in four adjacent IFOVs, represented by 186 values as specified in Table 15:

| *Values* | *Specification* |
|---|---|
| 4 | The surface pressure in each of the four IFOVs |
| 4 | The surface air temperature in each of the four IFOVs |
| 4 | The surface air dew point temperature in each of the four IFOVs |
| 4 | The surface skin temperature in each of the four IFOVs |

| *Values* | *Specification* |
|---|---|
| 4 | The cloud signal 'OmC' (observation minus clear forward model calculation brightness temperature) in each of the four IFOVs. [currently not output in the global products, used in the L2Pcore SST products] |
| 100 | Temperature and water vapour profiles on model levels for all four IFOVs represented as PC scores |
| 20 | Ozone profiles on model levels for all four IFOVs represented as PC scores |
| 20 | Emissivity at 10 wavelengths for all four IFOVs represented as PC scores |
| 4 | Surface pressure quality indicator in each of the four IFOVs |
| 4 | (Surface air) Temperature quality indicator in each of the four IFOVs |
| 4 | (Surface air) Humidity (dewpoint temperature) quality indicator in each of the four IFOVs |
| 4 | Surface skin temperature quality indicator in each of the four IFOVs |
| 4 | - currently not used - |
| 1 | Ozone quality indicator (one for all four IFOVs) |
| 1 | Emissivity quality indicator (one for all four IFOVs) |

*Table 15: PWLR³ output vector*

### 5.4.3 Regression predictors

Surface height, microwave radiances and infrared radiances constitute the predictors. The surface heights are represented as four values, $e^{-z_i/7000}$, where $z_i$ is the surface height in meters of each of the four IFOVs.

The microwave radiances are represented as 26 PC scores computed from the 15 AMSU radiance collocated with the current EFOV followed by the 5 collocated MHS radiances for each of the four IFOVs with the EFOV (in order $IFOV_1$, $IFOV_2$, $IFOV_3$, $IFOV_4$).
The microwave PC scores $p_j^{mw};\ j = 1..26$ are computed using the formula:

$$p_j^{mw} = \sum_{i=1}^{35} E_{ji}(X_i - xmean_i)/xstd_i \qquad \textit{Equation 20}$$

where the coefficients $E$, $xmean$ and $xstd$ are provided in the dataset `EV_MW4` [8.2.13] and $X$ is the vector of the 35 input radiances are detailed above.

The infrared radiances are represented as 200 PC scores computed from the 1200 (= 4*(90+120+90)) PC scores representing the IASI measurements in each of the four IFOVs within the EFOV (see section 5.1.1). In this case no normalisation is used such that the formula to compute the overall PC scores gets particularly simple:

$$p_j^{ir} = \sum_{i=1}^{1200} E_{ji}X_i \qquad \textit{Equation 21}$$

The eigenvectors $E$ are provided in the dataset `COF_EV4IR` [8.2.17] and $X$ is the vector of the input PC scores for the four IFVOs (in order $IFOV_1$, $IFOV_2$, $IFOV_3$, $IFOV_4$). For each IFOV the order of the PC scores is Band1, Band 2, Band3. In the case that one or more of the IASI IFOVs is flagged as bad, a special set of eigenvectors (essentially excluding the bad IFOVs) must be used. A total of 15 different sets of eigenvectors are provided in `COF_EV4IR`, the one which should be used depends on which IFOV numbers within the EFOV are flagged as bad. If we define $I_i\ ;\ i = 1,\ldots,4$ to be 0 if IFOV number $i$ is good and 1 if it is bad, the expression $I_1 + 2.I_2 + 4.I_3 + 8.I_4$ determines the index

of the set of eigenvectors to use. So if all IFOVs are good the first (index 0) set will be used. If all IFOVs are bad, no retrieval is possible and no set of eigenvectors is provided for index 15.

In total, this gives a vector of 230 (4 elevations + 26 PCs μ-wave + 200 PCs IASI) predictors to be used in the regression retrieval. In the case of infrared only retrieval the number of predictors is 204 (4 elevations + 200 PCs IASI). All coefficients for the joint microwave/infrared regression are provided in the dataset MWIR, whereas the infrared only coefficients are provided in the dataset IRON.

### 5.4.4 Regression class identification

The purpose of having different retrieval classes is to divide the training set into several parts in such a way that the type of atmosphere and surface within each class is relatively homogeneous and a linear function can provide a good approximation of the relationship between the inputs and the outputs. Of course the class definition must be based on the value of the inputs only and it can be done in many different ways. For the current scheme, a total of 480 (= 15 scan steps × 2 day/night × 16 k-mean clusters) classes have been used, which are defined as follows. The first 15 classes are defined based on the scan angle. The two EFOVs closest to nadir (i.e. position 14 and 15) belong to the first class, the next two (position 13 and 16) belong to the second class, and so on until the fifteenth class populated by EFOVs numbers 0 and 29. Next each of these 15 classes is divided into a day and a night class (sun zenith angle is greater than 90 degree). Each of these 30 classes is then divided into 16 further subclasses defined by k-means clustering. The final retrieval is obtained as the average of four individual retrievals, which differ only by the parameters which have been used in the clustering. For each of the four retrievals, the four first clustering predictors are $h_i = e^{-z_i/7000}$, where $z_i$ is the surface height in meters of each of the four IFOVs. This is followed by the first $nbrMW$ microwave PC scores and the first $nbrIR$ IASI PC scores, where the number of PC scores used in each of the four retrievals differs as follows: $(nbwMW = 4\,;\ nbrIR = 4)$, $(nbrMW = 2\,;\ nbrIR = 8)$, $(nbrMW = 8\,;\ nbrIR = 2)$ and $(nbrMW = 16\,;\ nbrIR = 16)$. Each clustering predictor is normalised by division with the standard deviation and the retrieval class, $i$, is chosen which minimizes

$$\sum_{j=1}^{4+nbrMW+nbrIR} \left(\frac{x_j}{cs_j} - centers_{ij}\right)^2 \qquad \textit{Equation 22}$$

Where:

| | |
|---|---|
| $x_j$ | are the clustering predictors, $x = (h_1, \dots, h_4, pcMW_1, \dots, pcMW_{nbrMW}, pcIR_1, \dots, pcIR_{nbrIR})$ |
| $cs_j$ | are the standard deviations associated with each input element $j$ |
| $centers_{ij}$ | define the centers of each of the 16 subclasses. |

The coefficients $cs$ and $centers$ are provided in the static auxiliary datasets `MWIR` and `IRON` [8.2.12].

### 5.4.5 Retrieval

The coefficients for the joint microwave / infrared regression are provided in four times 30 subgroups of the `MWIR` group [8.2.12] of the `IASI_SAD` [8.2] file. Each subgroup is named according the day/night classification, the scan angle class and $nbrMW/nbrIR$ (the number of microwave/infrared PC scores used in the classification) – for example `D_00_M16_I16` or `N_14_M02_I08`. Each of these groups contain the coefficients $cs$ and $centers$ for determining the regression class as well as 16 instances (one for each subclass) of the actual regression coefficients $R$, $ym$ and $xm$.

Once the retrieval class is determined, a vector $Y$ consisting of N = 186 parameters (see section 5.4.2) is retrieved by usual linear regression:

$$Y_j = ym_j + \sum_{i=1}^{M} R_{ji}(X_i - xm_i)$$

*Equation 23*

where:

| | |
|---|---|
| $xm_i$ | is extracted from one of the `MWIR` or `IRON` subgroups in `IASI_SAD` |
| $ym_j$ | is extracted from one of the `MWIR` or `IRON` subgroups in `IASI_SAD` |
| $R_{ji}$ | is extracted from one of the `MWIR` or `IRON` subgroups in `IASI_SAD` |

The temperature and water vapour profiles are retrieved together represented as 100 PC scores defining the profiles in all four IFOVs. These eight profiles (4 temperature and 4 water-vapour) must be reconstructed using the eigenvectors found in the dataset `EV_TW4 [8.2.15]`. The retrieved profiles are defined at ECMWF model levels plus a level at surface pressure and we use the retrieved surface pressure to compute the pressure at each of the 137 model levels. Following reconstruction, the profiles are interpolated to the standard 101 fixed level pressure grid as explained in 6.3.

The ozone profiles are retrieved as 20 PC scores defining the ozone profiles in all four IFOVs. The four ozone profiles are reconstructed using the eigenvectors found in the dataset `EV_OZ4` [8.2.14] and are provided at 137 model levels plus a level at surface pressure. Following reconstruction, the profiles are interpolated to the standard 101 fixed level pressure grid as explained in 6.3.

The water-vapour and ozone profiles are converted from dew point temperature to mixing ratio as explained in 6.13.

The retrieved temperature and water-vapour profiles must undergo a physical check at this stage, before they are further used by other subsequent functions in the IASI L2 processing chain. The check for super-saturation and over adiabatic conditions is explained in Section 5.8.7.

The retrieved surface emissivity is represented as 20 PC scores. When reconstructed (using the dataset `EV_EM4` [8.2.16]), the emissivity, $\tilde{e}$, at 10 selected wavelengths in each of the four IFOVs is obtained. In the product the emissivity is not provided at these 10 wavelengths, but at 12 other wavelengths. For this transformation, the high resolution mean emissivity spectrum, $\bar{e}$, and eigenvectors, $E$, found in the dataset `COF_EMS` [8.2.10], are used. First the PC scores, $p$, which fit the given emissivities best is found by least squares solution of $\tilde{e} - \bar{e}_S = E_S p$ (where subscript S indicates subselection corresponding to the ten wavelengths of $\tilde{e}$). Then the emissivities at the 12 final wavelengths are reconstructed from these PC scores.

### 5.4.6 Retrieval quality indicators

For each retrieved parameter, a simple but useful quality indicator is obtained by regression against the absolute value of the retrieval error. This regression retrieval of the absolute value of the primary retrieval errors uses the same predictors and the same retrieval classes as the primary retrieval. The regression coefficients for the quality indicators are embedded in the overall regression coefficients and have been included for the parameters listed in Table 16 below.

***Note:*** the quality indicators for surface pressure and emissivity are not presently provided for in the product.

| *Parameter* | *Quality Indicator* | *Product Field* |
|---|---|---|
| surface pressure | *not provided for* | |
| surface skin temperature | `FG_QI_SURFACE_TEMPERATURE` | [*IASIL2PFS*] |
| surface air temperature | `FG_QI_ATMOSPHERIC_TEMPERATURE` | [*IASIL2PFS*] |
| surface air dew point temperature | `FG_QI_ATMOSPHERIC_WATER_VAPOUR` | [*IASIL2PFS*] |
| ozone | `FG_QI_ATMOSPHERIC_OZONE` | [*IASIL2PFS*] |
| surface emissivity | *not provided for* | |

*Table 16: Regression coefficients per paramater*

For the quality indicators of surface pressure, surface skin temperature, surface air temperature and surface air dew point temperature an individual value for each of the four IFOVs is obtained, whereas for ozone and emissivity the quality indicator predicts the absolute error of the first PC score, representing all four IFOVs in the current EFOV, such that only a single value is obtained. If one or more of the four quality indicators provided in the product exceeds a threshold value, the PWLR[3] retrieval of all parameters is rejected. The acceptance threshold values are as follows:

| | |
|---|---|
| FG_QI_SURFACE_TEMPERATURE | 4.45 |
| FG_QI_ATMOSPHERIC_TEMPERATURE | 2.95 |
| FG_QI_ATMOSPHERIC_WATER_VAPOUR | 3.95 |
| FG_QI_ATMOSPHERIC_OZONE | 7.95 |

*Table 17: Acceptance threshold values for PWLR[3] retrievals*

The quantities retrieved with the all-sky statistical retrieval must be verified against configurable bounds. If a parameter retrieved with the statistical method is out of the expected range, the corresponding bit of the flag **FLG_FGCHECK** shall be raised and the exceeding value reset to the nearest bound. The profiles are treated as whole in **FLG_FGCHECK**. If the value of at least one pressure level is out of valid bounds then the entire profile is be flagged. The validity bounds are configurable and may vary with the geolocation and time in the year.

## 5.5 Clouds detection and retrieval

The identification of clouds in the IASI field of view is performed with three concurrent cloud tests described as follows:

| *Test* | *Full description in…* |
|---|---|
| NWP | Section 5.5.1 |
| AVHRR | Section 5.5.2 |
| ANN | Section 5.5.3 |

If a cloud is detected by at least one of the tests, its characterisation in terms of fractional coverage in the field of view and cloud top height is attempted using the $\chi^2$ and $CO_2$-slicing methods in Section 5.5.4. The combination of these detection and retrieval results is interpreted in the cloud classification summary as explained in Section 5.5.5.

The execution and outcome of the following tests shall be reflected in the processing flag **FLG_CLDTST** by raising the corresponding bits.

### 5.5.1 IASI Window channel test

This cloud-detection test compares the measured radiances in window channels against clear-sky simulated radiances. The simulated clear-sky radiances are calculated with the fast radiative transfer model—also referred to as forward model RTTOV. This is extensively documented in [RTTOVguide] and [RTTOVval]. The atmospheric state vector input to the forward modelling is taken from the collocated NWP information. If this is not available as per flag **FLG_NWPBAD**, it is taken from the statistical retrieval. Specifications are in Section 5.4.

$$R_{CALC,k} - \left(R_{OBS,k} + b_k\right) > \tau_k \qquad \textit{Equation 24}$$

where:

| | |
|---|---|
| $R_{CALC,k}$ | is the clear-sky calculated radiance at channel $k$, using RTTOV. |
| $R_{OBS,k}$ | is the observed radiance in channel $k$. |
| $b_k$ | is a bias correction offset, specific to channel $k$. |
| $\tau_k$ | is the threshold for cloud detection at channel $k$. |

$b_k$, $\tau_k$ and the channels $k$ are configurable parameters defined in the auxiliary dataset COF_CLDDET specified in Section 8.2.1.

### 5.5.2 AVHRR test

This test relies on the evaluation of the presence of clouds within the IASI field of view using collocated imager data only. The resulting fraction of a IASI field of view covered by cloud is provided in the L1C files, by the field ***GEUMAvhrr1BCldFrac***. If the integrated cloud amount exceeds a configurable threshold—set to 2 % in the processor Version 6—then the scene is declared cloudy according to the AVHRR test.

### 5.5.3 ANN Cloud detection

This test uses both IASI and collocated AVHRR measurements in combination and implements artificial neural networks to classify the scenes. The algorithm is detailed in the sub-sections following this section. The full equation is given in Section 5.5.3.4. This test returns a cloudiness estimate ranging from 1 to 4, based on the definitions below:

| *ANN test output* | *means* |
|---|---|
| 1 | Clear |
| 2 | Partially cloudy, small cover |
| 3 | Partially cloudy, high cover |
| 4 | Fully cloudy |

The scene is declared cloudy according to this test if the output exceeds a configurable threshold and the corresponding bit is set to *On* in **FLG_CLDTST**.

#### *5.5.3.1 Principle*

The artificial neural networks (ANN) are of the type multi-layer perceptron (MLP). Different architecture are designed for each of the *surface type/period of the day* combination:

- Sea/Day,
- Sea/Night,
- Land/Day,
- Land/Night.

The selection of the IASI channels is configured in the COF_CNN* groups of the IASI_SAD configuration file. See Section 8.2.5.

As for AVHRR measurements, there are two ANN inputs for each channel:

- *max(mean+std.dev)*
- *min(mean-std.dev)* computed over all AVHRR radiance clusters.

For cloud detection by day, channels 1, 2, 3a, 4 and 5 are used, leading to 10 ANN inputs.
For cloud detection by night, channels 3b, 4 and 5 only are available, leading to 6 ANN inputs.

Inputs for the AVHRR channels 1, 2 and 3a are expressed in reflectances which are linked to the channels radiances by this equation:

$$A_i = \frac{R_i \times \pi}{F_i \times cos(z_{sol})} \qquad \textit{Equation 25}$$

where:

| | |
|---|---|
| $A_i$ | is the reflectance in the channel *i*. |
| $R_i$ | the radiance in the channel *i*. |
| $F_i$ | the solar irradiance in the channel *i*, |
| $z_{sol}$ | is the solar zenith angle |

The values of the solar irradiance for the three channels are given in Table 18.

| *AVHRR Channel* | *Solar irradiance $F_i$ ($W/m^2$)* |
|---|---|
| 1 | 139.873215 |
| 2 | 232.919556 |
| 3a | 14.01647 |

*Table 18: Solar irradiances for the AVHRR channels 1, 2 and 3a*

Inputs for the AVHRR channels 3b, 4 and 5 are expressed in brightness temperatures which are linked to the channels radiances by the inverted Planck function:

$$BT_i = \frac{c_2 \times v_i}{ln(1 + c_1 \times \frac{v_i^3}{R_i})}$$ *Equation 26*

where:

| | |
|---|---|
| $BT_i$ | is the brightness temperature |
| $R_i$ | is the radiance |
| $v_i$ | is wavenumber of the channel *i* |
| $c_1 = 1.1910427 \times 10^{-16}$ Wm$^2$/s | is a Planck constant |
| $c_2 = 1.4387752 \times 10^{-2}$ m K | is a Planck constant |

Input/output vectors for the different surface type/period of the day configuration:

| | | |
|---|---|---|
| Sea/Day ANN | 18 IASI inputs + 10 AVHRR inputs | = 28 inputs |
| Sea/Night ANN | 18 IASI inputs + 6 AVHRR inputs | = 24 inputs |
| Land/Day ANN | 18 IASI inputs + 10 AVHRR inputs | = 28 inputs |
| Land/Night ANN | 18 IASI inputs + 6 AVHRR inputs | = 24 inputs |

#### *5.5.3.2 ANNs inner structure*

Four different structures are defined:

| | |
|---|---|
| Sea/Day ANN | two hidden layers: 12 , 5 neurons |
| Sea/Night ANN | three hidden layers: 8 , 4 × 2 neurons |
| Land/Day ANN | two hidden layers: 12 ,5 neurons |
| Land/Night ANN | three hidden layers: 8 , 4 × 2 neurons |

#### *5.5.3.3 Activation, input and output scaling functions*

The activation function of the input layer is the unity function. The neuron activation function of the hidden and output layers is the sigmoid function:

$$f(x) = \frac{1}{1 + e^{-x}}$$ *Equation 27*

Neurons input and output scaling functions are linear:

- Input scaling : $F_{in}$(input) = *InScale* × input + *InBias*
- Output scaling : $F_{out}$(output) = *OutScale* × output + *OutBias*

The parameters *InScale*, *InBias*, *OutScale* and *OutBias* are configurable and defined in the COF_CNN* auxiliary datasets defined in Section 8.2.5. In version 6, some of them are fixed:

- Input layer:
  - *InScale* = 1

- *InBias* = 0

- Hidden layers:
  - *InScale* = 1
  - *OutScale* = 1
  - *OutBias* = 0
- Output layer:
  - *InScale* = 1
  - *OutScale* = 3
  - *OutBias* = 1

#### *5.5.3.4 ANN cloud test equation*

The IFOV is declared cloudy if the following is true:

$$C > t \qquad \text{Equation 28}$$

where:

$$C = S^{out} * f\left(\sum_{i=1}^{N_H} w_i^{out} . o_i^H + b^{out}\right) + B^{out} \qquad \text{Equation 29}$$

with

$$\begin{cases} o_i^h = f\left(\sum_{j=1}^{N_{h-1}} w_{ij}^h . o_j^{h-1} + b_i^h\right) & ; h = 2 .. H \\ o_i^1 = f\left(\sum_{j=1}^{N_{in}} w_{ij}^1 . E_j + b_i^1\right) & ; h=1 \end{cases} \qquad \text{Equation 30}$$

and

$$E_i = S_i^{in} * e_i + B^{in} \qquad \text{Equation 31}$$

where:

| | |
|---|---|
| $t$ | configurable threshold |
| $C$ | retrieved cloudiness ; **C** $\in$ [1,4] |
| $S^{in/out}$ ; $B^{in/out}$ | scaling coefficients of the networks inputs/output |
| $f$ | activation function defined in Equation 27. |
| $H$ | number of hidden layers |
| $N_h$ | number of neurons in the hidden layer **h** |
| $w_i^{out}$ | weight of the connection between the output neuron and the **i**$^{th}$ neuron in the last hidden layer. |

| | |
|---|---|
| $b^{out}$ | bias of the output neuron |
| $o_i^h$ | activation value of the **i**th neuron in the **h**th hidden layer |
| $w_{ij}^h$ | weight of the connection between the **i**th neuron in the hidden layer **h** and its **j**th predecessor in the preceding layer (input or previous hidden layer). |
| $b_i^h$ | bias of the **i**th neuron in the **h**th hidden layer |
| $E_i$ | **i**th normalised entry in the input layer |
| $e_i$ | **i**th entry in the input vector |

### 5.5.4 Effective cloud amount and cloud top height assignment

If clouds have been detected by at least one of the window tests, either AVHRR and ANN, as captured in **FLG_CLDTST**, the calculation of the cloud-top pressure and fractional cloud cover from the IASI spectrum is done on single IASI IFOVs with the $CO_2$-slicing method as described by Menzel and Stewart [Menzel83] and Smith and Frey [Smith90] and detailed in Section 5.5.4.1. This method has limitations with low-contrast scenes, for example in the presence of low clouds of similar temperature as the surface or with small cloud amount. Therefore, it is complemented in such situations with the $\chi^2$ method explained in Section 5.5.4.2. The method was developed by Stubenrauch [Stub99].

The final choice of the method for cloud top height assignment shall be reflected in the processing flag **FLG_CLDFRM** by raising the corresponding bit.

Both the $CO_2$-slicing and $\chi^2$ methods require as input an atmospheric state vector corresponding to the scene observed in the IASI IFOV. These are the temperature, humidity and ozone profiles as well as the surface pressure, skin and air temperature and the surface air humidity. This information shall come from the collocated NWP data (see Section 5.1.8) or alternatively from the PWLR retrieval if no good NWP information flagged **FLG_NWPBAD** (**FLG_NWPBAD** > 0) is available. The origin of the atmospheric data (either NWP or PWLR) shall be reflected in the flag **FLG_CLDFRM** by raising the corresponding bit.

#### *5.5.4.1 The CO2-slicing method*

The $CO_2$-slicing method is applied on a selected subset of $N_S$ single IASI channels. The selection of this subset of channels is configurable but does not necessarily consist of subsequent channels and is specific to the $CO_2$-slicing method. For each channel of this subset the following expression is calculated for a number of possible cloud-top levels $n = 1..N_C$:

$$x_{k,n} = \frac{(R_k^{clr} - R_k^{cld,meas})}{(R_{k_R}^{clr} - R_{k_R}^{cld,meas})} - \frac{(R_k^{clr} - R_{k,n}^{bkc})}{(R_{k_R}^{clr} - R_{k_R,n}^{bkc})}$$

*Equation 32*

where:

| | |
|---|---|
| $R_k^{cld,meas}$ | = measured radiance in a cloudy or partly cloudy IFOV in channel $k$ |
| $R_{k,n}^{bkc}$ | = calculated outgoing blackbody radiance at space from the emission of the atmosphere above the level $n$ at wavenumber $k$ |
| $R_k^{clr}$ | = calculated radiance in channel $k$ for a completely clear IFOV |
| $k_R$ | = reference channel number |
| $k$ | = IASI channel index |
| $n$ | = pressure level number |

The initial channel selection and the pressure level are configured in COF_SLIC (8.2.6).

Equation 32 shall only be evaluated for channels where the first term on the right side falls within the range of values obtained from the second term on the right side, where the range is derived separately for each channel for all possible cloud-top levels. Channels which do not fulfil this condition must be excluded from the further evaluation. If no channel survives this test, the one with the greatest weight as calculated from Equation 32 below shall be retained.

Furthermore, Equation 32 shall only be evaluated if the radiances are greater than their respective measurement noise and if the absolute values of the denominators are greater than three times the respective measurement noise of the respective radiance. The number $N_S$ must be adjusted accordingly. If the number ends up as $N_S = 0$ the method fails and the $\chi^2$ method is invoked, which shall be flagged in **FLG_CLDFRM.** See Section 5.5.4.2.

There is only one reference channel, $k_R$, which is specified in the user-configurable auxiliary dataset COF_SLIC (8.2.6) per month and geographic location, and which is different from the channels of the aforementioned set of channels.

Equation 32 is evaluated for a selected range of pressure levels n ,where $N_{P1} \leq n \leq N_{P2}$ and $N_{P2}$ is selected such that it becomes the second pressure level above the surface. If the ratio of calculated radiance differences $(R_k^{clr} - R_{k,n}^{bkc}) / (R_{kR}^{clr} - R_{kR,n}^{bkc})$ shows inconsistent behaviour above some level whose pressure is lower than 400 hPa, $N_{P1}$ is lowered to the highest level just below the beginning of that inconsistent behaviour. To be precise, it is lowered to the pressure level where the first derivative of that ratio (with respect to the pressure) first changes from negative to zero when searching the pressure domain upwards. For each channel of the selected subset, a cloud top pressure $p_{C,k}$ —and thus the corresponding level number $n_{pc,k}$ —is calculated according to this equation:

$$p_{C,k} = p(\min(|x_{k,n}|)) \qquad \textit{Equation 33}$$

The cloud-top pressure that is finally assigned is the weighted mean of the cloud top pressure derived in single channels of the selected subset:

$$p_C = \frac{\sum_{k=1}^{N_S} w_k^2 \, p_{C,k}}{\sum_{k=1}^{N_S} w_k^2}$$

*Equation 34*

where:

$$w_k = \frac{\tau_{p_{C,k}} \times \frac{\partial B_k}{\partial T(p_{C,k})} \times \frac{\partial T(p_{C,k})}{\partial \ln p_{C,k}} \times [R_{k_R}^{clr} - R_{k_R}^{cld}(n_{p_{C,k}})] - \tau_{p_{C k_R}} \times \frac{\partial B_{k_R}}{\partial T(p_{C,k})} \times \frac{\partial T(p_{C,k})}{\partial \ln p_{C,k}} \times [R_k^{clr} - R_k^{cld}(n_{p_{C,k}})]}{[R_{k_R}^{clr} - R_{k_R}^{cld}(n_{p_{C,k}})]^2}$$

*Equation 35*

is the weighting function in channel $k$. The weighting function of a channel $k$ is set to 0 if the following is true:

$$|w_k| \le \beta \times \max(|w_j|), k = 1,\ldots,N_S$$

*Equation 36*

where β is a user-configurable constant.

The $k$ identifies here the number of the IASI channel within the selected subset of $N_S$ channels, renumbered from 1 to $N_S$ . Expressions in Equation 35 are calculated as follows:

$$\frac{\partial T(p_{C,k})}{\partial \ln p_{C,k}} = \frac{[T(n_{p_{C,k}} - 1) - T(n_{p_{C,k}} + 1)]}{\ln(p(n_{p_{C,k}} - 1)/p(n_{p_{C,k}} + 1))}$$

*Equation 37*

$$\frac{\partial B_k}{\partial T(p_{C,k})} = \frac{c_1 \cdot c_2 \cdot \nu_k^4 \cdot \exp(c_2 \nu_k / T(n_{p_{C,k}}))}{T(n_{p_{C,k}})^2 \cdot (\exp(c_2 \nu_k / T(n_{p_{C,k}})) - 1)^2}$$

*Equation 38*

where:

| | |
|---|---|
| $c_1$ | $= 1.1910427 \times 10^{-16}$ W.m$^2$.sr$^{-1}$ is a constant |
| $c_2$ | $= 1.4387752 \times 10^{-2}$ m K is a constant |

The cloud-to-space radiances and transmittances and respective temperatures and derivatives to be calculated for Equation 35 must be represented for cloud-top pressures on a fine vertical grid that is usually not represented in the FRTM used. Therefore, corresponding values must be linearly interpolated in the log(pressure) coordinate. A cloud-top pressure $p_{C,k}$ is excluded from the calculation of $p_C$ if the derived cloud fraction, as calculated from Equation 39 below with $p_{C,k}$ in place of $p_C$ is greater than 1.04. Furthermore, only those $p_{C,k}$ which belong to the histogram class with the greatest population in a histogram of all $p_{C,k}$ at a class width of 50 hPa are entered into the equation. In the event of two classes with the same greatest population, the one with the lower

pressure is chosen. If a preliminary evaluation of Equation 34 gives a result greater than 570 hPa and if there is a temperature inversion, then a new histogram is calculated with class width of 100 hPa and $p_{C,k}$ values falling into the class with the greatest population are retained. In the event of two classes with the same greatest population, the one with the higher pressure is chosen.

With the cloud-top pressure calculated by the $CO_2$-Slicing Method the cloud-top temperature is to be determined using a known temperature profile. The source of this temperature profile shall be the collocated NWP forecasts detailed in Section 5.1.8. If this is not available or of bad quality as specified in FLG_NWPBAD, the all-sky first-guess retrieval. See Section 5.4.

An interpolation as described in Section 6.3 has to be applied to interpolate the cloud-top temperature in the vertical temperature profile. The temperature profile must be examined with respect to inversions below 500 hPa. The pressure levels between the base of the inversion and the level 30 hPa above the one whose temperature is identical to the temperature at the base must not be used to evaluate Equation 33. Once the cloud top temperature is known, the effective cloud amount (total fractional cloud cover) is to be calculated in a window channel:

$$\alpha = \frac{R_{k_w} - R_{k_w}^{clr}}{B_{k_w}(T(p_c)) - R_{k_w}^{clr}} \qquad \textit{Equation 39}$$

where:

| | |
|---|---|
| $R_{kw}$ | = measured radiance in window-channel $k_w$ |
| $R_{kw}^{clr}$ | = clear-sky radiance in IASI window-channel $k_w$ |
| $B_{kw}$ | = Planck function in channel $k_w$ |

The clear-sky radiance is calculated using profiles and surface parameters either from collocated NWP or from the PWLR. This choice is made in the configuration file.

The threshold value, highest pressure level, and reference channel numbers are tabulated functions of latitude zone, month of the year, and surface type. These values are configured in the `COF_SLIC` group of `IASI_SAD`. See Section 8.2.6

#### *5.5.4.2 The $\chi^2$ method*

This method consists of modelling the differences between measured and simulated clear radiances with a mono-layer cloud for channels selected in $CO_2$ lines. It is based upon the minimisation of a weighted-$\chi^2$ function as reported by Stubenrauch et al [Stub99] and inspired by the minimum residual method of Eyre and Menzel [Eyre89], previously tested with HIRS data. The rationale of the minimum residual method is to find both the cloud top pressure *pc* and the equivalent cloud amount $\eta = f.\varepsilon$ , where f stands for cloud fraction and ε stands spectral mean cloud emissivity within $CO_2$ channels. This minimizes the residual:

$$\sum_i \{[I^{clr}(\nu_i) - I^{cld}(p_k, \nu_i)]\,\eta(p_k) - [I^{clr}(\nu_i) - I^{meas}(\nu_i)]\}^2 \qquad \textit{Equation 40}$$

where:

| | |
|---|---|
| $I^{clr}(\nu_i)$ | = the outgoing synthetic cloud-free |
| $I^{meas}(\nu_i)$ | = measured radiances |
| $I^{cld}(p_k, \nu_i)$ | = the outgoing radiance from a single blackbody on pressure level $p_k$ |
| $\nu_i$ | = is the wave number at channel $i$i |

The $\chi^2$-method has the advantage of always providing retrievals while the $CO_2$-slicing method is not applicable for approximately 30% of the IFOVs. According to Eyre and Menzel [Eyre89] the minimum residual method had shown good potential for high and middle level clouds when applied to HIRS channels, but poor performance for lower-level clouds.

### 5.5.5 Cloudiness summary

The various tests may conclude to contradictory clear/cloudy classifications because of different sensitivities and of the uncertainties associated with their respective methodologies (e.g. uncertainties in the *a priori* surface emissivity and temperature in the NWP test, lack of contrast between snow and clouds for the detection with AVHRR images or in the ANN classification). The different test results are consolidated into an enumerated flag, **FLG_CLDNES** that summarises the status of and the level of confidence in the clear-sky/cloudiness assessment within the IASI IFOV. This flag controls the choice of the subsequent retrieval methods in the processing chain.

This flag **FLG_CLDNES** is set as follows:

| ***Reason for flagging*** | ***Value*** |
|---|---|
| No clouds detected with the NWP, AVHRR and ANN cloud tests | 0 |
| Potential small cloud contamination (at least one cloud test detected a cloud) but a cloud could not be characterised with confidence | 1 |
| Cloud detected and characterised. The retrieved equivalent cloud amount is lower than 80% | 2 |
| Cloud detected and characterised. The retrieved equivalent cloud amount is higher than 80% | 3 |

The setting of the flag **FLG_CLDNES** is specified in the following table. It relies on various inputs, namely the detection performed by the three individual cloud tests and these cloud characteristics: cloud top pressure (CTP) and cloud fraction (CFR) as retrieved with the $CO_2$-slicing and the $\chi^2$ methods described in Section 5.5.4.

| ***Inputs*** | | | | **FLG_CLDNES** | ***Information*** | |
|---|---|---|---|---|---|---|
| *ANN* | *Win* | *AVHRR* | *Cloud parameters* | | *Assessment* | *Final Retrieval* |
| 0 | 0 | 0 | Cloud retrieval not invoked | 1 | Clear, high confidence | PWLR[3] + OEM |
| One of the tests disagree with the others: e.g. (1,0,0) or (0,1,0) or (0,1,1)... | | | Not a valid retrieval or CFR<25% \| CTP>750hPa | 2 | Clear, lower confidence | PWLR[3] + OEM |
| | | | CFR > 25% and CTP < 750 hPa | 3 | Cloudy | PWLR[3] |
| 1 | 1 | 1 | CFR < 80% | | | |
| | | | CFR > 80% | 4 | Very cloudy | PWLR[3] |

*Table 19: FLG_CLDNES settings.*

### 5.5.6 Cloud top phase characterisation

In cloudy conditions, the cloud phase, ϕ, shall be determined. The discrimination of ice from water clouds makes use of the difference:

$$T_b(8\mu m) - T_b(11\mu m)$$

compared to this difference:

$$T_b(11\mu m) - T_b(12\mu m)$$

If this equation is true:

$$\{T_b(8\,\mu\text{m}) - T_b(11\,\mu\text{m})\} - \{T_b(11\,\mu\text{m}) - T_b(12\,\mu\text{m})\} > t_1 \qquad \textit{Equation 41}$$

then the cloud phase is ice ($\phi = 2$), else if:

$$t_1 > \{T_b(8\,\mu\text{m}) - T_b(11\,\mu\text{m})\} - \{T_b(11\,\mu\text{m}) - T_b(12\,\mu\text{m})\} > t_2 \qquad \textit{Equation 42}$$

then the cloud is of mixed phase ($\phi = 3$). Otherwise, the cloud is of liquid phase ($\phi = 1$), where $t_1$ and $t_2$ are threshold values for this test. The threshold values are tabulated functions of latitude zones and month of the year. In clear situations the cloud phase must not be determined ($\phi = 0$).

### 5.5.7 Dust detection

For the aerosol detection, the Dust indicator has to be evaluated.

Given the radiance *r* and the auxiliary information:

- Geographic coordinates (lat, long),
- Surface type (OCEAN/LAND)

| *Surface type* | *flg_landsea* |
|---|---|
| OCEAN | 0 |
| LAND | [1 5] |

- Time (AM/PM)

| *Time* | *Solar Zenith Angle* |
|---|---|
| AM | [0 90[ |
| PM | [90 180] |

the dust indicator is given by the following equation:

$$R = \sum_{i=0}^{n\_dust} G(i) \cdot \big(r\big(ch(i)\big) - \mu(i)\big) - bias \qquad \textit{Equation 43}$$

where:

| | |
|---|---|
| *G* | = the gain matrix |
| *m* | = is the background spectrum |
| *bias* | = a value to be subtracted, to obtain the correct Dust indicator |
| *ch = (ch(1),...,ch(n_dust))* | = the vector of the *n_dust* wavelength channels that capture the majority of the aerosol information. |

These parameters are configurable and defined in the COF_DUST auxiliary datasets defined in Section 8.2.18.

### 5.5.8 Thin cirrus detection

Currently, no thin cirrus cloud test is available, but one is expected in the near future. The flag must be set to two by default.

## 5.6 Surface state

### 5.6.1 Sea-ice detection

The land-sea atlas is only a static land-sea mask. Without further information, the scenes containing sea-ice would be inconsistently processed along with retrieval algorithms configured for plain open water.

To avoid this, the presence of sea ice is evaluated for all IFOVs fully covered by oceans at latitudes higher than 45°. This is achieved with collocated AMSU measurements taken from [Grody]. This algorithm is applied only if AMSU collocated data of good quality are available, as reflected in the quality flag **FLG_AMSUBAD**.

To compute the sea ice fraction, the emissivity at AMSU Channel 1 (23.8 GHz) $ems_1$ is first retrieved from a linear combination of the brightness temperatures in the AMSU channels 1, 2 and 3; written as $TB_1$, $TB_2$ and $TB_3$ in the following equation:

$$\varepsilon_1 = a + bTB_1 + cTB_2 + dTB_2 \qquad \textit{Equation 44}$$

where:

$$\begin{cases} a = 1.84 - 0.723.\mu; \\ b = -0.00088; \\ c = 0.0066 + 0.0029.\mu; \\ d = -0.00926 \end{cases} \qquad \textit{Equation 45}$$

with

$$\mu = \cos(\hat{z}_{sat}) \qquad \textit{Equation 46}$$

and $\hat{z}_{sat}$ is the satellite zenith angle.

The theoretical emissivity of water, $ems_{water}$, is a function of the viewing angle:

$$\varepsilon_{water} = 0.1824 + 0.9048.\mu - 0.6221.\mu^2 \qquad \textit{Equation 47}$$

The emissivity of ice, $ems_{ice}$, is evaluated as follows:

$$\varepsilon_{ice} = \begin{cases} 0.93, & \text{if } (TB_1 - TB_2) < 5\,K \\ 0.87, & \text{if } 5 < (TB_1 - TB_2) < 10\,K \\ 0.83, & \text{if } 10 < (TB_1 - TB_2) \end{cases} \qquad \textit{Equation 48}$$

Finally, the sea ice concentration $sea_{ice}$ is expressed in percentage and is computed using Equation 44 to Equation 48, and Equation 49:

$$sea_{ice} = 100 * (\varepsilon_1 - \varepsilon_{water}) / (\varepsilon_{ice} - \varepsilon_{water})\, 0.1824 + 0.9048.\mu - 0.6221.\mu^2 \qquad \textit{Equation 49}$$

### 5.6.2 Land surface emissivity

The land surface emissivity is retrieved with the PWLR[3] method as described in 5.4.

***Note:*** For emissivity product users, the full emissivity spectrum for all 8461 IASI channels can be constructed from the emissivity provided at selected wavelengths in the IASI L2 products. This is possible using a base of emissivity eigenvectors, like for instance defined in [UWIREMS].

$$\boldsymbol{\varepsilon} = \boldsymbol{\Omega}.\left(\tilde{\boldsymbol{\Omega}}^T\tilde{\boldsymbol{\Omega}}\right)^{-1}\tilde{\boldsymbol{\Omega}}^T(\tilde{\boldsymbol{\varepsilon}} - \langle\tilde{\boldsymbol{\varepsilon}}\rangle) + \langle\boldsymbol{\varepsilon}\rangle \qquad \textit{Equation 50}$$

where:

| | |
|---|---|
| $\varepsilon$ | is the land surface emissivity spectra on all IASI channels |
| $\tilde{\varepsilon}$ | is the land surface emissivity spectra in the selected channels for L2 products |
| $\langle\boldsymbol{\varepsilon}\rangle$ | is the average emissivity in all IASI channels |
| $\langle\tilde{\boldsymbol{\varepsilon}}\rangle$ | is the average emissivity in the selected channels |
| $\boldsymbol{\Omega}$ | is the eigenvector spanning all the IASI channels |
| $\tilde{\boldsymbol{\Omega}}$ | is the eigenvectors spanning the selected IASI channels |

$\langle\boldsymbol{\varepsilon}\rangle$, $\langle\tilde{\boldsymbol{\varepsilon}}\rangle$, $\boldsymbol{\Omega}$ and $\tilde{\boldsymbol{\Omega}}$ are static configuration data, publicly available on line.

## 5.7 Atmospheric composition

### 5.7.1 ANN retrieval of trace gases

The state vector to be retrieved by the trace-gas retrieval is as follows:

$$\mathrm{x} = \left(\mathrm{C}_{\mathrm{CO}_2}, \mathrm{C}_{\mathrm{CH}_4}, \mathrm{C}_{\mathrm{N}_2\mathrm{O}}\right) \qquad \textit{Equation 51}$$

where $\mathrm{C}_{\mathrm{CO}_2}, \mathrm{C}_{\mathrm{CH}_4}, \mathrm{C}_{\mathrm{N}_2\mathrm{O}}$ are the total columnar amounts of the trace gases $\mathrm{CO}_2, \mathrm{CH}_4, \mathrm{N}_2\mathrm{O}$. The amounts have to be expressed in kg/m$^2$. A separate network of one output, the total columnar amount, is formulated for each gas. These quantities are retrieved with artificial neural networks (ANN). The nets consist of fully connected feed-forward networks with one entrance layer, two hidden layers, and one output layer of neurons. The parameters forming the input layer are as follows:

- a number of $N_R \leq 200$ IASI level 1c radiances
- the surface temperature and a coarse temperature profile, represented on M ≤ 30 levels.
- the surface pressure
- the secant of the satellite zenith angle

The transfer function of the hidden neurons is as follows:

$$f(z) = \tanh(z) = \frac{\mathrm{e}^{z} - \mathrm{e}^{-z}}{\mathrm{e}^{z} + \mathrm{e}^{-z}} \qquad \textit{Equation 52}$$

and the transfer function of the output layer is as follows:

$$g(z) = z \qquad \textit{Equation 53}$$

so that the global transfer function for the output $O_q$ ; $\mathrm{q} = (\mathrm{CO}_2, \mathrm{CH}_4, \mathrm{N}_2\mathrm{O})$ reads:

$$O_q = g\left\{\sum_{k=1}^{S_2} w_{qk}^3 . f\left(\sum_{j=1}^{S_1} w_{kj}^2 . f\left(\sum_{i=1}^{N_1} w_{ji}^1 . I_i' + b_j^1\right) + b_k^2\right) + b_q^3\right\} \qquad \textit{Equation 54}$$

where:

| | |
|---|---|
| $S_1$ | is the number of neurons in the first hidden layer |
| $S_2$ | is the number of neurons in the second hidden layer |
| $w_{ji}^1$ | weight for the connections between the successive layers |
| $w_{kj}^2$ | weight for the connections between the successive layers |
| $w_{pk}^3$ | weight for the connections between the successive layers |

The biases associated with the neurons are combined into the vectors $b_j^1$, $b_k^2$, and $b_l^3$, and for the first and second hidden layer and the output layer, respectively. The normalised input vector I′ is computed from the raw inputs I with respective pairs of scaling coefficients *($C_1$; $C_2$ )* and the relation:

$$I'_i = 0.9 \times \frac{I_i - C_i^1}{C_i^2}$$ *Equation 55*

where $i$ refers to the $i^{th}$ input element; $i = 1..N_I$.

The input vector writes:

$$I = (R'_1, \ldots, R'_{Na}, R_1, \ldots, R_{N_q}, Ts, T_1, \ldots, T_{Nt}, Ps, \hat{s})$$ *Equation 56*

where:

| | |
|---|---|
| $N_a$ | Number of absorption channels |
| $N_q$ | Number of baseline channels |
| $R'_m$ | Absorption in the m$^{th}$ selected absorption channel |
| $R_p$ | Radiance in the p$^{th}$ selected baseline channel |
| $Ts$ | Surface temperature |
| $T_k$ | Temperature at the k$^{th}$ selected pressure level |
| $Ps$ | Surface pressure |
| $\hat{s}$ | Secant of the satellite zenith angle. |

The absorptions R'$_i$ are defined as follows:

$$R'_i = B_i - R_i$$ *Equation 57*

with $B_i$, the baseline radiance at selected channel $i$.

$$B_i = \frac{2hc^2\nu_i^3}{\exp\left(\frac{hc\nu_i}{k_B\overline{T_b}}\right) - 1}$$ *Equation 58*

and the mean baseline brightness temperature:

$$\overline{T_b} = \frac{1}{N_q}\sum_{n=1}^{N_q} \frac{hc\nu_q(n)}{k_B \ln\left(\frac{2hc^2\nu_q^3(n)}{R_q(n)} + 1\right)}$$ *Equation 59*

where:

| | |
|---|---|
| $k_B$ | = Boltzmann's constant |
| $H$ | = Planck's constant |
| $C$ | = speed of light |
| $N_q$ | = number of IASI channels defining the baseline |
| $v_q(n)$ | = a baseline wavenumber |
| $R_q(n)$ | = a baseline radiance |
| $n$ | = an index in the array of channels used to define the baseline |

The trace gas amounts resulting from Equation 54 are normalised values and have to be rescaled to physical units with associated pairs of de-normalisation coefficients $(D^1;D^2)$ and the following formula:

$$\bar{O}_q = O_q . \frac{D_q^2}{0.9} + D_q^1 \qquad \textit{Equation 60}$$

The number of neurons, the weights and biases, the input and output scaling coefficients as well as the channel and the pressure level selections named in this section are configurable constants. They are stored in the auxiliary datasets COF_TRG* See Section 8.2.9. The retrieved columnar amounts $\bar{O}_q$ with this configuration come then in molecules per cm$^2$. They can be further converted to kg/m$^2$, the standard units for EPS IASI level 2 products as follows:

$$kg/m^2 = molecules/cm^2 \times m_q \times 10^4 \qquad \textit{Equation 61}$$

with $m_q$ being the molecular mass of the respective gas $\mathrm{q} = (\mathrm{CO_2}, \mathrm{CH_4}, \mathrm{N_2O})$.

The error covariance associated with this retrieval is assumed to be diagonal, and constant.
The ANN retrieval of trace gases can be vulnerable to sun glint and must be flagged as such.

## 5.8 Optimal estimation retrieval of geophysical thermodynamic parameters

In clear sky situations, an optimal estimation retrieval is performed [Rodgers] The optimal estimation uses the all-sky statistical retrieval, not only as first guess (FG), but also as a-priori (background). The **FLG_CLDNES**, supplemented with two additional cloud tests (Section 5.8.2 and Section 5.8.1), is used for the selection of applicable clear-sky cases. Specifications for this selection are in Section 5.8.2 and Section 5.8.1.

### 5.8.1 AVHRR homogeneity test

This test assumes that clear-sky scenes are homogeneous to an extent in the infrared. A simple measure of the inhomogeneity $\eta$ of AVHRR measurements within a IASI FOV is computed as follows:

$$\eta = \left(\frac{\sigma_4}{\mu_4} + \frac{\sigma_5}{\mu_5}\right)/2 \qquad \textit{Equation 62}$$

where:

| | |
|---|---|
| $\mu_4$ | is the overall mean radiance of AVHRR channel 4 |
| $\mu_5$ | is the overall mean radiance of AVHRR channel 5 |
| $\sigma_4$ | is the standard deviation for mean radiance of AVHRR channel 4 |
| $\sigma_5$ | is the standard deviation for mean radiance of AVHRR channel 5 |

The scene is declared cloud-free according to this test if the inhomogeneity measure $\eta$ is less than the configurable threshold defined in `MaxInhomogeneity`, from the configuration file `iasi2_ppf.conf`. The execution and the outcome of this test shall be reflected in the flag **FLG_CLDTST**.

### 5.8.2 IASI/AMSU test

This test compares the brightness temperature observed in channel 6980, $T_{6980}^{obs}$, with a clear-sky predicted value based on the collocated AMSU measurement, $T_{6980}^{clr}$.

The clear-sky predicted brightness temperature of IASI channel 6980, $T_{6980}^{clr}$, is computed as follows:

$$T_{6980}^{clr} = 44.007 - 0.272T_4 + 1.837T_5 - 0.738T_6 + 0.004c_{sz} + 6.391(1 - c_{view}) \qquad \textit{Equation 63}$$

where:

| | |
|---|---|
| $T_4$ | is the brightness temperatures of AMSU channel 4 |
| $T_5$ | is the brightness temperatures of AMSU channel 5 |
| $T_6$ | is the brightness temperatures of AMSU channel 6 |
| $c_{sz}$ | is the cosine of the sun zenith angle |
| $c_{view}$ | is the cosine of the AMSU scan angle |

The scene is declared cloud-free according to this test if the following Equation 64 is true:

$$T_{6980}^{clr} - T_{6980}^{clr} > \tau \qquad \textit{Equation 64}$$

where $\tau$ is configured in the field *MinIasiMinusAmsu* from the configuration file `iasi2_ppf.conf` described in Section8.3. The execution and the outcome of this test is reflected in the flag **FLG_CLDTST**.

### 5.8.3 The cost function

The optimal estimation retrieval of the geophysical thermodynamic parameters is performed by minimisation of a cost function, $J$, consisting of two terms, the background ($J_x$) and the observation ($J_y$) terms, which we describe separately below.

$$J = J_x + J_y \qquad \textit{Equation 65}$$

#### *5.8.3.1 Background term of the cost function*

Given the equation:

$$\boldsymbol{J_x = (x - x_a)^T S_x^{-1} (x - x_a)} \qquad \textit{Equation 66}$$

The state-vector $x \in R^n$ represents the quantities to be retrieved:

- temperature profile (T),
- water vapour profile (W),
- ozone profile (O)
- surface skin temperature (Ts)

$$x = (T_1, \dots, T_{N_T}, W_1, \dots, W_{N_W}, O_1, \dots, O_{N_O}, T_S) \qquad \textit{Equation 67}$$

where:

| | |
|---|---|
| $N_T$ | number of levels in the profiles of temperature to be retrieved |
| $N_W$ | number of levels in the profiles of water to be retrieved |
| $N_O$ | number of levels in the profiles of ozone to be retrieved |

$N_T$, $N_W$ and $N_O$ < 250.

For the minimisation, the profiles are represented as principal component (PC) scores of the deviation with respect to the a-priori. In the IASI L2 PPF version 6, $x \in R^n$ writes as follows:

$$x = (t_1, \dots, t_{n_t}, w_1, \dots, w_{n_w}, o_1, \dots, o_{n_o}, T_S) \qquad \textit{Equation 68}$$

where:

| | |
|---|---|
| $n_t$ | is the number of PCS used to represent the profiles of temperature |
| $n_w$ | is the number of PCS used to represent the profiles of water vapour |
| $n_o$ | is the number of PCS used to represent the profiles of ozone |

The number of principal component scores used for each of the three types of profiles are configurable. In the IASI L2 PPF version 6,

$$n_T = 28, n_W = 18,\ n_O = 10.$$

The total number of state-vector elements is $n = n_T + n_W + n_O + 1$. $\boldsymbol{S_x}$ is diagonal matrix.

The elements on the diagonal can be extracted from the static auxiliary dataset `COF_STV`. This dataset is defined in Section 8.2.8 and summarised in Table 20:

| *Stave-vector component* | *Dimension* | *Unit (of corresponding PCs)* | *Diagonal of Sx* |
|---|---|---|---|
| $x_T$ | $n_T$ | K | /COF_STV/T_covariance |
| $x_W$ | $n_W$ | ln(ppmv) | /COF_STV/W_covariance |
| $x_O$ | $n_O$ | ln(ppmv) | /COF_STV/O_covariance |
| $x_{Ts}$ | 1 | K | $9K^2$ |

*Table 20: Elements on the diagonal can be extracted from the static auxiliary dataset `COF_STV`.*

As the PC scores used in the state-vector representation of the profiles are based on deviations from an a-priori profile given at the 101 fixed pressure levels RTTOV grid, the a-priori $x_a$ in this representation is zero —except for the last element corresponding to Ts. The principal components required to expand the PC scores into profiles represented at 101 pressure levels are also given in the dataset `COF_STV`. See Section 8.2.8.

#### *5.8.3.2 Observation term of the cost function*

$$\boldsymbol{J_y = (F(x) - y)^T S_y^{-1} (F(x) - y)} \qquad \textit{Equation 69}$$

The IASI observations are represented as a subset of reconstructed IASI L1C radiances with the unit $mW/m^2/sr/cm^{-1}$. The channel selection currently consists of $m = 139$ channels, which are specified in `COF_SY)`. A different observation error covariance matrix, $S_y$ (unit: $(mW/m^2/sr/cm^{-1})^2$ ), is used over land and sea, they are provided in `COF_SY_LAN [8.2.2] and COF_SY_SEA` respectively [8.2.3].

$S_y$ is the combined measurement and forward model error. The channel selection is provided with an assumed IASI channel numbering from 0 to 8460.

The forward model F: $R^n \rightarrow R^m$ is composed of two functions:

- the state-vector representation function X: $R^n \rightarrow R^N$
- and the RTTOV 10.2 implemented function f: $R^N \rightarrow R^m$.

Here, $N = 304$, corresponding to the atmospheric temperature in K, the atmospheric water vapour concentration in ppmv and the atmospheric ozone concentration in ppmv. All are at 101 fixed pressure levels each. This includes the surface skin temperature. The state-vector representation function is computed individually for each component. For T we have $X_T = X_T^a + E_T x_T$ , where $E_T \in R^{N_T \times n_T}$ are the $n_T$ leading principal components found in the dataset `/COF_STV/T_eigenvectors [8.2.8]` and $X_T^a$ is the a priori temperature profile in K at 101 levels which is obtained by piecewise linear regression within each individual field of view (see Section 5.4). This is similar for W and O, except that the principal components are based on ln(ppmv) such that we get the following:

$X_W = \exp(\ln(X_W^a) + E_W x_W)$ and $X_O = \exp(\ln(X_O^a) + E_O x_O)$,

where $X_W^a$ and $X_O^a$ are the a priori water vapour and ozone concentrations in ppmv at 101 levels.

The reconstructed radiances, y, are obtained from the IASI L1C PC scores provided in the PRP files. The eigenvector files (with format as described in section 8.1) are needed to reconstruct IASI L1C radiances from the PC scores, as described in the pseudo code in Figure 13:

```
K  = [FirstChannel .. FirstChannel+NbrChannels[
P1 = [1 .. NBSxP1]
P2 = [NBSxP1 + 1 .. NBSxP1 + NBSxP2]
P3 = [NBSxP1 + NBSxP2 + 1 .. NBSxP1 + NBSxP2 + NBSxP3]
P  = [1 .. NBSxP1 + NBSxP2 + NBSxP3]

Input data:
Noise(K) [unit: W/m2/sr/m-1]       // from eigenvector file
Mean(K)                            // from eigenvector file
PcScoresBxP1(P1)                   // from MDR-PCS
PcScoresBxP2(P2)                   // from MDR-PCS
PcScoresBxP3(P3)                   // from MDR-PCS
Eigenvectors(K,P)                  // from eigenvector file
SQ = ScoreQuantisationFactor(x)    // from GIADR-IPCC

Output:
Radiance(K)  [unit: W/m2/sr/m-1]

Algorithm:
Radiance(K) = Noise(K)*(
                          Mean(K)
                          + SQ*sum(P1, PcScoresBxP1(P1)*Eigenvectors(K,P1))
                          + SQ*sum(P2, PcScoresBxP2(P2)*Eigenvectors(K,P2))
                          + SQ*sum(P3, PcScoresBxP3(P3)*Eigenvectors(K,P2))
```

*Figure 13: Pseudo code (reconstruction of radiances in band x0.*

To suppress Instrument artefacts, this is followed by a projection onto the forward model subspace as defined by the first 62 vectors in `IASI_EV1_1C_M02_FS.hdf5` and the first 77 vectors in `IASI_EV2_1C_M02_FS.hdf5`.

***Note:*** No channels from Band 3 enter the retrievals.

Finally, the double-filtered radiances are bias-corrected. The bias correction to be applied:

$bc_j$ (for j=1..N),

is subtracted from the double-filtered measurement radiances. It is a linear function of the following:

- the $M_1$ leading PC scores in band 1,
- the leading $M_2$ PC scores in band 2
- the secant of the scan angle, $secz = \sec \hat{z}_{sat} = 1/\cos \hat{z}_{sat}$.

If $x$ is a vector with $M_1 + M_2 + 1$ elements composed as described above:

$$p = \left(PCS_1^{B_1}, \ldots, PCS_{M_1}^{B_1}, PCS_1^{B_2}, \ldots, PCS_{M_1}^{B_2}, secz\right)$$

the bias correction can be computed as follows:

$$bc_j = \overline{bc_j} + \sum_{i=1}^{M1+M2+1} \mathcal{B}_{ji}(x_i - \bar{p}_i) \qquad \textit{Equation 70}$$

where the coefficients $\mathcal{B}_{ji}$, $\bar{p}_i$ and $\overline{bc_j}$ are defined in COF_BC. Specifications are in Section 8.2.7.

### 5.8.4 The minimisation method and convergence criterion

The cost function $J(x) = J_x(x) + J_y(x)$ detailed in Equation 71 is smooth and for any point, $x$, we can compute its gradient:

$g(x) \in R^n$ in Equation 72

and its Hessian matrix,

$H(x) \in R^{n \times n}$ as per Equation 73.

The cost function and its first two derivatives (gradient and Hessian) write:

$$J_n = (F(x_n) - y)^T . S_y^{-1} . (F(x_n) - y) + (x_n - x_a)^T . C^{-1} . (x_n - x_a) \qquad \textit{Equation 71}$$

$$J_n' = K_n^T . S_y^{-1} . (F(x_n) - y) + S_x^{-1} . (x_n - x_a) \qquad \textit{Equation 72}$$

$$J_n'' = K_n^T . S_y^{-1} . K_n^T + S_x^{-1} \qquad \textit{Equation 73}$$

where:

| | |
|---|---|
| $x_n$ | is the atmospheric state at iteration $n$ |
| $J_n$ | is the cost function at iteration $n$ |
| $F(x_n)$ | is the forward model computation, or calculated radiances, with $x_n$ See Section 5.8.5. |
| $y$ | is the observation vector, from the measured radiances |
| $K_n$ | is the derivative of the forward model function to the state vector components, also called Jacobians |

The method is considered to have converged in these cases:

- if the norm as computed in Section 6.10 of the gradient, $\|\vec{g}\|$, is lower than a configurable threshold `ConvergenceThreshold` in the `iasi2_ppf.conf`. See Specifications in Section 8.3.
- or if the relative Newton step size, $\|d\|/\|x\|$, is below 0.00000001.

Furthermore a configurable maximum number of iterations is imposed ("`MaxIterations`" in `iasi2_ppf.conf` (see Section 8.3). The minimisation function shall be exited when this maximum number of iterations is reached.

Minimisation of the cost function is only attempted if the initial value (computed for the first guess) is below a configurable threshold ("`FGCostMax`" in `iasi2_ppf.conf`). In case minimisation is attempted, two separate configurable thresholds, `RTCostMax_X` and `RTCostMax_Y` in `iasi2_ppf.conf` are applied to the resulting values of the background and observation terms of the cost function: $J_{x,n}$ and $J_{y,n}$ respectively. All of this sequence is detailed in Section 5.8.4. The optimal estimation retrieval is only accepted if both terms of the cost function are below their

respective thresholds. The overall minimisation and acceptance process is summarised in the pseudo-code in Figure 14:

***Note***: The optimal estimation retrieval can be accepted –and therefore be available in the product– even if the iterations did not converge and the minimisation was stopped after reaching the maximum number of iterations.

01: $\alpha = 1; n = 0; x_0 = FG$
02: **if** $(J(x_0) >$ FGCostMax) **then** return */* do not attempt minimisation */*
03: **while** $(n <$ MaxIterations) **do**
04: $d = H(x_n)^{-1} g(x_n)$
05: **if** $\left(J(x_n - \alpha d) < J(x_n)\right)$ **then**
06: $x_{n+1} = x_n - \alpha d;\ \alpha = 1$
07: **else**
08: $\alpha = \frac{\alpha}{2}$; **goto 3**
09: $n = n + 1$
10: **if** $\left( \begin{matrix} (\|g\| < \text{ConvergenceThreshold}) \\ \textbf{OR}\ (\|d\|/\|x_n\| < 10^{-8}) \end{matrix} \right)$ **then** *converged* **break**
11: **endwhile**
12: **if** $\left(\left(J_{x,n} < \text{RTCostMax\_X}\right)\ \textbf{AND}\ \left(J_{y,n} < \text{RTCostMax\_Y}\right)\right)$ **then** *accept_retrieval*

*Figure 14: The overall minimisation and acceptance process pseudo-code.*

where:

| | |
|---|---|
| $d$ | is the step in the state space $x$, after the Newton descent |
| $\alpha$ | is the fraction of the step $d$ to be applied to the state vector |

The flag **FLG_ITCONV** is set according to the outcome of the optimal estimation as summarised in Table 11:

| *Value* | *Reason for flagging* |
|---|---|
| 0 | The FOV was not considered sufficiently clear for clear sky optimal estimation. FLG_CLDNES>2 or (at least) one of the two additional cloud test was not passed. |
| 1 | The minimisation of cost function not attempted due to high cost of the first guess. |
| 2 | The minimisation did not converge and the solution was not accepted. |
| 3 | The solution was accepted, even though the minimisation did not converge. |
| 4 | The minimisation converged, but the solution was not accepted. |
| 5 | The solution was accepted and the minimisation converged. |

*Table 21: Settings for flag FLG_ITCONV .*

The number of iteration performed shall be copied into the flag **FLG_NUMIT**.

### 5.8.5 The radiative transfer model

RTTOV 10.2 is configured using coefficients based on LBLRTM v.12.2 with 101 levels, predictors version 7 and a creation date of 28 March 2013 is used as a radiative transfer model [RTTOVguide] With these coefficients, the trace gases $CO_2$, CO, $N_2O$ and $CH_4$ are not variable and their concentrations do not need to be input. The state vector input to RTTOV reads as follows:

$$x = \left(\boldsymbol{T_1}, \dots, \boldsymbol{T_{N_T}}, \boldsymbol{W_1}, \dots, \boldsymbol{W_{N_W}}, \boldsymbol{O_1}, \dots, \boldsymbol{O_{N_O}}, \boldsymbol{T_S}, T_a, W_a, P_S, \hat{z}_{sat}, h, \varepsilon_1, \dots, \varepsilon_{N_k}\right) \quad \textit{Equation 74}$$

Besides the optimal estimation state-vector parameters–in bold in Equation 74, there are only few parameters which need to be fed to RTTOV in order to compute the forward model radiances. These parameters are kept fixed for each field of view and their origins are specified below. The satellite zenith angle and the surface height are taken from the PRP file: the satellite zenith angle originates directly from the IASI L1C file, the surface height is co-located from the topography atlas as described in Section 5.1.3. The two-meter air temperature $T_a$ and humidity $W_a$ as well as the surface pressure $P_S$ are taken from PWLR. The land surface emissivity $(\varepsilon_1, \dots, \varepsilon_{N_k})$ in the $N_k$ selected channels is reconstructed from the emissivities retrieved with the PWLR[3] in section 5.4.

### 5.8.6 Retrieval error estimate and averaging kernels

The optimal estimation retrieval error covariance matrix estimate, $S$, is given by the inverse of the Hessian matrix, i.e.

$$S = (K^T S_y^{-1} K + S_x^{-1})^{-1} \quad \textit{Equation 75}$$

where:

| | |
|---|---|
| $K \in R^{m \times n}$ | is the matrix of partial derivates (Jacobian) of the forward model F: $R^n \rightarrow R^m$ evaluated at the optimal solution. The forward model is introduced in Section 5.8.3.2. |

This retrieval error covariance matrix refers to the error in the principal component space in which the retrieval was performed. See Section 5.8.3.1. The minimisation is performed assuming no cross-correlation between temperature, water-vapour and ozone profiles, such that $S$ writes:

$$S = \begin{pmatrix} S_T & & \\ & S_W & \\ & & S_O \end{pmatrix} \qquad \textit{Equation 76}$$

The diagonal blocks corresponding to temperature, water vapour and ozone are provided in the output product separately.

***Note***: The averaging kernel (in PC space), ***A***, can be computed with this formula:

$$A = I - SS_x^{-1} \qquad \textit{Equation 77}$$

where:

| | |
|---|---|
| $I$ | is the identity matrix |
| $S$ | is the computed after Equation 75 and Equation 76. |
| $S_x^{-1}$ | is the background error covariance matrix introduced in Section 5.8.3.1 and configured in COF_STV Section 8.2.8. |

Both the retrieval error covariance matrix and the averaging kernel expressed in the principal components of the atmospheric state $S_{PC}$ and $A_{PC}$ can be transformed to the 101 level pressure grid of RTTOV -$S_{SV}$ and $A_{SV}$- by pre and post multiplication with the $N \times n$ matrix of atmospheric state eigenvectors $V$ provided in `COF_STV`. This is defined in Section 8.2.8:

$$S_{SV} = VS_{PC}V^T \qquad \textit{Equation 78}$$
$$A_{SV} = VA_{PC}V^T \qquad \textit{Equation 79}$$

### 5.8.7 Check for physical adiabiatic and saturation conditions

The temperature and humidity profiles resulting from the optimal estimation and accepted as described in 5.8.4 shall be verified against physical boundary conditions. The profiles deviating the super-saturation and super-adiabatic conditions shall be modified and flagged accordingly in **FLG_PHYSCHECK**, as specified in the sections 6.14 and 6.15.

## 5.9 Optimal estimation retrieval of atmospheric composition parameters

### 5.9.1 FORLI-CO

The IASI L2 PPF integrates the FORLI algorithm [FORLI] as an external library for the retrieval CO profiles, forming the EUMETSAT AC SAF IASI CO products. The reader is invited to consult the FORLI-CO ATBD for a detailed description of the algorithm and implementation [FORLIatbd].

### 5.9.2 Brescia-$SO_2$

The IASI L2 PPF integrates the Brescia-$SO_2$ algorithm as an external library for the retrieval of $SO_2$ partial columns, forming the EUMETSAT AC SAF IASI SO2 products. The reader is invited to consult de Brescia-$SO_2$ ATBD for a detailed description of the algorithm and implementation [BresciaATBD].

## 5.10 Generation of the IASI L2Pcore product

The SST retrieved within the IASI L2 PPF is also recorded in isolation in the IASI L2Pcore products, which form the seed to the IASI L2P SST product. The IASI L2Pcore SST is encoded in netCDF and contains the core products elements after GHRRST (the Group for High Resolution SST) standards. It is then augmented at the EUMETSAT OSI SAF with additional meta and contextual information as required by GHRSST [*GHRSSTspe*]. The IASI L2Pcore contains the fields identified in Table 22.

| *Field* | *Description* |
|---|---|
| Latitude | Latitude (degrees North) |
| Longitude | Longitude (degrees East) |
| Time | Reference time of SST data array |
| Sea_surface_temperature | Skin SST measurement values (full resolution) |
| Sst_dtime | Deviation of observation time from reference time |
| L2P_flags | Flag qualifying SST input data |
| SSES_bias | Single Sensor Error Statistics bias |
| SSES_standard _deviation | Single Sensor Error Statistics standard deviation uncertainty |
| Satellite_zenith_angle | Satellite zenith angle (degrees) |
| Solar_zenith_angle | Solar zenith angle (degrees) |
| Quality_level | L2P data quality, from 2 (first useable data) to 5 (best quality) |
| Wind_speed | 10-metre ECMWF wind speed (m/s) |
| obs_minus_calc | Sum of observed minus calculated radiances in window region (experimental) |
| dust_index | Pseudo-quantitative dust index FLG_DUSTCLD (experimental) |

*Table 22: IASI L2Pcore SST field description*

As per GHRSST standards, the retrieved SST are classified into quality classes:

- Quality Level 5: best
- Quality Level 4: good
- Quality Level 3: fair
- Quality Level 2: first usable quality
- Quality Level 1: bad

A single sensor error estimate (SSES) field provides the information on the bias (accuracy) and standard deviation (precision) associated with each quality class. This is determined off-line from routine monitoring against in situ drifting buoys, the OSTIA model and 3-way analyses with sondes and other satellite high spatial resolution products (e.g. AVHRR SST). The SSES are configured in the auxiliary dataset files IASI_L2P_xxx_* (Section 8.3).

The stratification per quality classes is done upon the 'OmC' cloud signal retrieved with the PWLR[3] (see section 5.4) as follows:

| *Quality classes* | *OmC condition* |
|---|---|
| Q5 | $\|OmC\| < 0.5$ |
| Q4 | $0.5 \leq \|OmC\| < 1.$ |
| Q3 | $1 \leq \|OmC\| < 2$ |
| Q2 | $1 \leq \|OmC\| < 3$ |
| Q1 | $\|OmC\| \geq 3$ |

## 5.11 Quality control of the final products

The quantities retrieved in complement to the first guess retrieval must be verified against configurable bounds before being copied into the final IASI L2 products. If a parameter retrieved with the statistical method is out of the expected range, the corresponding bit of the flag **FLG_RETCHECK** shall be raised and the exceeding value reset to the nearest bound. The profiles are treated as whole in **FLG_RETCHECK**, this means that if the value of at least one pressure level is out of valid bounds then the entire profile is be flagged. The validity bounds are configurable and may vary with the geolocation and time in the year.

# 6 GENERIC FUNCTIONS

While the first part of this document described the processing functions in sequence, this section contains the details and specifications for generic functions which may be invoked by different processing modules.

## 6.1 Instrument foot-print size and Earth coordinates

Let ζ be the satellite zenith angle at the observation point defined by the IASI IFOV centre and let $\theta$ be the scanning angle, defined from Nadir. The relationship between ζ and $\theta$ writes:

$$\zeta = \operatorname{asin}\left(\frac{(R_\oplus + h)}{R_\oplus}\sin\theta\right) \qquad \textit{Equation 80}$$

$$\theta = \operatorname{asin}\left(\frac{R_\oplus}{(R_\oplus + h)}\sin\zeta\right) \qquad \textit{Equation 81}$$

Let α be the angle defined by the sub-satellite point, the Earth centre and the IFOV centre. Then:

$$\alpha = \zeta - \theta \qquad \textit{Equation 82}$$

And from Equation 81, it follows:

$$\alpha = \operatorname{asin}\left(\frac{(R_\oplus + h)}{R_\oplus}\sin\theta\right) - \theta \qquad \textit{Equation 83}$$

The projection on the Earth ground of the field of view is, approximately, an ellipse:

- the semi-major axis in the scan direction is $a_{scan}$
- the semi-minor axis in the track direction is $a_{track}$,

are approximated as follows:

$$a_{scan} = \frac{1}{2}.R_\oplus.|\alpha_1 - \alpha_2| \qquad \textit{Equation 84}$$

Where $\alpha_1$ and $\alpha_2$ are the angles defined by the sub-satellite point, the Earth centre and the bounding points of the footprint in the scan direction.

Given $\vartheta_{scan}$, the IFOV angular aperture in the scan direction, $\alpha_1$ and $\alpha_2$ can be computed with Equation 83 and the viewing angles $\theta_1 = \theta - \vartheta_{scan}/2$ and $\theta_2 = \theta + \vartheta_{scan}/2$, respectively.

$$a_{track} = \frac{1}{2}.R_\oplus.\vartheta_{track}.\frac{\sin(\zeta - \theta)}{\sin\theta} \qquad \textit{Equation 85}$$

Where $\vartheta_{track}$ is the IFOV angular aperture in the flight direction.

## 6.2 IPSF pixels weight and geolocation

The instrument point spread function defines the geometric distribution of the contribution to the IASI measurements within each IFOV and is different for each of the four detectors within an EFOV. For each detector the IPSF is sampled on a regular grid in viewing angle in the so-called cold space. The dimensions $N_Y$ and $N_Z$ are variable and are defined for each product in the fields *IDefPsfSondNbLin* and *IDefPsfSondNbCol* of the GIADR-quality in the IASI L1C products. Each grid cell is identified by its indices $i = 1..N_Y$ and $j = 1..N_Z$ and its angular coordinates $\hat{y}_i$ and $\hat{z}_j$ in the frame of reference summarised in Figure 15. $\hat{y}_i$ and $\hat{z}_j$ are stored in the fields *IDefPsfSondY* and *IDefPsfSondZ* of the L1C GIADR-quality. The IPSF weights $\Psi_{i,j}$ at grid points $(i;j)$ are defined in the field *IDefPsfSondWgt* of the L1C GIADR-quality.

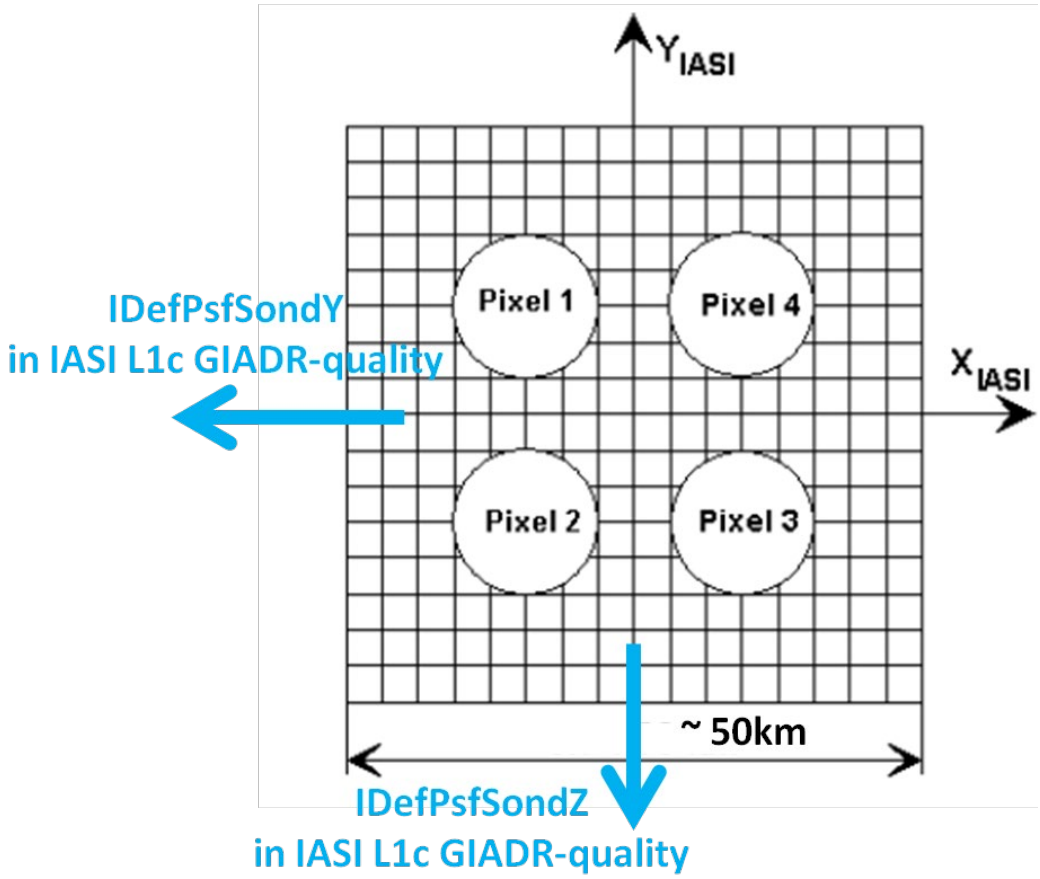


*Figure 15: Definition of the PSF grid coordinates in the IASI Nadir viewing, adapted from IASIL1spe.*

The geolocation of the centre of each of the IPSF grid cell in the IFOV $u$, $\lambda_u(i,j)$ and $\varphi_u(i,j)$, is computed from the geolocations of the centres of the four IFOVs assuming a local linear relationship between the geolocations and the $(\hat{Z},\hat{Y})$ viewing angle coordinates. This is done in turn in each IFOV $u = 1..4$ using the 3-point barycentric interpolation with the two direct neighbours as listed in Equation 88. See also Section 6.9.

$$\lambda_u(i,j) = baryInterp\left((\Lambda_u,\hat{Y}_u,\hat{Z}_u),(\Lambda_v,\hat{Y}_v,\hat{Z}_v),(\Lambda_w,\hat{Y}_w,\hat{Z}_w),(\hat{y}_{u,i},\hat{z}_{u,j})\right) \quad \textit{Equation 86}$$

$$\varphi_u(i,j) = baryInterp\left((\Phi_u,\hat{Y}_u,\hat{Z}_u),(\Phi_v,\hat{Y}_v,\hat{Z}_v),(\Phi_w,\hat{Y}_w,\hat{Z}_w),(\hat{y}_{u,i},\hat{z}_{u,j})\right) \quad \textit{Equation 87}$$

where:

| | |
|---|---|
| $\Lambda_{1..4}$ | is the latitude of the centre of the IFOVs 1 to 4. |
| $\Phi_{1..4}$ | is the longitude of the centre of the IFOVs 1 to 4. |
| $\hat{Y}_{1..4}$ | is an angular coordinate of the centre of the IFOVs 1 to 4 in the viewing frame. |
| $\hat{Z}_{1..4}$ | is an angular coordinate of the centre of the IFOVs 1 to 4 in the viewing frame. |
| $\lambda_u(i,j)$ | is the latitude of the centre of the PSF grid cell (i;j) in the IFOV $u = 1..4$. |
| $\varphi_u(i,j)$ | is the longitude of the centre of the PSF grid cell (i;j) in the IFOV $u = 1..4$ |
| $\hat{y}_{u,i}$ | is an angular coordinate of the centre of the PSF grid cell (i;j) in the IFOV $u = 1..4$. |
| $\hat{z}_{u,j}$ | is an angular coordinate of the centre of the PSF grid cell (i;j) in the IFOV $u = 1..4$. |

$$for\ u = \begin{cases} 1\ then\ v = 2\ and\ w = 4 \\ 2\ then\ v = 1\ and\ w = 3 \\ 3\ then\ v = 2\ and\ w = 4 \\ 4\ then\ v = 1\ and\ w = 3 \end{cases} \qquad \textit{Equation 88}$$

The $baryInterp$ function is the 3-point barycentric interpolation function.

Close to the poles, the latitude and longitude coordinates are not monotone continuous functions and the barycentric interpolation cannot be applied to the original geolocations. The interpolation must be performed in a Polar azimuthal projection. If the latitude of one of the four IFOVs is above 87 degrees ($|lat| > 87$ deg) then the geolocations of the four IFOVs $(\Lambda_{1..4}, \Phi_{1..4})$ must be transformed into Polar azimuthal coordinates $(\Upsilon_{1..4}^{Paz}, Z_{1..4}^{Paz})$ using Equation 89 and Equation 90. The barycentric interpolation as listed in Equation 86 to Equation 88 to Equation 87 is performed with these Polar azimuthal coordinates instead of the original latitudes and longitudes. The resulting PSF grid interpolated Polar coordinates $\upsilon_u^{Paz}(i,j)$ and $\zeta_u^{Paz}(i,j)$ are transformed back to latitudes and longitudes with Equation 91 and Equation 92.

The Polar azimuthal projection writes:

$$\upsilon = (90. - |\lambda|) * \cos\varphi \qquad \textit{Equation 89}$$
$$\zeta = (90. - |\lambda|) * \sin\varphi \qquad \textit{Equation 90}$$

where $(\upsilon; \zeta)$ are the projected coordinates of the point at latitude $\lambda$ and longitude $\varphi$.

The conversion from Polar projected coordinates to latitudes and longitudes writes:

$$|\lambda| = \left(90. - \sqrt{\upsilon^2 + \zeta^2}\right) \qquad \textit{Equation 91}$$
$$\varphi = sign(\zeta) * \cos^{-1}\left(\frac{\upsilon}{\sqrt{\upsilon^2 + \zeta^2}}\right) \qquad \textit{Equation 92}$$

## 6.3 Vertical interpolations of atmospheric temperature and constituent profiles

The temperature, water-vapour and ozone profiles are interpolated according to the following interpolation schemes. The temperature varies approximately linearly with the height, whereas the pressure decreases exponentially with height, so that a suitable interpolation of temperature $T$ at pressure $p$ in a pressure-level grid reads as follows:

$$T = T_0 + \frac{T_1 - T_0}{\ln\left(\frac{p_1}{p_0}\right)} . \ln\left(\frac{p}{p_0}\right)$$ *Equation 93*

where:

| | |
|---|---|
| $p_0$ | is a pressure level surrounding $p$. |
| $p_1$ | is a pressure level surrounding $p$. |
| $T_0$ | is a corresponding temperature value. |
| $T_1$ | is a corresponding temperature value. |

The water-vapour mixing ratio $W$ decreases exponentially with height, so that the interpolation at $p$ on a pressure grid is double-logarithmic ($p_0 > p > p_1$):

$$\ln W = \ln W_0 + \frac{\ln\left(\frac{W_1}{W_0}\right)}{\ln\left(\frac{p_1}{p_0}\right)} . \ln\left(\frac{p}{p_0}\right)$$ *Equation 94*

where:

| | |
|---|---|
| $p_0$ | is a pressure level surrounding $p$. |
| $p_1$ | is a pressure level surrounding $p$. |
| $W_0$ | is a corresponding water vapour value. |
| $W_1$ | is a corresponding water vapour value. |

Ozone profiles are interpolated in the same way as water-vapour.

## 6.4 Vertical integration of atmospheric constituent concentrations

Let $p_i$ and $\mu_i$ be the pressure and mixing ratio of a given atmospheric constituent defining a vertical profile on $N_{lev}$ levels. With $p_i$ and $\mu_i$ expressed in hPa and kg/kg, respectively, the partial columnar amount $c_i$ in kg/m$^2$ of this atmospheric constituent in the layer between two pressure levels $p_i > p_{i+1}$ is given by the formula:

$$c_i = \frac{\bar{\mu}(p_i - p_{i+1})}{g(\bar{z}, \phi)}; i = 0..N_{lev} - 2$$ *Equation 95*

where:

$$\bar{\mu} = \frac{\mu_i - \mu_{i+1}}{2} \qquad \textit{Equation 96}$$

$$\bar{z} = (z_i - z_{i+1})/2 \qquad \textit{Equation 97}$$

are the average mixing ratio and altitude of the layer defined by pressure levels $p_i$ and $p_{i+1}$.

| | |
|---|---|
| $g(\bar{z}, \phi)$ | is the local gravitational acceleration depending on latitude, ϕ |
| $\bar{z}$, | is height as defined in Equation 105. |

The conversion from pressure levels to height in Equation 97 is done as described in Section 5.13.5, starting from the surface level, whose elevation is known (5.1.3). Alternatively, it may also be approximated as follows:

$$\bar{z} = -4000(\log\left(\frac{p_i}{1013}\right) + \log\left(\frac{p_{i+1}}{1013}\right)) \qquad \textit{Equation 98}$$

To compute the integrated total columnar amount $TC$ of an atmospheric constituent, all partial columnar amounts of layers between the successive pressure levels on which the mixing ratio profile is provided must be computed as in Equation 95 and summed. To compute the partial columnar amount $c_{surf}$ in the layer between the surface pressure and the first pressure grid level above the surface on which the profile is defined, the mixing ratio is assumed constant in this layer and equal to the mixing ratio at the first pressure grid level above the surface. Hence:

$$c_{surf} = \mu_0(P_S - p_0)/g(\bar{z}, \phi) \qquad \textit{Equation 99}$$

where:

| | |
|---|---|
| $P_S$ | is the surface pressure |
| $\bar{z}$ | $= (z_{surf} - z_0)$ |
| $z_{surf}$ | is the surface elevation |
| $z_0$ | is the height of the first pressure grid level |

Finally, the total column writes:

$$TC = c_{surf} + \sum_{i=0}^{N_{lev}-2} c_i \qquad \textit{Equation 100}$$

## 6.5 Conversion from pressure to height levels

The conversion between pressure and height levels is done with the barometric equation. It is important that this equation is applied layer-wise as it represents an integration where constant temperature and humidity is assumed between the two consecutive levels defining a layer. The height difference between two levels $i$ and $j$ with known pressures $p_i$ and $p_j$ is given by the following:

$$z_i - z_j = \frac{-R_L \bar{T}_v}{g(z_i, \phi)} . ln\left(\frac{p_i}{p_j}\right) \qquad \textit{Equation 101}$$

Alternately, for known heights and the ratio of the pressures at levels *i* and *j* is as follows:

$$\frac{p_i}{p_j} = exp\left(\frac{-g(z_i, \phi)(z_i - z_j)}{R_L \bar{T}_v}\right) \qquad \textit{Equation 102}$$

where:

| | |
|---|---|
| $R_L$ | $= 287.06\ \mathrm{J.K^{-1}.kg^{-1}}$ is the gas constant for dry air |
| $\bar{T}_v$ | is the layer mean virtual temperature, represented as Equation 103 |

$$\bar{T}_v = (T_{v,i} + T_{v,j})/2 \qquad \textit{Equation 103}$$

where:

$$T_{v,i} = T_i(1 + 0.608 q_i) \qquad \textit{Equation 104}$$

with:

| | |
|---|---|
| $T_i$ | the temperature (in K) at level *i* |
| $q_i$ | is the specific humidity at level *i* (in kg/kg). |

The acceleration due to gravity $g$ (in m.s$^{-2}$) is a function of geographic latitude $\phi$ and height $z$ (in m):

$$g(z,\phi) = 9.80616\left(1 - 0.0026373\cos(\phi) + 0.0000059\cos^2(\phi)\right) - (3.085462 * 10^{-6} + 2.27 * 10^{-9} * \cos(\phi))z + (7.254 * 10^{-13} + 10^{-20} * \cos(\phi))z^2 - (1.517 * 10^{-19} + 6 * 10^{-22} * \cos(\phi))z^3$$ *Equation 105*

The form of Equation 101 and Equation 102 requires that the calculations always begin at a level with known start values of $z$ and $p$. Usually, surface pressure and surface height are the known start values and Equation 101 and Equation 102 are iterated towards the top of the atmosphere. The surface height for each IASI IFOV is retrieved as specified in 5.1.3 from the topography atlas.

## 6.6 Linear interpolation

The linear interpolation of a function *y(x)* at point *x* from the function values $y_0$ and $y_1$ at points $x_0$ and $x_1$ writes:

$$y = y_0 + (y_1 - y_0)\frac{(x - x_0)}{(x_1 - x_0)}$$ *Equation 106*

## 6.7 Bilinear interpolation

The bi-linear interpolation of a function *f(x,y)* at the point *(x;y)* from the function values $f_{00}$, $f_{01}$, $f_{11}$ and $f_{10}$ at points $(x_0; y_0)$, $(x_0; y_1)$, $(x_1; y_1)$, $(x_1; y_0)$ on a regular 2D-grid writes:

$$f(x,y) = \alpha_{00}(x_1 - x)(y_1 - y) + \alpha_{10}(x - x_0)(y_1 - y) + \alpha_{01}(x_1 - x)(y - y_0) + \alpha_{11}(x - x_0)(y - y_0)$$ *Equation 107*

where $\alpha_{ij} = \frac{f(x_i, y_j)}{(x_1 - x_0)(y_1 - y_0)}$

## 6.8 Three-point barycentric interpolation

The barycentric interpolation of a function $f$ at the coordinate point $(x, y)$ from the function values $f_1$, $f_2$, $f_3$ at coordinate points $(x_1, y_1)$, $(x_2, y_2)$, $(x_3, y_3)$ writes:

$$f(x,y) = \frac{\alpha_1 f_1 + \alpha_2 f_2 + \alpha_3 f_3}{\alpha_1 + \alpha_2 + \alpha_3}$$ *Equation 108*

where:

$$\alpha_1 = (x_2 - x)(y_3 - y) - (x_3 - x)(y_2 - y)$$ *Equation 109*

$$\alpha_2 = (x_3 - x)(y_1 - y) - (x_1 - x)(y_3 - y)$$ *Equation 110*

$$\alpha_3 = (x_1 - x)(y_2 - y) - (x_2 - x)(y_1 - y)$$ *Equation 111*

## 6.9 Euclidean norm

The Euclidean norm of a vector $\vec{V} = [v_1, v_2, \ldots, v_n]$ of dimension $n$, noted $\|\vec{V}\|$, writes:

$$\|\vec{V}\| = \sqrt{\sum_{i=1}^{n} v_i^2} \qquad \textit{Equation 112}$$

## 6.10 Dot product

The dot product, also called scalar product, of two vectors:

$\vec{U} = [u_1, u_2, \ldots, u_n]$ and

$\vec{V} = [v_1, v_2, \ldots, v_n]$

of dimension *n* writes:

$$\vec{U} \cdot \vec{V} = \sum_{i=1}^{n} u_i \, v_i \qquad \textit{Equation 113}$$

### 6.10.1 Vector product

The vector product, also called cross product, of two vectors $\overrightarrow{V_1}$ and $\overrightarrow{V_2}$ in Cartesian coordinates (x,y,z) writes:

$$\overrightarrow{V_1} \times \overrightarrow{V_2} = \begin{pmatrix} x_1 \\ y_1 \\ z_1 \end{pmatrix} \times \begin{pmatrix} x_2 \\ y_2 \\ z_2 \end{pmatrix} = \begin{pmatrix} y_1 z_2 - y_2 z_1 \\ z_1 x_2 - z_2 x_1 \\ x_1 y_2 - x_2 y_1 \end{pmatrix} \qquad \textit{Equation 114}$$

## 6.11 Geolocation conversion to Cartesian coordinates

In the Cartesian coordinate system, the x-axis goes through (longitude, latitude = 0,0), the y-axis goes through (longitude, latitude = 90,0) and the z-axis goes through the poles. The conversion of longitude φ and latitude λ to Cartesian co-ordinates $(x, y, z)$ writes:

$$\begin{cases} x = R_\oplus \cos\lambda \cos\varphi \\ y = R_\oplus \cos\lambda \sin\varphi \\ z = R_\oplus \sin\lambda \end{cases} \qquad \textit{Equation 115}$$

Where $R_\oplus$ is the Earth radius.

## 6.12 Water-vapour density definitions and relationships

The humidity concentrations can be expressed in different units. We detail here the representations used in various functions of the processor and detail their relationships.

### The water-vapour pressure, $p_{H_2O}$

The vapour pressure of moist air is defined as the partial pressure of the water-vapour present in the air mass. It is said to be with respect to liquid (or ice) water if the air mass is over a plane surface of liquid (or ice) water at the same temperature and pressure.

### The water-vapour saturation pressure, $e_S$

The water-vapour saturation pressure is defined as the water-vapour pressure where two phases of water co-exist in neutral equilibrium. It is said to be with respect to liquid (or ice) water if the air mass is over a plane surface of liquid (or ice) water at the same temperature and pressure. The saturation water-vapour pressure, $e_S$, is given by the integrated Clausius Clapeyron equation, as formulated by the Goff Gratch equations [SmithMet].

Over water, the saturation water-vapour pressure in hPa is as follows:

$$\log_{10}(e_S) = -7.90298 * \left(\frac{T_S}{T} - 1\right) + 5.02808 * \log_{10}\left(\frac{T_S}{T}\right) - 1.3816 * 10^{-7} * \left(10^{11.344*\left(1-\frac{T}{T_S}\right)} - 1\right) + 8.1328 * 10^{-3} * \left(10^{-3.49149*\left(\frac{T_S}{T}-1\right)} - 1\right) + \log_{10}(e_{wS})$$

*Equation 116*

where:

| | |
|---|---|
| $T$ | = the temperature in K. |
| $T_S$ | = 373.16 $K$ |
| $e_{wS}$ | = 1013.246 hPa |

Over ice, the saturation water vapour pressure in hPa is as follows:

$$\log_{10}(e_S) = -9.09718 * \left(\frac{T_0}{T} - 1\right) - 3.56654 * \log_{10}\left(\frac{T_0}{T}\right) + 0.876793 * \left(1 - \frac{T}{T_0}\right) + \log_{10}(e_{i0})$$

*Equation 117*

where:

| | |
|---|---|
| $T_0$ | = 273.16 K. |
| $e_{i0}$ | = 6.1071 hPa. |

### Specific humidity, $q$

The specific humidity is the ratio of water-vapour mass to the air parcel's total mass, approximated as the mixing ratio of the mass of water-vapour in an air parcel to the mass of dry air for the same parcel. It is expressed in kg/kg.

$$q = \frac{M_{H_2O}}{M_L}.\frac{p_{H_2O}}{p - p_{H_2O}}$$ *Equation 118*

Conversely, $p_{H_2O}$ can be retrieved from $q$ as follows:

$$p_{H_2O} = \frac{p}{1 + \frac{M_{H_2O}}{M_L}.\frac{1}{q}}$$ *Equation 119*

where:

| | |
|---|---|
| $M_{H_2O}$ | = 18.01534 $g/mol$ is the Molar mass of water. |
| $M_L$ | = 28.964$g/mol$ is the Molar mass of dry air. |
| $p$ | = total atmospheric pressure of water-vapour in the air parcel |
| $p_{H_2O}$ | = partial atmospheric pressure of water-vapour in the air parcel |

### Volume mixing ratio, $w$

Another representation of water-vapour density is the volume mixing ratio, $w$. It is usually expressed in parts per million by volume or ppmv. It relates to the mass mixing ratio $q$ (in kg/kg) as follows:

$$w = 10^6.\frac{M_L}{M_{H_2O}}.q$$ *Equation 120*

or

$$w = 10^6.\frac{p_{H_2O}}{p - p_{H_2O}}$$ *Equation 121*

and

$$p_{H_2O} = \frac{10^{-6}.w.p}{1 + 10^{-6}.w}$$ *Equation 122*

**Dew point Temperature, $T_{dew}$**

The dew point temperature is the saturation temperature for the water-vapour in the air parcel at initial pressure and moisture content. It can be approximated with the following formula:

$$T_{dew} = \frac{T_n}{\frac{m}{log(p_{H_2O}/A)} - 1} \qquad \textit{Equation 123}$$

where:

| | |
|---|---|
| $T_n$ | is a configurable parameter |
| $m$ | is a configurable parameter |
| $A$ | is a configurable parameter |

**The Relative Humidity, %RH**

The relative humidity of an air-water mixture is defined as the ratio of the partial pressure of water-vapour present at a given temperature and pressure, $p_{H_2O}$, to the partial pressure of the water present at saturation for the given temperature and pressure, $e_S$ . These are defined after Equation 116 and Equation 117. Thus the relative humidity of air is a function of both water content and temperature. It is expressed in percentage and writes as follows:

$$\%RH = 100.\frac{p_{H_2O}}{e_S} \qquad \textit{Equation 124}$$

## 6.13 Check for Supersaturation of Water Vapour

The check for super saturation requires the comparison of the retrieved water-vapour amount with its saturation value. For each pressure level of a given profile, the saturation mixing ratio $q_S$ is computed with Equation 118 using as $p_{H_2O}$the saturation water-vapour pressure $e_S$ from Equation 116 and Equation 117. If the actual mixing ratio $q$ is higher than $q_S$, then it is reset to $q_S$ and the correction for super-saturation is recorded in the flag **FLG_PHYSCHECK**.

Bit 1 of **FLG_PHYSCHECK** shall be set if the super-saturation is found in the first guess water-vapour profile. See Section 5.4. The bit 3 of **FLG_PHYSCHECK** shall be set if the super-saturation is found in the water-vapour profile retrieved with the optimal estimation as specified in Section 5.8.

## 6.14 Check for Super-Adiabatic Layering

The adiabatic layering between an upper and a lower level with temperatures $T_0$ and $T_1$ and pressure levels $P_0$ and $P_1$, respectively, with $P_1 < P_0$ is given by the following:

$$b = \left(\frac{T_{0,adia}}{T_{1,adia}}\right) = \left(\frac{P_0}{P_1}\right)^{R_L/c_p} \qquad \textit{Equation 125}$$

where:

| | |
|---|---|
| $R_L$ | $= 287.06\, J.kg^{-1}.K^{-1}$ is the specific gas constant for dry air. |
| $c_p$ | $= 1004.71\, J.kg^{-1}.K^{-1}$ is the specific heat of dry air at constant pressure. |

If the ratio $T_0/T_1$ < b, then a correction term has to be calculated according to the following:

$$a = \frac{bT_1 - T_0}{1 + b} \qquad \textit{Equation 126}$$

If $a$ is greater than the standard deviation of the temperature, then $T_0$ has to be increased by $a$ and $T_1$ must be decreased by $a$. The correction is reported in the flag **FLG_PHYSCHECK** by setting the bit 2 to on if the check and correction applies to the first guess retrieval, as described in Section 5.4. Also bit 4 must be set if this applies to the temperature profile retrieved with the optimal estimation. See Section5.8.

# 7 PROCESSING AND QUALITY FLAGS

A collection of processing flags records the configuration and mode in which the different retrieval functions are executed. They capture the availability and quality of the expected input data (e.g. measurements, model data). The flags also detail the classification of the scene sensed by IASI and reflect the quality of the L2 products. This information is intended to the users of the IASI L2 products to support the selection of the IASI L2 products to use, depending on their applications. The processing and quality flags are also used within the L2 PPF itself, to trigger calls to different functions and configurations.

| *Flag name* | *Description* |
|---|---|
| FLG_AMSUBAD | Availability and quality of AMSU measurements |
| FLG_AVHRRBAD | Availability and quality of AVHRR measurements |
| FLG_CLDFRM | Origin of characterisation of the cloud formations |
| FLG_CLDNES | Cloudiness assessment summary |
| FLG_CLDTST | Details of cloud tests executed and their results |
| FLG_DAYNIT | Discrimination between day and night |
| FLG_DUSTCLD | Indicates presence of dust clouds in the IFOV |
| FLG_FGCHECK | Check that geophysical parameters from the first guess are within bounds |
| FLG_IASIBAD | Availability and quality of IASI L1 measurements |
| FLG_INITIA | Indicates the measurements used in the first guess retrieval |
| FLG_ITCONV | Convergence and acceptance of the OEM result |
| FLG_LANSEA | Specifies surface type |
| FLG_MHSBAD | Availability and quality of MHS measurements |
| FLG_NUMIT | Number of iterations in the OEM |
| FLG_NWPBAD | Availability and quality of NWP data |
| FLG_PHYSCHECK | Indicates potential corrections for superadiabatic and supersaturation conditions |
| FLG_RETCHECK | Check that geophysical parameters from the OEM are within bounds |
| FLG_SATMAN | Indication of satellite manouevre |
| FLG_SUNGLNT | Identification of sun glint |
| FLG_THICIR | Thin cirrus cloud test |

*Table 23: IASI Level 2 processing and quality flags*

The flags can be of enumerated type of encoded in bit streams. When bit streams are specified, the bit 1 refers to the lowest weight–there is no bit 0 and bit N = 2N-1. Table 23 summarises the flag list and signification. A detailed explanation for each flag is given in the following individual tables, in alphabetic order.

## 7.1 Quality Flag: FLG_AMSUBAD

| *Value* | *Meaning* |
|---|---|
| 0 | The expected AMSU measurements are available, of good quality and collocated with IASI for processing. |
| 1 | AMSU-A data are available but of degraded quality (according to AMSU L1 flags or QC tests) and not used for processing. |
| 2 | No coincident (time and space) AMSU measurements available for processing. |

## 7.2 Quality Flag: FLG_AVHRRBAD

| *Value* | *Meaning* |
|---|---|
| 0 | The expected AVHRR radiance analyses are available and of good quality for processing. |
| 1 | The radiance clusters are available but of degraded quality (according to IASI L1c flags or QC tests) and not used for processing. |
| 2 | No radiance clusters available for processing. |

## 7.3 Quality Flag: FLG_CLDFRM

| *Value* | *Meaning* |
|---|---|
| 0 | No cloud products retrieved. |
| Bit 1 | Height assignment performed with NWP forecasts. |
| Bit 2 | Height assignment performed with statistical first guess retrieval. |
| Bit 3 | Cloud products retrieved with the $CO_2$-slicing. |
| Bit 4 | Cloud products retrieved with the $\chi^2$ method. |

## 7.4 Quality Flag: FLG_CLDNES

| *Value* | *Meaning* |
|---|---|
| 1 | The IASI IFOV is clear. |
| 2 | Small cloud contamination possible. |
| 3 | The IASI IFOV is partially covered by clouds. |
| 4 | High or full cloud coverage. |

## 7.5 Quality Flag: FLG_CLDTST

| *Value* | *Meaning* |
|---|---|
| Bit 1 | IASI Window cloud test executed. |
| Bit 2 | IASI Window cloud test indicates a cloud. |
| Bit 3 | AMSU cloud test executed. |
| Bit 4 | AMSU cloud test indicates a cloud. |
| Bit 5 | AVHRR integrated cloud fraction assessed. |
| Bit 6 | AVHRR integrated cloud fraction indicates a cloud. |
| Bit 7 | IASI-AVHRR ANN cloud test executed. |
| Bit 8 | IASI-AVHRR ANN cloud test indicates a cloud. |
| Bit 9 | AVHRR heterogeneity test executed. |
| Bit 10 | AVHRR heterogeneity test indicates a cloud. |
| Bit 11 | Spare |
| Bit 12 | Spare |
| Bit 13 | Spare |
| Bit 14 | Spare |
| Bit 15 | Spare |
| Bit 16 | Spare |

## 7.6 Quality Flag: FLG_DAYNIT

| *Value* | *Meaning* |
|---|---|
| 0 | Day |
| 1 | Night |
| 2 | Twilight |

## 7.7 Quality Flag: FLG_DUSTCLD

| *Value* | *Meaning* |
|---|---|
| [0 .; 25.4]<br>(scale factor 10) | The FLG_DUSTCLD is a scalar unitless indicator providing a pseudo-quantitative information of the dust load in the IASI pixels. The values typically range between 0 and 10, but can reach higher values in exceptional dust outbreaks. The presence of dust is suspected when the index in greater than approximately two. |
| All bits set | Test not executed |

## 7.8 Quality Flag: FLG_FGCHECK

| *Value* | *Meaning* |
|---|---|
| 0 | Retrieved values are within valid bounds. |
| Bit 1 | Temperature profile is out of valid bounds. |
| Bit 2 | Water-vapour profile is out of valid bounds. |
| Bit 3 | Ozone profile is out of valid bounds. |
| Bit 4 | Surface temperature is out of valid bounds. |
| Bit 5 | Surface emissivity is out of valid bounds. |
| Bit 6 | CO concentration is out of valid bounds. |
| Bit 7 | $N_2O$ concentration is out of valid bounds. |
| Bit 8 | $CH_4$ concentration is out of valid bounds. |
| Bit 9 | $CO_2$ concentration is out of valid bounds. |
| Bits 10-16 | Spare |

## 7.9 Quality Flag: FLG_IASIBAD

| *Value* | *Meaning* |
|---|---|
| 0 | The IASI measurements and side information are available and of good quality for L2 processing |
| 1 | The IASI L1c products are of degraded quality according to IASI L1c flags, no L2 processing. |
| 2 | Quality control indicates that the IASI L1c data are of degraded quality (not indicated by the IASI L1c flags), no L2 processing. |

## 7.10 Quality Flag: FLG_INITIA

| *Value* | *Meaning* |
|---|---|
| 0 | Default value, no OEM attempted |
| Bit 1 | IASI included |
| Bit 2 | AMSU included |
| Bit 3 | MHS included |
| Bits 4-8 | Spare |

## 7.11 Quality Flag: FLG_ITCONV

| *Value* | *Meaning* |
|---|---|
| 0 | OEM not attempted. |
| 1 | OEM aborted because first guess residuals too high. |
| 2 | The minimisation did not converge, sounding rejected. |
| 3 | The minimisation did not converge, sounding accepted. |
| 4 | The minimisation converged but sounding rejected. |
| 5 | The minimisation converged, sounding accepted. |

## 7.12 Quality Flag: FLG_LANSEA

| *Value* | *Meaning* |
|---|---|
| 0 | The IASI IFOV is completely covered by water. |
| 1 | The IASI IFOV is completely covered by land, variability of the surface topography is low. |
| 2 | The IASI IFOV is completely covered by land, variability of the surface topography is high. |
| 3 | The IASI IFOV covers land and water, the variability of the surface topography is low. |
| 4 | The IASI IFOV covers land and water, the variability of the surface topography is high. |
| 5 | The IASI IFOV contains sea-ice. |

## 7.13 Quality Flag: FLG_MHSBAD

| *Value* | *Meaning* |
|---|---|
| 0 | The expected MHS measurements are available, of good quality and collocated with IASI for processing. |
| 1 | MHS data are available but of degraded quality (according to MHS L1 flags or QC tests) and not used for processing. |
| 2 | No coincident (time and space) MHS measurements available for processing. |

## 7.14 Quality Flag: FLG_NUMIT

| *Value* | *Meaning* |
|---|---|
| 0 | No iterations |
| N | Number of iterations |

## 7.15 Quality Flag: FLG_NWPBAD

| *Value* | *Meaning* |
|---|---|
| 0 | The expected NWP forecasts are available, of good quality and collocated with IASI for processing. |
| 1 | The expected NWP forecasts are available but of suspect quality, not used for processing. |
| 2 | No coincident NWP forecasts available for processing. |

## 7.16 Quality Flag: FLG_PHYSCHECK

| *Value* | *Meaning* |
|---|---|
| 0 | No superadiabatic or supersaturation found. |
| Bit 1 | Superadiabatic conditions in the first guess. |
| Bit 2 | Supersaturation conditions in the first guess. |
| Bit 3 | Superadiabatic conditions in the OEM retrieval. |
| Bit 4 | Supersaturation conditions in the OEM retrieval.. |
| Bit 5 –8 | Spare |

## 7.17 Quality Flag: FLG_RETCHECK

| *Value* | *Meaning* |
|---|---|
| 0 | Retrieved values are within valid bounds. |
| Bit 1 | Temperature profile is out of valid bounds. |
| Bit 2 | Water-vapour profile is out of valid bounds. |
| Bit 3 | Ozone profile is out of valid bounds. |
| Bit 4 | Surface temperature is out of valid bounds. |
| Bit 5 | Surface emissivity is out of valid bounds. |
| Bit 6 | CO concentration is out of valid bounds. |
| Bit 7 | $N_2O$ concentration is out of valid bounds. |
| Bit 8 | $CH_4$ concentration is out of valid bounds. |
| Bit 9 | $CO_2$ concentration is out of valid bounds. |
| Bits 10 –16 | Spare |

## 7.18 Quality Flag: FLG_SATMAN

| *Value* | *Meaning* |
|---|---|
| 0 | The platform is not undergoing a manoeuvre. |
| 1 | The platform is undergoing a manoeuvre, nominal processing. |
| 2 | The platform is undergoing a manoeuvre, no processing. |

## 7.19 Quality Flag: FLG_SUNGLNT

| *Value* | *Meaning* |
|---|---|
| 0 | No Sun glint |
| 1 | IASI observes in Sun glint. |

## 7.20 Quality Flag: FLG_THICIR

| *Value* | *Meaning* |
|---|---|
| 0 | No thin cirrus detected. |
| 1 | Thin cirrus detected. |
| 2 | Test failed or not executed. |

# 8 STATIC CONFIGURATION DATASETS

## 8.1 IASI_EV*

The eigenvector files are used for the compression as well as the reconstruction of Level 1C radiances. There is one file for each of the three IASI bands. The three eigenvector file types (IASI_EV1, IASI_EV2 and IASI_EV3) all share the same format. They are HDF5 files containing three Attributes and four Datasets, all belonging to the root group, as detailed in Table 21 below:

All entities, except noise, have no unit measure. The unit of noise is $W/m^2/sr/m^{-1}$.

The eigen values are provided for comparison only and are not used for compression or reconstruction.

| *Name* | *Type* | *Data Type* | *Rank* | *Dim 1* | *Dim 2* | *Description* |
|---|---|---|---|---|---|---|
| /FirstChannel | Attribute | 32-bit integer | 0 | | | Channel number (between 1 and 8461) of the first channel of the band. |
| /NbrChannels | Attribute | 32-bit integer | 0 | | | Number of channels in the band. |
| /NbrEigenvectors | Attribute | 32-bit integer | 0 | | | Number of eigenvectors included in the file. Can be greater, but not smaller, than the number of PC scores (for the corresponding band) included in the L1 PCS product. |
| /Noise | Dataset | 64-bit floating-point | 1 | /NbrChannels | | Random component of the Instrument noise assumed for the noise normalisation within the PC compression scheme. [unit: $W/m^2/sr/m^{-1}$] |
| /Mean | Dataset | 64-bit floating-point | 1 | /NbrChannels | | Noise-normalised radiance means assumed for the PC compression scheme. |
| /Eigenvalues | Dataset | 64-bit floating-point | 1 | /NbrEigenvectors | | The eigenvalues corresponding to the eigenvector included in the file. Not used for compression/ reconstruction. |
| /Eigenvectors | Dataset | 64-bit floating-point | 2 | /NbrEigenvectors | /NbrChannels | The eigenvectors used for the compression/reconstruction of IASI L1C radiances. |

*Table 24: HDF5 objects contained in the eigenvector files.*

## 8.2 IASI_SAD

The IASI_SAD static auxiliary dataset is an HDF5 file organised in several groups serving as configuration and coefficients for various aspect of the IASI L2 processor. In this section each group is presented in a subsection.

### 8.2.1 COF_SY

| *ID* | *Type* | *DIM1* | *DIM2* | *Description* |
|---|---|---|---|---|
| nbrChannels | Int32 | 1 | | Number of channels used in the optimal estimation observation vector |
| channels | Int32 | nbrChannels | | Channel index numbers (in [0..8460]) of used channels |
| observationErrorCovariance | Double | nbrChannels | nbrChannels | Observation error covariance matrix |

### 8.2.2 COF_SY_LAN

| *ID* | *Type* | *DIM1* | *DIM2* | *Description* |
|---|---|---|---|---|
| observationErrorCovariance | Double | nbrChannels | nbrChannels | Observation error covariance matrix over land |

### 8.2.3 COF_SY_SEA

| *ID* | *Type* | *DIM1* | *DIM2* | *Description* |
|---|---|---|---|---|
| observationErrorCovariance | Double | nbrChannels | nbrChannels | Observation error covariance matrix over sea |

### 8.2.4 COF_CLDDET

| *ID* | *Type* | *DIM1* | *DIM2* | *DIM3* | *DIM4* | *Description* |
|---|---|---|---|---|---|---|
| L | Int32 | 1 | | | | Number of latitude zones for threshold |
| M | Int32 | 1 | | | | Number of month intervals for threshold |
| N | Int32 | 1 | | | | Number of cloud detection channels |
| biasCorrection | Double | N | | | | Bias correction (K) for cloud detection channels |
| channel | Int32 | N | | | | Selected cloud detection channels |
| differenceThreshold | Double | 4 | L | M | N | Threshold difference, per type:<br>• LandDay<br>• LandNight<br>• SeaDay<br>• SeaNight<br>latitude zone, month interval and channel. |
| latitudeId | Double | L | | | | Latitude zone definition |
| monthId | Int32 | M | | | | Month interval definition |

### 8.2.5 COF_CNN*

| *ID* | *Type* | *DIM1* | *DIM2* | *Description* |
|---|---|---|---|---|
| L | Int32 | 1 | | Number of neural network layers |
| N | Int32 | 1 | | Number of inputs |
| N1 | Int32 | 1 | | Number of input IASI channels |
| N2 | Int32 | 1 | | Number of input AVHRR channels |
| S | Int32 | 1 | | Number of neural network weights |
| T | Int32 | 1 | | Number of neural network nodes |
| U | Int32 | L | | Number of nodes per layer |
| avhrrChannels | Int32 | N2 | | Identification of input AVHRR channels |
| bias | Double | T | | NN node bias |
| iasiChannels | Int32 | N1 | | Identification of input IASI channels |
| inputOffset | Double | N | | Offset applied to inputs |
| inputSlope | Double | N | | Scaling applied to inputs |
| threshold | Double | 1 | | Cloud identification threshold |
| weights | double | S | | Neural network weights |

Four groups follow this pattern..

| *Group* | *Control Name* |
|---|---|
| land at day (DL) | COF_CNNDL |
| water at day (DW) | COF_CNNDW |
| land at night (NL) | COF_CNNNL |
| water at night (NW) | COF_CNNNW |

### 8.2.6 COF_SLIC

| *ID* | *Type* | *DIM1* | *DIM2* | *Description* |
|---|---|---|---|---|
| K | Int32 | 1 | | Number of CO2 channels |
| Channel | Int32 | K | | CO2 channels |
| highestLevelNbr | Int32 | 1 | | Level index of highest possible cloud |
| radianceBias | Double | 8461 | | Radiance bias for CO2 slicing |
| referenceChannel | Int32 | 1 | | Reference channel |
| windowChannel | Int32 | 1 | | Window channel |

### 8.2.7 COF_BC

| *ID* | *Type* | *DIM1* | *DIM2* | *Description* |
|---|---|---|---|---|
| N | Int32 | 1 | | Number of channels (equal to /COF_SY/nbrChannels) |
| M1 | Int32 | 1 | | Number of band 1 PC scores used |
| M2 | Int32 | 1 | | Number of band 2 PC scores used |
| coefs | Double | N | M1+M2+1 | Regression operator |
| xmean | Double | M1+M2+1 | | Input mean values |
| ymean | Double | N | | Output mean values |

### 8.2.8 COF_STV

| *ID* | *Type* | *DIM1* | *DIM2* | *Description* |
|---|---|---|---|---|
| T_covariance | Double | 30 | | Background temperature error covariance (along first 30 eigenvectors) |
| T_eigenvectors | Double | 30 | 101 | First 30 eigenvectors of background temperature error covariance |
| W_covariance | Double | 30 | | Background temperature error covariance (along first 30 eigenvectors) |
| W_eigenvectors | Double | 30 | 101 | First 30 eigenvectors of background temperature error covariance |
| O_covariance | Double | 30 | | Background temperature error covariance (along first 30 eigenvectors) |
| O_eigenvectors | Double | 30 | 101 | First 30 eigenvectors of background temperature error covariance |

### 8.2.9 COF_TRG*

| *ID* | *Type* | *DIM1* | *DIM2* | *Description* |
|---|---|---|---|---|
| K | Int32 | 1 | | Number of absorption channels |
| L1 | Int32 | 1 | | Number of inputs |
| L2 | Int32 | 1 | | Number of first layer inputs |
| L3 | Int32 | 1 | | Number of second layer inputs |
| L4 | Int32 | 1 | | Number of outputs |
| M | Int32 | 1 | | Number of baseline channels |
| N | Int32 | 1 | | Number of temperature pressure levels |
| absorbtionChannel | Int32 | K | | Identification of absorption channels |
| absorbtionScale | Double | 2 | K | Offset and scale for absorption channels |
| b1 | Double | L2 | | Offset for first layer inputs |
| b2 | Double | L3 | | Offset for second layer inputs |
| b3 | Double | L4 | | Offset for output layer |
| baselineChannel | Int32 | M | | Identification of baseline channels |
| baselineScale | Double | 2 | M | Offset and scale of baseline channels |
| molecularMass | Double | 1 | | Molecular mass |
| outputScale | Double | 2 | | Offset and scale for output |
| pressureLevel | Int32 | N | | Identification of temperature levels |
| surfacePressureScale | Double | 2 | | Offset and scale for surface pressure |

| *ID* | *Type* | *DIM1* | *DIM2* | *Description* |
|---|---|---|---|---|
| temperatureScale | Double | 2 | 1+N | Offset and scale for temperature |
| w1 | Double | L2 | L1 | Weights first layer |
| w2 | Double | L3 | L2 | Weights second layer |
| w3 | Double | L3 | | Weights output layer |
| zenithScale | Double | 2 | | Offset and scale for zenith angle |

These four groups all follow this pattern:

- COF_TRGCO
- COF_TRGCH4
- COF_TRGN2O
- COF_TRGCO2

### 8.2.10 COF_EMS

| *ID* | *Type* | *DIM1* | *DIM2* | *Description* |
|---|---|---|---|---|
| N | Int32 | 1 | | Number of emissivity eigenvectors |
| eigenvector | Double | N | 8461 | Emissivity eigenvectors at IASI spectral resolution |
| mean | Double | 8461 | | Mean emissivity spectrum |

### 8.2.11 COF_MWCHAN

| *ID* | *Type* | *DIM1* | *DIM2* | *Description* |
|---|---|---|---|---|
| amsuChannels | Int32 | 15 | | Indication of which AMSU channels to check (1 means check, 0 means do not check) |
| mhsChannels | Int32 | 5 | | Not used yet |

### 8.2.12 MWIR/IRON

Both the MWIR and the IRON group contain 120 subgroups which all have the same format as shown below. The subgroup names follow the pattern

<daynight>_<scanclass>_M<nbrMW>_I<nbrIR>

Where:

| | |
|---|---|
| <daynight> | = either ‘D’ for day or ‘N’ for night |
| <scanclass> | = indicates the scan class (see section 5.4.4) |
| <nbrMW> | = the number of microwave PC scores used for classification |
| <nbrIR> | = the number of infrared PC scores used for classification |

| *ID* | *Type* | *DIM1* | *DIM2* | *DIM3* | *Description* |
|---|---|---|---|---|---|
| R | Double | 16 | 230 | 186 | Regression coefficients |
| centers | Double | 4+nbrMW+nbrIR | 16 | | |
| cs | Double | 4+nbrMW+nbrIR | | | |
| xm | Double | 16 | 230 | | |
| ym | Double | 16 | 186 | | |

### 8.2.13 EV_MW4

| *ID* | *Type* | *DIM1* | *DIM2* | *Description* |
|---|---|---|---|---|
| E | Double | 35 | 35 | Microwave eigenvectors (for AMSU plus four time MHS) |
| Mean | Double | 35 | | Microwave mean radiances |
| Std | Double | 35 | | Microwave radiance normalisation factors |

### 8.2.14 EV_OZ4

| *ID* | *Type* | *DIM1* | *DIM2* | *Description* |
|---|---|---|---|---|
| E | Double | 20 | 552 | Ozone eigenvectors (4 IFOVs a 138 levels) |
| Mean | Double | 552 | | Ozone mean profiles (4 IFOVs a 138 levels) |

### 8.2.15 EV_TW4

| *ID* | *Type* | *DIM1* | *DIM2* | *Description* |
|---|---|---|---|---|
| E | Double | 100 | 1096 | Temperature and humidity eigenvectors (4 IFOVs a 138 levels) |
| Mean | Double | 1096 | | Temperature and humidity mean profiles (4 IFOVs a 138 levels) |

### 8.2.16 EV_EM4

| *ID* | *Type* | *DIM1* | *DIM2* | *Description* |
|---|---|---|---|---|
| E | Double | 20 | 40 | Emissivity eigenvectors (4 IFOVs a 10 wavelengths) |
| Mean | Double | 40 | | Emissivity mean profiles (4 IFOVs a 10 wavelengths) |

### 8.2.17 COF_EV4IR

| *ID* | *Type* | *DIM1* | *DIM2* | *DIM3* | *Description* |
|---|---|---|---|---|---|
| E | Double | 15 | 300 | 1200 | 15 sets of PC score eiegenvectors |

### 8.2.18 COF_DUST

| *ID* | *Type* | *DIM1* | *DIM2* | *DIM3* | *Description* |
|---|---|---|---|---|---|
| channels | Int | *n_dust* | | | Channels used for dust indicator evaluation |
| gain_ocean | Double | *n_dust* | | | Gain matrix when surface type is ocean (for AM and PM) |
| gain_land_AM | Double | *n_dust* | | | Gain matrix when surface type is land for AM |
| gain_land_PM | Double | *n_dust* | | | Gain matrix when surface type is land for PM |
| mi_ocean | Double | *n_dust* | | | Background spectrum when surface type is ocean (for AM and PM) |
| mi_land | Double | *n_dust* | | | Background spectrum when surface type is land (for AM and PM) |
| bias_land_AM | Double | 721 | 1441 | | Bias to be subtracted for land (for AM) |
| bias_land_PM | Double | 721 | 1441 | | Bias to be subtracted for land (for PM) |

Where *n_dust* is the number of channels used for the dust detection.

## 8.3 IASI_L2P

The IASI_L2P static auxiliary dataset is an HDF5 file containing the bias and standard deviation look-up table for the production of the IASI L2Pcore SST files. It is made of one group named COF_L2PLUT.

| *ID* | *Type* | *DIM1* | *DIM2* | *Description* |
|---|---|---|---|---|
| bias | Double | 4 | 1 | SST bias for each quality class from “best” “first usable quality” |
| standardDeviation | Double | 4 | 1 | SST standard deviation for each quality class from “best” to “first usable quality” |

## 8.4 iasi2_ppf.conf

A configuration file of XML format, `iasi2_ppf.conf`, completes the static auxiliary datasets described in the previous section. It contains the paths to static databases, Installed with the PPF itself, and specifies the values of a few additional parameters, mostly thresholds, as well as switches triggering alternative retrieval functions and configurations.

An example of this file is given Figure 16.

```
<!-- Configuration file for the IASI2 PPF.-->

<Iasi2PpfConfig>

  <Processing>
    <DoBiasCorrection>yes</DoBiasCorrection>
    <DoFSFilter>yes</DoFSFilter>
    <UseSSTRegression>no</UseSSTRegression>
    <UseMWIRPWLRforCo2Slicing>no</UseMWIRPWLRforCo2Slicing>

    <SADFile>wo</SADFile>

    <MaxIterations>3</MaxIterations>
    <ConvergenceThreshold>1</ConvergenceThreshold>
    <FGCostMax> 500 </FGCostMax>
    <RTCostMax_X> 20 </RTCostMax_X>
    <RTCostMax_Y>  300 </RTCostMax_Y>

    <CloudTestAvhrrThreshold>0.02</CloudTestAvhrrThreshold>
    <CloudTestNwpThresholdOffset>0</CloudTestNwpThresholdOffset>

    <MaxInhomogeneity>0.04</MaxInhomogeneity>
    <MinIasiMinusAmsu>-1</MinIasiMinusAmsu>

    <nbrScoresB1>  90 </nbrScoresB1>
    <nbrScoresB2> 120 </nbrScoresB2>
    <nbrScoresB3>  80 </nbrScoresB3>

    <ForwardModelEv1File>/home/iasi2/PPF-
IASI2/data/pcc/IASI_EV1_1C_M02_FS.hdf5</ForwardModelEv1File>
    <ForwardModelEv2File>/home/iasi2/PPF-
IASI2/data/pcc/IASI_EV2_1C_M02_FS.hdf5</ForwardModelEv2File>
    <ForwardModelEv3File>/home/iasi2/PPF-
IASI2/data/pcc/IASI_EV3_1C_M02_FS.hdf5</ForwardModelEv3File>

    <ZhouPath>/home/iasi2/PPF-IASI2/data/dz_regression_v4/</ZhouPath>
    <EmissivityPath>/home/iasi2/PPF-IASI2/data/atlas_ems/</EmissivityPath>
    <LandSeaFile>/home/iasi2/PPF-
```

```
IASI2/data/land_cover/clo.10.00.prd</LandSeaFile>
    <GtopoFile>/home/iasi2/PPF-
IASI2/data/topography/GlobalGtopo2.DEM</GtopoFile>
    <RtiasiPath> /home/iasi2/PPF-IASI2/data/rtiasi4/ </RtiasiPath>
    <RttovPath> /home/iasi2/PPF-IASI2/data/rttov/ </RttovPath>

  </Processing>
</Iasi2PpfConfig>
```

*Figure 16: A configuration file of XML format, `iasi2_ppf.conf`.*

## 8.5 ipcc_ppf_M0[12].conf

The IASI PCC function needs additional configuration not contained in the eigenvector (IASI_EVx) files. This function is described in Section 5.1.1. These additional pieces of information shall be read from the XML configuration files `ipcc_ppf_M0[12].conf`. A sample file is shown in Figure 17. The additional pieces of information are as follows for each band: x = 1,2,3):

- Number of scores (per storage width). (nbrScoresBxP1, nbrScoresBxP2, nbrScoresBxP3)
- Outlier threshold (on the normalised residual RMS for detector 1). (outlierThresholdBxD1)
- Outlier threshold (on the normalised residual RMS for detector 2). (outlierThresholdBxD2)
- Outlier threshold (on the normalised residual RMS for detector 3). (outlierThresholdBxD3)
- Outlier threshold (on the normalised residual RMS for detector 4). (outlierThresholdBxD4)
- Outlier slope. (outlierSlopeBx)
- Quantisation factor for the scores. (scoreQuantisationFactorBx)
- Quantisation factor for the residuals. (residualQuantisationFactorBx)

```
<IpccPpfConfig>
  <Processing>
    <nbrScoresB1P1>   1  </nbrScoresB1P1>
    <nbrScoresB1P2>  41  </nbrScoresB1P2>
    <nbrScoresB1P3>  48  </nbrScoresB1P3>

    <nbrScoresB2P1>   2  </nbrScoresB2P1>
    <nbrScoresB2P2>  61  </nbrScoresB2P2>
    <nbrScoresB2P3>  57  </nbrScoresB2P3>

    <nbrScoresB3P1>   1  </nbrScoresB3P1>
    <nbrScoresB3P2>  44  </nbrScoresB3P2>
    <nbrScoresB3P3>  45  </nbrScoresB3P3>

    <outlierThresholdB1D1> 1.1232 </outlierThresholdB1D1>
    <outlierThresholdB1D2> 1.1804 </outlierThresholdB1D2>
    <outlierThresholdB1D3> 1.1539 </outlierThresholdB1D3>
    <outlierThresholdB1D4> 1.1029 </outlierThresholdB1D4>

    <outlierThresholdB2D1> 1.1318 </outlierThresholdB2D1>
    <outlierThresholdB2D2> 1.0161 </outlierThresholdB2D2>
    <outlierThresholdB2D3> 1.0131 </outlierThresholdB2D3>
    <outlierThresholdB2D4> 1.0261 </outlierThresholdB2D4>

    <outlierThresholdB3D1> 0.9825 </outlierThresholdB3D1>
    <outlierThresholdB3D2> 0.9482 </outlierThresholdB3D2>
    <outlierThresholdB3D3> 1.0333 </outlierThresholdB3D3>
    <outlierThresholdB3D4> 1.0386 </outlierThresholdB3D4>

    <outlierSlopeB1> 0.0305687 </outlierSlopeB1>
    <outlierSlopeB2> 0.220026  </outlierSlopeB2>
    <outlierSlopeB3> 3.54998   </outlierSlopeB3>

    <scoreQuantisationFactorB1> 0.5 </scoreQuantisationFactorB1>
    <scoreQuantisationFactorB2> 0.5 </scoreQuantisationFactorB2>
    <scoreQuantisationFactorB3> 0.5 </scoreQuantisationFactorB3>

    <residualQuantisationFactorB1> 0.5 </residualQuantisationFactorB1>
    <residualQuantisationFactorB2> 0.5 </residualQuantisationFactorB2>
    <residualQuantisationFactorB3> 0.5 </residualQuantisationFactorB3>
  </Processing>
</IpccPpfConfig>
```

*Figure 17: XML configuration files `ipcc_ppf_M0[12].conf`.*

# APPENDIX A: EXTENDED DOCUMENT CHANGE RECORD

| *Issue/Revision* | *Date* | *DCN No.* | *Changed Pages / Paragraphs* |
|---|---|---|---|
| Issue 3, Draft A | 15/11/2000 | DCN.SYS. DCN.025 | Re-structuring of the document. |
| Issue 4, RevisionA | 04/01/2001 | | Sect. 5.11.7.5.3.4: Added detailed specification of check for super saturation of water vapour |
| | | | Sect. 5.11.7.5.3.4: Added detailed specification of check for super adiabatic layering |
| | | | Sect. 5.11.7.5.2: Added detailed specification of checks and corrections for super saturated and super adiabatic situations |
| | | | Sect 5.11.6.2: AMSU-MHS-IASI interchannel regression cloud clearing method has been removed |
| | | | Sect. 3.2.2.7.2: Removed inter-channel regression cloud clearing method |
| | | | Sect. 5.11.7.5.2: Added detailed specification of artificial neural network for trace gas retrieval |
| | | | Sect 2.1: Changed first sentence |
| | | | Sect 1.11.1: Added applicable document |
| | | | Sect 1.11.2: Added reference document |
| | | | Sect 1.6: Changed sentence |
| | | | Sect 2.2: Update of table 2 |
| | | | Sect 3.1.3.1: editorial changes |
| | | | Sect 3.2.2.2: change of wording |
| | | | Sect 5.3.2.8: Table 4 re-arranged and more details included |
| | | | Sect 5.3.5: Completed ALG.A0.50 according to Table 4?, detailed ALG.A0.30 |
| | | | Sect 5.5: ALG.A2.10 deleted, ALG.A2.60: included missing verb |
| | | | Sect 4.1: detailed REQ.IASI.PGS.L2.000100, completed REQ.IASI.PGS.L2.00300 according to Table 4 |
| | | | Sect 5.6.2: Added detail in ALG.A32.50 |
| | | | Sect 5.6.3: Corrected number of ALG.A33.10 |
| | | | Sect 5.7.2: Added requirement to ALG.A42.10, added detail to ALG.A42.30 |
| | | | Sect 5.7.3: Added requirement to ALG.A43.10 |
| | | | Sect 5.7.4: Added requirement to ALG.A44.10 |
| | | | Sect 5.7.5: Added requirement to ALG.A45.10 |
| | | | Sect. 5.11.7.5.3.4: Added requirement to calculate ozone columnar amount |

| Issue/Revision | Date | DCN No. | Changed Pages / Paragraphs |
|---|---|---|---|
| | | | Sect. 5.7.5: Updated Flag FLG_HIRSBAD |
| | | | Sect 5.9: Added detail to general description |
| | | | Sect. 5.9.2: Refinement of ALG.A62.10 |
| | | | Sect 5.9.4: Changed title to reflect contents |
| | | | Sect. 5.10.5: Replaced “cloud mask” by “scenes analysis” |
| | | | Sect. 5.11.1: Requirement ALG.A81.10 refined and extended |
| | | | Sect. 5.11.2.1: Added requirements to ALG.A4821.40 |
| | | | Sect. 5.11.2.1: Refinement of ALG.A4821.50 |
| | | | Sect. 5.11.3.1.2: Removed requirement from ALG.A8312.20 |
| | | | Sect 5.11.3.1.5: Refinement of ALG.A8314.07 |
| | | | Sect. 5.11.3.2: Refinement of ALG.A832.05 |
| | | | Sect. 5.11.3.2: Refinement of ALG.A832.10, and added requirement |
| | 01/03/2001 | | Sect 5.11.3.3: Corrected reference number of ALG.A8233.20 to A833.20 |
| | | | Sect. 5.11.5.4: Refinement of requirement ALG.A854.40 |
| | | | Sect. 5.11.2.1: Added requirement ALG.A4821.35 |
| | | | Entire document: Moved scientific details and algorithms to section 6. |
| | | | Sect. 5.11.2.1: Added requirement to ALG.A4821.50 |
| | | | Sect. 5.11.7.5.2: Removed requirement ALG.A8752.70 |
| | | | Sect 5.11.7.5.2: Removed algorithm description from ALG.A487534.30 and combined with ALG.A487534.50 |
| | | | Sect 5.11.7.5.2: Removed requirement ALG.A487534.60 |
| | | | Sect 5.11.2: Changed body text including requirement to numbered item ALG.A4821.A5 |
| | | | Sect 5: Moved all SADT diagrams to Section 3 |
| | | | Sect 4: Moved all operations concept to section 3 |
| | | | Section 5 becomes section 4 |
| | | | Section 4: Moved all flag descriptions to annex |
| | 02/03/2001 | | Section 4.6.2, ALG.A0.110: Refinement and relaxation of requirement |
| | | | Section 4.6.2, ALG.A0.120: refinement |
| | | | Section 4.6.2, ALG.A0.130: refinement |
| | | | Section 4.7, added requirement ALG.A1.25 |
| | | | Section 4.7, ALG.A1.50: refinement |
| | | | Section 4.7, ALG.A1.60: refinement |

| *Issue/Revision* | *Date* | *DCN No.* | *Changed Pages / Paragraphs* |
|---|---|---|---|
| | | | Section 4.8, ALG.A2.20: refinement |
| | | | Section 4.8, ALG.A2.50: refinement |
| | | | Section 4.8, ALG.A2.60: refinement |
| | 21/03/2001 | | Section 1.11.2: added reference |
| | | | Section 4.12.4, ALG.A64.20: refinement |
| | | | New Section 5.4 on bilinear interpolation |
| | 27/03/2001 | | Refinement of Section 5.5 |
| | | | Refinement of Section 5.8 |
| | | | Refinement of Section 5.1 |
| | 02/04/2001 | | Update of Section 5.3, describing predictors for trace gases |
| | | | Section 4.14.3.2, ALG.A4832.30: refinement |
| | | | Section 4.14.3.2, ALG.A4832.35: refinement |
| | 03/04/2001 | | Section 4.14.7.5.3.3, ALG.A87533.60: refinement and added requirement |
| | | | Section 5.16:Added detail on trace-gas profile scaling |
| | 04/04/2001 | | Section 5.7: Refined description of cloud detection tests |
| | | | Section 5.8: Refined description of CO2 slicing method |
| | | | Section 5.9: Refined description of threshold values |
| | | | Section 10: Refined description of threshold values |
| | 05/04/2001 | | Annex: Removed flag FLG_FRTM |
| | | | Sect. 4.14.2, ALG.A82.5: Removed choice of FRTM |
| | | | Sect. 4.14.2, ALG.A82.10: Refinement |
| | | | Sect. 4.14.2, ALG.A82.20: Refinement |
| | | | Sect. 4.14.30, ALG.A82.30: Removed |
| | | | Sect. 4.14.2, ALG.A82.40: Removed requirement |
| | | | Sect. 4.14.2.1, ALG.A4821.07: Refinement |
| | | | Annex: Removed IASI_L2_PGS_SEL_FRTM |
| | | | Sect. 4.14.7.3.1, ALG.A8731.10: Refinement |
| | | | Sect. 4.14.7.3.1, ALG.A8731.20: Refinement |
| | | | Sect 4.14.7.3.2.1: Removed FRTM choice |
| | | | Sect. 4.14.7.5.3.4, ALG.A87534.100: Refinement |
| | | | Sect. 3.1.2: Updated figures 8 and 18 |
| | | | Sect. 4.14.3.3: Removed explicit cloud clearing, choice of clear, cloudy, or variational cloud clearing is made |
| | | | Sect. 4.14.3.3: ALG.A853.10: Refined |
| | | | Sect: 4.14.5.4: Removed section |
| | | | Sect 4.14.6: Section replaced by section |

| Issue/Revision | Date | DCN No. | Changed Pages / Paragraphs |
|---|---|---|---|
| | | | 4.14.6.2 |
| | | | Section 4.14.6.1: Removed section |
| | | | Section 4.14.6.2: Removed section |
| | | | Sect. 4.14.6, ALG.A862.20: refined |
| | | | Annex: removed FLG_CLDCOR |
| | 09/04/2001 | | Sect. 3.1.2: Removed figure on decomposition of A86 |
| | | | Sect 3.1.2: Removed figure on decomposition of A85 |
| | | | Sect 3.1.2: Updated decomposition of A8 |
| | | | Sect. 4.14.5: Renamed section and changed functionality to selection of retrieval type |
| | | | Sect. 4.14.5.1: Made requirement explicit algorithm ALG.A851.10 |
| | | | Sect. 4.14.7.5.3.4, ALG.A487534.70: Changed requirement |
| | | | Sect. 4.14.7.5.3.4: Renamed second requirement to ALG.A487534.20 |
| | | | Sect. 4.14.5.1: Section removed, renamed ALG.A851.10 to ALG.A85.10 |
| | | | Sect. 4.14.5.2: Section removed, renamed ALG.A852.10 to ALG.A85.20 |
| | | | Sect. 4.14.5.3: Section removed, renamed ALG.A853.10 to ALG.A85.30 |
| | | | New section 5.16, describing super and pseudo channels |
| | | | New section 5.18, describing selection of iterative retrieval |
| | 10/04/2001 | | Sect 4.7, ALG.A1.60: refined, PSF extracted from dataflow |
| | | | Sect 4.7, ALG.A1.70: refined |
| | | | New section 5.3 describing the PSF |
| | | | New section 5.3.1 describing the calculation of the fractional land cover |
| | | | New section 5.3.2 describing the calculation of the weighted fractional surface type cover |
| | | | New section 5.3.3 describing the calculation of the mean surface height and the surface height distribution |
| | | | Section 4.8, ALG.A2.30: refined |
| | | | Section 4.8, ALG.A2.40: removed |
| | | | Section 4.8, ALG.A2.60: refined |
| | | | Section 4.8, ALG.A2.70: refined |
| | | | Sect. 4.14.7.5.2, ALG.A8752.150: refined |

| Issue/Revision | Date | DCN No. | Changed Pages / Paragraphs |
|---|---|---|---|
| | | | Added section 5.17.1 describing the initialisation of the iterative retrieval and of the FRTM |
| | 12/04/2001 | | Sect. 5.17.1: Added description of sea surface emissivity calculation |
| | | | Added section 5.19, describing the radiance tuning. The introductory part of section 4.9.3 has been shortened accordingly |
| | | | Section 3.1.2: removed function A8751 from Figure 17 |
| | | | Section 4.14.7.5.1: removed, ALG.A8751.10 de-scoped and renamed to ALG.A8752.10 and moved to section 4.14.7.5.2 |
| | | | Added new Annex: Contents description of user-configurable auxiliary databases |
| | 23/04/2001 | | Annex C: Refinement |
| | 24/04/2001 | | Section 4.14.7.5.2.6: Section renamed, ALG.A87536.40 refined |
| | | | Added section 5.20, describing interpolation to user levels |
| | | | Section 3.1.2: Updated figure 3.1.2 |
| | | | Section 4.9.2: Added requirement ALG.A32.70 on handling missing or corrupted channels |
| | 25/04/2001 | | Section 4.14.7.5.2.6: Refinement of ALG.A87536.40 |
| | 04/05/2001 | | Section 4.14.3.2: Refinement of ALG.A832.50 |
| | | | Section 4.14.3.2: Refinement of ALG.A832.70 |
| | 07/05/2001 | | Combined section 4.8 with section 4.7 |
| | | | New section 4.8: Acceptance and validation of NWP forecast |
| | 08/07/2001 | | Moved requirements of sections 4.2, 4.3, 4.4, 4.5 into section 4.6, which became new section 4.2 |
| | | | Section 4.5.2, refined ALG.A32.40 |
| | | | Section 4.6.2, refined ALG.A42.20 |
| | | | Section 4.6.3, refined ALG.A43.20 |
| | | | Section 4.6.4, refined ALG.A44.20 |
| | | | Section 4.6.5, refined ALG.A45.20 |
| | | | Section 4.7.2, refined ALG.A52.20 |
| | | | Section 4.10.3.2, refined ALG.A832.15 |
| | | | Section 4.10.3.2, refined ALG.A832.40 |
| | | | Section 4.6.10, refined ALG.A862.20 |
| | | | Section 4.10.7.2.3, removed ALG.A8723.20 |
| | | | Section 4.14.7.5.2.6, refined ALG.A87536.10 |

| Issue/Revision | Date | DCN No. | Changed Pages / Paragraphs |
|---|---|---|---|
| | | | Section 4.14.7.5.2.6, refined ALG.A87536.20 |
| | | | Section 4.14.7.5.2.6, added ALG.A87536.65 |
| | 10/05/2001 | | New section 1.11.3, listing references to background information |
| | | | Sections 3 and 4: Removed HIRS level 1 dataflow as input from the PF |
| | | | Section 3: removed subsection on operations concept |
| | | | Moved subsections giving the product generation overview from section 3 to 4. |
| | | | Section 4.2.2: Split ALG.A0.130 into sub-requirements |
| | | | Section 4.2.2: Removed requirement ALG.A0.150 |
| | | | Section 4.2.2: Removed sub-req. 10 of ALG.A0.10 |
| | | | Removed section 4.2.3 |
| | | | Section 4.3, split ALG.A1.25 |
| | | | Section 4.3, split ALG.A1.60 |
| | | | Section 2.2.2, added ALG.A0.180 |
| | | | Section 4.3, split ALG.A1.120 |
| | | | Section 4.3, split ALG.A1.130 |
| | | | Section 4.4, split ALG.A1.10 |
| | | | Section 4.4, refined ALG.A1.30 |
| | | | Section 4.5.2, split ALG.A32.50 |
| | | | Section 4.6.2, split ALG.A42.20 |
| | | | Removed section 4.6.5 |
| | | | Section 4.8.4, split ALG.A64.20 into sub- requirements |
| | | | Section 4.9.5, split ALG.A75.10 |
| | | | Section 4.9.5, split ALG.A75.20 |
| | | | Section 4.9.5, split ALG.A75.40 |
| | | | Section 4.9.5: Added requirement ALG.A75.35 |
| | | | Section 4.10.1: Removed requirement ALG.A81.20 |
| | | | Section 4.10.2, split ALG.A82.05 |
| | | | Section 4.10.2.1, split ALG.A821.20 |
| | | | Section 4.10.2.1, split ALG.A821.35 |
| | | | Section 4.10.2.1, split ALG.A821.50 |
| | | | Section 4.10.3.1.3, removed requirement from ALG.A8313.10 |
| | | | Section 4.10.3.1.5, split ALG.A8314.07 |
| | | | Section 4.10.3.1.5, split ALG.A8314.08 |
| | | | Section 4.10.3.1.5, split ALG.A8314.40 |

| Issue/Revision | Date | DCN No. | Changed Pages / Paragraphs |
|---|---|---|---|
| | | | Section 4.10.3.1.5, split ALG.A8314.90 |
| | | | Section 4.10.3.1.5, split ALG.A8314.130 |
| | | | Section 4.10.3.2, refined ALG.A832.05 |
| | | | Section 4.10.3.2, split and refined ALG.A832.10 |
| | | | Section 4.10.3.2, split ALG.A832.15 |
| | | | Section 4.10.3.2, split and refined ALG.A832.40 |
| | | | Section 4.10.3.3, removed ALG.A833.10 |
| | | | Section 4.10.3.3, split ALG.A833.20 |
| | | | Section 4.10.3.4, removed ALG.A843.10 |
| | | | Section 4.10.4.1, split ALG.A841.30 |
| | | | Section 4.10.4.2, split ALG.A842.20 |
| | | | Section 4.10.4.3, refined ALG.A843.40 |
| | | | Section 4.10.5, split ALG.A85.30 |
| | | | Section 4.10.6, split ALG.A862.60 |
| | | | Section 4.10.7.3.1, split ALG.A8731.20 |
| | | | Section 4.10.7.3.2.2, removed ALG.A87322.60 |
| | | | Section 4.10.7.3.2.3, refined ALG.A87323.10 |
| | | | Section 4.10.7.3.2.3, removed ALG.A87323.30 |
| | | | Section 4.10.7.5.1, split and refined ALG.A8752.10 |
| | | | Section 4.10.7.5.1, split ALG.A8752.40 |
| | | | Section 4.10.7.5.1, split ALG.A8752.80 |
| | | | Section 4.10.7.5.1, split ALG.A8752.120 |
| | | | Section 4.10.7.5.1, refined ALG.A8752.125 |
| | | | Section 4.10.7.5.1, split ALG.A8752.130 |
| | | | Section 4.10.7.5.1, refined ALG.A8752.140 |
| | | | Section 4.10.7.5.1, split and refined ALG.A8752.150 |
| | | | Section 4.10.7.5.2.2, refined ALG.A87532.10 |
| | | | Section 4.10.7.5.2.2, refined ALG.A87532.30 |
| | | | Section 4.10.7.5.2.3, removed ALG.A87533.10 |
| | | | Section 4.10.7.5.2.3, removed ALG.A87533.20 |
| | | | Section 4.10.7.5.2.3, new requirement ALG.A87533.05 |
| | | | Section 4.10.7.5.2.3, removed ALG.A87533.30 |
| | | | Section 4.10.7.5.2.3, new requirement ALG.A87533.15 |
| | | | Section 4.10.7.5.2.3, new requirement ALG.A87533.25 |
| | | | Added section 5.17.2 |
| | 11/05/2001 | | Section 4.10.7.5.2.3, refined ALG.A87533.60 |
| | | | Section 4.10.7.5.2.3, split ALG.A87533.70 |

| *Issue/Revision* | *Date* | *DCN No.* | *Changed Pages / Paragraphs* |
|---|---|---|---|
| | | | Section 4.10.7.5.2.3, refined ALG.A87533.80 |
| | | | Section 4.10.7.5.2.3, refined ALG.A87533.100 |
| | | | Section 4.10.7.5.2.4, split ALG.A87534.20 |
| | | | Section 4.10.7.5.2.4, split ALG.A87534.70 |
| | | | Section 4.10.7.5.2.4, split ALG.A87534.75 |
| | | | Section 4.10.7.5.2.4, split ALG.A87534.110 |
| | | | Section 4.10.7.5.2.4, refined ALG.A87534.160 |
| | | | Section 4.10.7.5.2.4, split ALG.A87534.190 |
| | | | Section 4.10.7.5.2.4, split and refined ALG.A87534.210 |
| | | | Section 4.10.7.5.2.4, split ALG.A87534.220 |
| | | | Section 4.10.7.5.2.4, split and refined ALG.A87534.230 |
| | | | Section 4.10.7.5.2.4, split and refined ALG.A87534.250 |
| | | | Section 4.10.7.5.2.6, split ALG.A87536.40 |
| | | | Section 4.10.7.5.2.6, split ALG.A87536.50 |
| | | | Table 3 revised and moved to section 4.1.1.8 |
| | 15/05/2001 | | Section 4.2.2, refined ALG.A0.50 |
| | | | Section 4.2.2, refined ALG.A0.60 |
| | | | Section 4.2.2, refined ALG.A0.10 |
| | | | Section 4.2.2, refined ALG.A0.110 |
| | | | Section 4.5.1, refined ALG.A31.30 |
| | | | Section 4.10.2.1, new requirement ALG.A821.08 |
| | | | Section 4.5.1, new requirement ALG.A31.40 |
| | | | Section 4.5.1, refined ALG.A31.30 |
| | | | Section 4.5.2, refined ALG.A32.30 |
| | | | Section 5.4.2, moved ALG.A32.50, ALG.A52, ALG.A55, ALG.A58 to section 4.2.2, renamed to ALG.A0.190, ALG.A0.200, ALG.A0.210, ALG.A0.220 |
| | | | Section 4.2.2, new ALG.A0.230 |
| | | | Section 4.5.3, new ALG.A33.20 |
| | | | Section 4.5.4 removed |
| | | | Section 4.6.2, removed ALG.A42.25 |
| | | | Section 4.7.1, refined ALG.A51.10 |
| | | | Section 4.7.1, new ALG.A51.20 |
| | | | Section 4.7.3 removed |
| | | | Section 4.8.1, split and refined ALG.A61.10 |
| | | | Section 4.8.2, split and refined ALG.AA62.10 |
| | | | Section 4.9.4, removed ALG.A74.10 |

| Issue/Revision | Date | DCN No. | Changed Pages / Paragraphs |
|---|---|---|---|
| | | | Section 4.9.4, refined ALG.A74.20 |
| | | | Section 4.10.1, split and refined ALG.A81.10 |
| | | | Section 4.10.2, removed ALG.A82.20 |
| | | | New section 5.5 describing the interpretation of the AVHRR radiance analysis |
| | 17/05/2001 | | Section 4.9.5, new ALG.A75.05 |
| | | | Section 4.9.5, refined ALG.A75.15 |
| | | | Section 4.10.2.1, refined and split into ALG.A821.40 |
| | | | Section 4.10.2.1, removed ALG.A8312.20 |
| | | | Section 4.10.3.1.3, refined ALG.A8313.20 |
| | | | Added section 5.7, describing calculation of brightness temperature Section 4.10.3.1.5, refined ALG.A8315.40 |
| | | | Section 4.10.3.1.5, refined ALG.A8315.100 |
| | | | Section 4.10.3.1.5, refined ALG.A8315.140 |
| | | | Section 4.10.3.1.5, refined ALG.A8315.160 |
| | | | Section 4.10.4, refined ALG.A841.10 |
| | | | Section 4.10.5, removed ALG.A85.20 |
| | | | Section 4.10.5, refined ALG.A85.30 |
| | | | Section 4.10.6, refined and split ALG.A862.20 |
| | | | Section 4.10.6, new ALG.A862.70 |
| | | | Section 4.10.7.2, split and refined |
| | | | Section 4.10.7.21 removed |
| | | | Section 4.10.7.2.2 removed |
| | | | Section 4.10.7.2.3removed, requirements moved to section 4.10.7.5.2.1 |
| | | | Section 4.10.7.2.4 removed |
| | | | Added section 5.23.2, describing valid bounds on cloud parameters |
| | | | Added section 5.26 on quality control |
| | | | Section 4.10.7.3.1, ALG.A8731.10 removed |
| | | | Section 4.10.7.3.2.1, ALG.A87321.40 removed |
| | | | Section 4.10.7.3.2.2 removed |
| | | | Section 4.10.7.3.2.1 removed |
| | | | Section 4.10.7.3.2.3 removed |
| | | | Section 4.10.7.5.1, ALG.A8752.40 refined |
| | | | Section 4.10.7.5.1, ALG.A8752.110 removed |
| | | | Section 4.10.7.5.1, ALG.A8752.50 removed |
| | | | Section 4.10.7.5.1, ALG.A8752.100 removed |

| Issue/Revision | Date | DCN No. | Changed Pages / Paragraphs |
|---|---|---|---|
| | | | Section 4.10.7.5.1, ALG.A8752.90 removed |
| | | | Section 4.10.7.5.2.3, ALG.A87533.120 removed |
| | | | Section 4.10.7.5.1, ALG.A8752.40 refined |
| | | | Section 4.10.7.5.1, ALG.A8752.100 removed |
| | | | Section 4.10.7.5.1, ALG.A8752.90 removed |
| | | | Section 4.10.7.5.1, ALG.A8752.110 removed |
| | | | Section 4.10.7.5.2.3, ALG.A87533.120 removed |
| | | | Section 4.10.7.5.2.4, ALG.A87534.70 removed |
| | | | Section 4.10.7.5.2.4 |
| | | | Section 4.10.7.5.2.4 |
| | 21/05/2001 | | Section 4.10.7.5.2.2 |
| | | | Section 3.2 |
| | 23/05/2001 | | Section 5.6.2, detailed description of Jacobians |
| | 28/05/2001 | | 28/05/2001 Added section 5.3 on line and pixel numbering scheme |
| | 30/5/2001 | | Added section 3.3.1, PGF States and Transitions |
| | | | Added requirement ALG.A0.25 |
| Issue 5, Draft | 25/09/2001 | | Removed Annex F |
| | | | Section 1.7: Removed statement on two concurrent |
| | | | numbering schemes |
| | | | Section 5.13: Refinement |
| | | | Section 5.19: Correction and refinement |
| | | | Section 5.23.1: Refinement of trace-gas retrieval |
| | | | Section 4.3, ALG.A1.60: Correction of typo |
| | | | Section 4.10.1, ALG.A81.10: Refinement |
| | | | Section 4.10.3.1.5, ALG.A8315.07: Correction of typos |
| | | | Section 5.7, Equation 15: Correction of equation 15 |
| | | | Section 5.12: Correction of equation 228 |
| | | | Section 5.23: Correction of equation 252 |
| | | | Section 4.6.4, ALG.A44.20: Correction of typo |
| | | | Section 4.6.5, ALG.A46.10: Renamed to ALG.A45.10 |
| | | | Section 4.8.3, ALG.A63.10: Correction of typo |
| | | | Section 4.9.5, ALG.A75.35: Correction of typos |
| | | | Section 1.6: Adapted to Issue 5, revision 0. Changed text related to TBC and TBD |
| | | | Section 1.10: Updated list of acronyms |
| | | | Section 4.8.4, ALG.A64.30: Renamed to make numbering unique |

| Issue/Revision | Date | DCN No. | Changed Pages / Paragraphs |
|---|---|---|---|
| | | | Section 5.7.2, equations 19,22,23: Corrections |
| | | | Section 5.7: Refinements |
| | | | Section 5.22: Changed definition and calculation of super channels |
| | 04/10/2001 | | Annex C.: Changed upper limit of number of levels to 100 |
| | 31/10/2001 | | Section 4.10.7.5.2.4: Deleted requirement ALG.A87534.90 |
| | | | Section 5.23.3: Added details |
| | | | Section 5.23.4: Added details |
| | | | Section 5.26: Added details |
| | | | Section 4.10.7.5.2.4: Added detail to ALG.A87534.250 |
| | | | Section 4.10.7.5.2.4: Changed ALG.A87534.110 |
| | | | Section 5.23.1: Added details |
| | | | Section 4.10.3.2: Changed ALG.A832.50 |
| | | | Section 4.10.3.2: Changed ALG.A832.10 |
| | | | Section 4.10.3.2: Changed ALG.A832.15 |
| | | | Section 5.10: Added details |
| | | | Annexes B and C: Corrected description of IASI_L2_PGS_COF_SLIC |
| | | | Annexes B and C: Added description of IASI_L2_PGS_THR_CLCMP |
| | | | Section 5.11: Added details |
| | | | Annex C: Completed description of IASI_L2_PGS_COF_CLDPHA |
| | | | Annexes B and C: Description of IASI_L2_PDS_THR_DAYNIT has been added |
| | | | Section 4.10.3.1.4: Changed ALG.A8315.07 |
| | | | Section 5.23: Correction of equations |
| | | | Section 5.25: Added detail |
| | | | Section 4.5.3: Added requirements to ALG.A33.10 and ALG.A33.20 |
| | | | Section 4.10.3.1.4: Function A8314 deleted |
| | | | Section 4.8.4: Added detail to ALG.A64.22 |
| | | | Section 4.8.4: Added detail to ALG.A64.24 |
| | | | Section 4.8.4: Added detail to ALG.A64.26 |
| | | | Section 4.7.2: Added detail to ALG.A52.20 |
| | | | Section 4.9.5: Added requirements to ALG.A75.10 |
| | | | Section 4.9.5: ALG.A75.50 |

| Issue/Revision | Date | DCN No. | Changed Pages / Paragraphs |
|---|---|---|---|
| | 01/11/2001 | | Section 3.2: Updated figures 2, 7, and 10 |
| | | | Section 5.15: Text included |
| | | | Section 5.16: Text included |
| | 06/12/2001 | | Section 4.5.1: Changed introductory sentence |
| | | | Section 4.5.2, ALG.A32.50: Refinement |
| | | | Section 4.8.2, ALG.A62.20: Removed requirement |
| | | | Section 4.8.3, ALG.A64.22: Refinement |
| | | | Section 4.8.3, ALG.A64.24: Refinement |
| | | | Section 4.8.3, ALG.A64.26: Refinement |
| | | | Section 4.10.3.1.3, ALG.A8313.10 refined |
| | | | Added section 5.7.2 describing band correction |
| | | | Section 4.10.3.1.5, ALG.A8315.130: removed duplicated requirement |
| | | | Section 4.10.3.2, ALG.A832.06: Refinement |
| | | | Annexes B and C: Removed IASI_L2_PGS_THR_IACLD and changed IASI_L2_PGS_THR_IACLR |
| | | | Section 4.10.3.2, ALG.A832.30 refined |
| | | | Annex C: Updated IASI_L2_PGS_COF_SLIC |
| | | | Section 4.10.3.3, ALG.A833.10: Changed reference to database |
| | | | Annexes B and C: Removed ASI_L2_PGS_THR_CLTHR |
| | | | Section 4.10.7.3, ALG.A8731.20:changed requirement |
| | | | Annex E: Change of FLG_CHNSEL |
| | | | Entire document: replaces IASI pixels by IASI IFOVs |
| | | | Section 4.10.7.5.1: Re-phrased introductory sentence |
| | | | Section 4.10.7.5: Changed introductory remarks |
| | | | Section 4.10.7.5.2.1: Function A87531 is obsolete and has been emptied, the section is not removed to keep the numbering scheme intact |
| | | | Section 4.10.7.5.1, ALG.A8752.120: refinement |
| | | | Section 4.10.7.5.2.2, ALG.A87532.30: refinement |
| | | | Section 4.10.7.5.1, ALG.A8752.140 renamed to ALG.A8752.05 |
| | | | Section 4.10.7.5.1, ALG.A8752.05: removed part of the requirements |
| | 10/12/2001 | | Section 4.10.7.5.2.3, ALG.A87533.25: refinement |
| | | | Section 4.10.7.5.2.4, ALG.A87534.260 removed |
| | | | Section 4.10.7.5.2.3, ALG.A87533.15: refinement |

| Issue/Revision | Date | DCN No. | Changed Pages / Paragraphs |
|---|---|---|---|
| | | | Section 5.23: Added details |
| | | | Section 4.10.7.5.2.3, ALG.A87533.25: refinement |
| | 11/12/2001 | | Section 5.7.2: Corrected equations 133, 134, and 135 |
| | | | Section 5.7: Added note to equation 77 |
| | | | Section 5.7 and subsections: Removed equation (45) and replaced $P$ by $p$ in all equations |
| | | | Section 5.7: Added details |
| | | | Section 5.7.2: Corrected equation (88) |
| | | | Section 5.7.2: Added details |
| | 12/12/2001 | | Section 5.2: Refinement |
| | | | Section 1.5: Refinement |
| | | | Section 1.11.3: Added detail |
| | | | Section 5.3: Refinement |
| | | | Section 5.4.2: Added detail, refinement |
| | | | Annex C: Added details |
| | | | Section 5.17: Simplified equations |
| | | | Section 5.6: Added details |
| | | | Section 5.9: Corrected equation (213) |
| | | | Section 4.10.6, ALG.A862.20 refined |
| | | | Annex B and C: Added IASI_L2_PGS_DAT_VARCLR |
| | | | Section 5.14: Added details |
| | | | Section 5.18: Text included |
| | | | Section 5.25: Refinement |
| | | | Section 5.7.2: Removed comment following equation |
| | | | Section 5.7.2: Removed comment following equation |
| | | | Section 5.14: Added detail and changed equations |
| | 10/01/2002 | | Section 5.7.3: Corrected equation (133) |
| | | | Section 5.7.3: Corrected expressions in Table 8 |
| | 15/01/2002 | | Section 5.4: Added detail |
| | 17/01/2002 | | Section 5.17: Modifications on water-vapour and ozone retrieval |
| | | | Section 5.9: Modification of EOF residual check |
| | | | Section 4.3, ALG.A1.25: Refinement |
| | | | Annex A: Update with new symbols |
| | | | Annex D: FLG_FINCHC updated and combined with FLG_CLDRET |
| | | | Section 4.10.5, ALG.A85.30: FLG_CLDRET replaced by flag FLG_FINCHC |

| *Issue/Revision* | *Date* | *DCN No.* | *Changed Pages / Paragraphs* |
|---|---|---|---|
| | | | Section 4.10.7.5.2.4, ALG.A487534.75: FLG_CLDRET replaced by FLG_FINCHC |
| | | | Section 4.10.6, ALG.A862.20: FLG_CLDRET replaced by FLG_FINCHC |
| | | | Section 5.23: Added detail |
| | | | Section 4.10.7.5.2.6, ALG.A87536.50: Removed redundant information |
| | | | Appendix C: Updated IASI_L2_PGS_DAT_VGRD |
| | | | Section 4.10.7.5.2.2, ALG.A87532.10: Added requirement |
| | | | Annex D: Corrected IASI_L2_PGS_THR_AVH |
| | | | Annex D: Updated IASI_L2_PGS_THR_FRTCLR |
| | | | Annex D: Updated IASI_L2_PGS_THR_CLDDET |
| | | | Section 4.9: Rephrased remark on PSF in introductory paragraph |
| | | | Section 5.7: Removed Table 7 |
| | | | Section 4.10.7.5.1, ALG.A8752.40: Refinement and replacement of FLG_PRECHC by FLG_FINCHC |
| | | | Section 4.10.2, ALG.A82.05: Replaced IASI_L2_PGS_SEL_PRESEL by IASI_L2_PGS_TYP_INI |
| | | | Annexes B and C: Removed IASI_L2_PGS_SEL_PRESEL |
| | | | Annex D: Removed flag FLG_PRECHC |
| | | | Annexes B and C: Added IASI_L2_PGS_COV_NWP |
| | | | Section 4.10.7.5.2.4, ALG.A87534.20: Added extraction of NWP covariance matrix |
| | | | Section 4.2.4, ALG.A0.200: Added requirement |
| | 30/01/2002 | | Section 5.23: Added convergence checks |
| | | | Section 4.10.7.5.2.6, ALG.A87536.65: Added requirement |
| | | | Annexes B and C: Added IASI_L2_PGS_DAT_GTSLEV |
| | | | Section 5.7: Changed predictors for FRTM |
| | | | Section 5.7.3: Changed Jacobians according to changed predictors in FRTM |
| | 31/01/2002 | | Inclusion of section 5.30 describing the error covariance compression and the information there generated for the product |
| | | | Section 4.10.7.5.32.6, ALG.A87536.30: Refinement |
| | | | Annexes B and C: Added IASI_L2_PGS_STERR |
| Issue 5 | 07/02/2002 | | Section 4.10.7 and subsections: |

| *Issue/Revision* | *Date* | *DCN No.* | *Changed Pages / Paragraphs* |
|---|---|---|---|
| | | | Annex E: Changed FLG_IASIBAD |
| | | | Section 4.5.2, ALG.A32.50: Refinement and added information |
| | | | Section 4.2.2, ALG.A0.230: Modification |
| | | | Section 4.3, ALG.A1.60: Typo corrected |
| | | | Section 5.7: Removed Curtis-Godson approximation for calculation of layer-mean values |
| | | | Section 4.10.3.1.3, ALG.A8315.20: Resolved duplicated number of requirement |
| | | | Section 4.10.2, ALG.A82.05: Changed dataset name |
| | | | Section 4.10.7.2, ALG.A872.10: Refinement |
| | | | Section 4.10.7.5.2, ALG.A87532.50: Removed requirement because of duplication of ALG.A872.10 |
| | | | Section 4.10.7.5.2.4: Corrected numbering of algorithms beginning with ALG.A4. |
| | | | Section 5.7: Added information related to gamma-correction of transmittance |
| | | | Section 5.9, Equation (228) corrected. |
| | | | Section 5.20: Refinement |
| | | | Annex D: Corrected entry in IASI_L2_PGS_COF_FRTM |
| | | | Added new section 5.31 on the use of flags |
| | | | Removed flag FLG_IASIGEO from Annexes D and E |
| | | | Section 4.3, ALG.A1.50: FLG_IASIGEO replaced by FLG_IASIBAD, refinement |
| | | | Annex E: Refined FLG_ATOVINT |
| | | | Annexes B and C: Removed IASI_L2_PGS_SEL_CHAN |
| | | | Section 4.8.4, ALG.A64.24: Added requirement |
| | | | Section 64, ALG.A64.26: Added requirement |
| | | | Annexes B and C: Removed IASI_L2_PGS_COF_WINCOR and updated IASI_L2_PGS_THR_WINCOR |
| | | | Section 4.10.3.1.5, ALG.A8315.130: Replaced IASI_L2_PGS_COF_WINCOR by IASI_L2_PGS_THR_WINCOR |
| | | | Annex B: Removed IASI_L2_PGS_THR_ADIAB |
| | | | Annex C: IASI_L2_PGS_DAT_CLIM: corrected |
| | | | Annex C: IASI_L2_PGS_THR_DESSTR: corrected |
| | | | Annex C: IASI_L2_PGS_TYP_INI: updated |

| *Issue/Revision* | *Date* | *DCN No.* | *Changed Pages / Paragraphs* |
|---|---|---|---|
| | | | Annex E: FLG_FGCHECK corrected |
| | | | Annexes D and E: Flag FLG_FGSUPAD has been removed |
| | | | Annexes D and E: Flag FGSUPSAT has been removed |
| | | | Annex D: Removed flag FLG_INTCLR |
| | | | Section 5.6: Added information |
| | | | Section 5.2: Removed cloud top pressure, cloud phase and cloud emissivity from state vector |
| | | | Annex C: added information to IASI_L2_PGS_SEL_SUPCH |
| | | | Section 5.23: Added information on measurement covariance update during variational cloud clearing |
| | | | Section 4.3 |
| | | | Section 4.3 |
| | | | Annex C: Removed IASI_L2_PGS_COF_IPSF |
| | | | Section 4.9.3, ALG.A73.20: Updated |
| | | | Section 4.10.7.5.1, ALG.A8752.05: Added information |
| | | | Section 4.10.1, ALG.A81.10: Refinement |
| | | | Section 3.2: Updated figure 8 |
| | | | Section 4.10.7.5.1, ALG.A8752.05: Added detail |
| | | | Section 4.10.3.1.5, ALG.A8315.08: Refinement |
| | | | Annex C: Added IASI_L2_PGS_COF_ANN |
| | | | Annex C: Updated IASI_L2_PGS_TYP_HTASS |
| | | | Annexes B and C: Updated IASI_L2_PGS_DAT_GTSLEV |
| | | | Annex C: Updated IASI_L2_PGS_DAT_VARCLR |
| | | | Section 5.15: Added information |
| | | | Section 5.23.1: Added information on initialisation of temperature |
| | 12/02/2002 | | Annex E: Updated FLG_INITIA |
| | | | Section 5.1: Note added how to discriminate between AMSU-A1 and AMSU-A2 |
| | | | Combined sections 5.13 and 5.24 into section 5.13 |
| | | | Section 4.10.2.1: Moved ALG.A821.10 to section 4.5.3 and renumbered it to ALG.A33.05 |
| | | | Section 4.5.3: Refinement of ALG.A33.05, ALG.A33.10, and ALG.A33.15 |
| | | | Annexes B and C: Updated IASI_L2_PGS_COF_ISRF |
| | | | Section 3.2: Updated figure 3 |

| Issue/Revision | Date | DCN No. | Changed Pages / Paragraphs |
|---|---|---|---|
| | | | Section 5.22: Added information |
| | | | Section 4.10.7.5.2.3, ALG.A87533.50: Refined |
| | | | Annex E: Updated FLG_ITRBOU |
| | | | Section 4.10.7.5: Added requirement ALG.A8752.170 |
| | | | Annexes B and C: Added IASI_L2_PGS_COV_CLDPAR |
| Issue 5, Rev 1 | 21/02/2002 | EUM.EPS.SYS.DCR.0.2.114 | Annexes B and C: Updated IASI_L2_PGS_THR_STERR |
| | | | Annex C: Updated IASI_L2_PGS_THR_CLDPHA |
| | | | Section 3.2: Removed mention of pseudo channels from caption to figure 14 |
| | | | Section 5.7: added detail and corrected equation (28) |
| | | | Section 5.7: changed equation (32) and added information |
| | | | Annexes B and C: Added items to IASI_L2_PGS_COF_SOL |
| | | | Section 5.7, before equation (44): changed “cloud levels” to “levels” |
| | | | Section 5.7.3: Completed equation (94) |
| | | | Section 5.7.3: Completed equation (103) |
| | | | Section 5.3.7: Corrected derivatives in table 7 |
| | | | Section 5.3.7: Moved partial derivative wrt emissivity up before table 7 |
| | | | Section 5.7.3: Corrected equations |
| | | | Section 5.23: Changed state vector for cloudy cases |
| | | | Section 4.10.2.1, ALG.A821.15: Added requirement |
| | | | Section 4.2.3: ALG.A0.190 renumbered to ALG.A0.240 |
| | | | Section 4.2.4: ALG.A0.200 renumbered to ALG.A0.250 |
| | | | Section 4.2.5: ALG.A0.210 renumbered to ALG.A0.260 |
| | | | Annex C: Updated IASI_L2_PGS_DAT_LEMI |
| | 28/03/2002 | | Section 5.7: Removed obsolete equation (83) |
| | | | Section 5.7.3, Table 7: Corrected predictor derivative |
| | | | Section 5.1: Corrected equation (1) |
| | | | Section 5.27: Corrected equation (285) |
| | | | Section 1.3: Added detail |
| | | | Section 3.4.1: Typos corrected |
| | | | Section 4.1: Removed introductory paragraph |
| | | | Section 3.3.1: Typo corrected |

| *Issue/Revision* | *Date* | *DCN No.* | *Changed Pages / Paragraphs* |
|---|---|---|---|
| | | | Section 3.3.1: Typo corrected |
| | | | Section 4.1.1.3: Removed incorrect detail |
| | | | Section 4.1.1.4: Removed incorrect detail |
| | | | Section 4.1.1.5: Removed incorrect detail |
| | | | Section 4.1.1.8, Table 3: Added detail |
| | | | Section 4.1.1.8: Added detail on product quality |
| | | | Sections 4.1.2 – 4.1.6: Corrected typos |
| | | | Section 4.2.1, ALG.A0.10: Added detail to numbers 4, 8, and 15 |
| | | | Section 4.2.1, ALG.A0.20: Added detail and removed requirement |
| | | | Section 4.2.2, ALG.A0.40: Typo corrected |
| | | | Section 4.2.2, ALG.A0.120: Typo corrected |
| | | | Section 4.4, ALG.A2.30: Added detail |
| | | | Section 4.5.1, ALG.A31.30: Typo corrected |
| | | | Section 4.8.1, ALG.A61.10: Added detail |
| | | | Section 4.8.4, ALG.A64.10: Added detail |
| | | | Section 4.10.2.1, ALG.A821.40: Added detail |
| | | | Section 4.10.3.1.5, ALG.A8315.170: Removed TBC |
| | | | Section 4.10.7.1.1, ALG.A8711.10: Added detail |
| | 30/04/2002 | | Section 5.29: Added detail |
| | | | Section 5.10: Added detail and corrected equations |
| | | | Section 4.10.7.1.2, ALG.A8712.10: Changed requirement to simplify calculation |
| | | | Section 4.10.7.3.2, ALG.A8732.40 and ALG.A8732.50: Changed requirements to simplify calculations |
| | | | Section 4.10.7.5.2.2: Changed requirement ALG.A87532.30 to simplify calculations |
| | | | Section 5.31: Added detail |
| | | | Section 5.23: Added detail |
| | | | Section 5.19: Added detail to ANN trace gas retrieval (equations modified) |
| | | | Annex C: Update of dataset contents |
| | | | Annex B and C: Renamed IASI_L2_PGS_THR_STERR into IASI_L2_PGS_COF_STERR and updated data set |
| | | | Annex E: Updated FLG_STERR |
| | | | Section 4.10.7.5.2.6, ALG.A87536.65: Refinement |
| | | | Section 4.9: Added detail |

| Issue/Revision | Date | DCN No. | Changed Pages / Paragraphs |
|---|---|---|---|
| | | | Section 4.9.4, ALG.A74.20: Added detail |
| | 06/05/2002 | | Section 5.23: Changed cloud top temperature to pressure in state vector |
| Issue 5 Rev 2 | 07/06/2002 | EUM.EPS.SYS. DCR.02.131 | Section 3.2, Updated Figure 7 |
| | | | Section 4.10.2.1, ALG.A821.08: Corrected detail |
| | | | Annex C: Corrected entry in IASI_L2_PGS_THR_GLWAVE |
| | | | Section 4.10.7.3.1, ALG.A8731.20: Changed details |
| | | | Section 5.15: Added detail |
| | | | Section 5.16: Added detail |
| | | | Section 5.7: Changed details |
| | 12/06/2002 | | Section 5.7.1: Changed details |
| | | | Section 5.23.3: Corrected equation |
| | | | Annex D: Updated IASI_L2_PGS_THR_NWP |
| | | | Annexes C and D: Inclusion of IASI_L2_PGS_DAT_NWPLEV |
| | | | Added new section 5.34 describing NWP data contents |
| | | | Section 5.20: Added detail |
| | | | Section 4.4, ALG.A2.30: Added detail |
| | | | Section 4.4, ALG.A2.40: Added detail |
| | | | Section 5.8: Completed algorithm description |
| | | | Section 5.29: Added detail |
| | | | Section 4.3, ALG.A1.122: Refinement |
| | | | Section 5.4.3.1: Refinement |
| | | | Section 5.12: Correction included |
| | | | Annex C: Correction of IASI_L2_PGS_THR_CIRDET |
| | 18/06/2002 | | Annexes B and C: Added IASI_L2_PGS_DAT_EMIS |
| | | | Section 5.23.1: Added detail |
| | | | Annex C: Added detail to IASI_L2_PGS_COF_SOL |
| | | | Section 5.7: Added detail |
| | | | Section 5.10: Added detail |
| | | | Annex C: Removed entry from IASI_L2_PGS_DAT_LEMI |
| | | | Annex C: Completed IASI_L2_PGS_DAT_CEMI |
| | | | Section 4.10.2: Corrected ALG.A82.05 |
| | | | Added new section 5.35 on Integrity of IASI Data |
| | | | Annex E: Updated definition of FLG_RETCHC |

| Issue/Revision | Date | DCN No. | Changed Pages / Paragraphs |
|---|---|---|---|
| | | | Section 4.10.1, ALG.A81.10: Minor change |
| | | | Section 5.23: Added detail |
| | | | Section 5.29: Equation corrected |
| | | | Annex C: Corrected IASI_L2_PGS_COV_CLDPAR |
| | | | Section 5.1: Corrected references |
| | | | Annex D: Added flag description for FLG_SFCAVH |
| | | | Section 5.9: Added detail |
| | | | Section 5.18: Added detail |
| | | | Section 5.19: Added detail |
| | | | Section 4.10.1: Corrected ALG.A81.10.1 |
| | | | Annex E: Updated FLG_RETCHC |
| | | | Section 4.10.7.2, ALG.A872.10.3: Added flag update |
| | | | Section 4.10.3.3, ALG.A833.20: Added flag update |
| Issue 5, Rev 3 | 16/08/2002 | EUM.EPS.SYS.DCR.02.154 | Correction of coefficients in equation 295 |
| | | | Section 4.3, ALG.A1.25: Added information |
| | | | Section 5.4: Correction of equation (8) |
| | | | Section 5.4: Added new equation (6a) |
| | | | Section 4.10.7.5.1, ALG.A8752.05.1: Changed requirement |
| | | | Section 5.7.4: Correction of equation (141) |
| | | | Section 5.17: Removed TBC |
| | | | Section 5.23: Correction of equation (267) |
| | | | Section 5.4.2: Correction of table 4 |
| | | | Annex C: Added info to IASI_L2_PGS_THR_DESSTR |
| | | | Annex C: Added info to IASI_L2_PGS_THR_POLCLD |
| | | | Annex C: Added info to IASI_L2_PGS_COF_IASAMS |
| | | | Annex C: Added info to IASI_L2_PGS_COF_IASINT |
| | | | Annex C: Added info to IASI_L2_PGS_DAT_CLIM |
| | | | Annexes B and C: Added dataset ASI_L2_PGS_DAT_NWPLEV |
| | | | Annex C: Added info to IASI_L2_PGS_DAT_USLEV |
| | | | Annex C: Added info to dataset IASI_L2_PGS_THR_HORCO |
| Issue 5, Rev 4 | 07/03/2003 | EUM.EPS.SYS.DCR.03.062 | Section 4.3, ALG.A1.30: Refinement for clarification |
| | | | Section 5.19: Correction of equations for ANN trace gas retrieval and definition of input and scaling parameters by adding five equations |

| Issue/Revision | Date | DCN No. | Changed Pages / Paragraphs |
|---|---|---|---|
| | | | Annex C: Completion of data set definition for IASI_L2_PGS_COF_TRGAS |
| | | | Annex C: Correction of maximum number of IASI_L2_PGS_COF_ANN |
| | | | Section 5.15: Removed unnecessary entries from table related to setting of flag FLG_FINCHC |
| Issue 5, Rev 5 | 31/03/2004 | EUM.EPS SYS.DCR. 04.019 | Section 1.10.2: Added reference document [RD-501]. |
| | | | Annex B: Added reference to RD-501 |
| | | | Annex B: Removed contents, added reference to RD-501 |
| | | | Section 5.22: Added paragraph on handling of missing channels |
| | | | Section 5.18: Added description of input and output scaling and comments for clarification |
| | | | Section 5.1: Added transformation of IASI L1C channel numbering into IASI Level 2 channel numbering. |
| | | | Section 5.29: removed TBW, added detailed description of entropy encoded eigenvector scores compression method |
| | | | Section 5.35: added description on setting of flag FLG_IASIBAD and implied consequences for the processing |
| | | | Section 1.10.2: Added reference documents |
| | | | Section 4.10.7.5.2.7: Removed ALG.A87534.80 |
| | | | Section 5.15: Changed setting of flag FLG_FINCHC |
| | | | Section 5.7: removed TBD |
| | | | Section 4.9.5: changed ALG.A75.50 |
| | | | Added section 5.30.1: Setting of flag FLG_RETCHC |
| | | | Added section 5.30.2: Setting of flag FLG_ATOVCMP |
| | | | Added section 5.30.3: Setting of flag FLG_ATOVCLR |
| | | | Added section 5.30.4: Setting of flag FLG_CLDSUM |
| | | | Section 4.10.3.1.3: Changed ALG.A8313.20 |
| | | | Section 4.10.3.1.3: Removed ALG.A8313.10 |
| | | | Annexes D and E: removed FLG_THICOR |
| | | | Section 4.10.4.2: Section deleted |
| | | | Section 4.10.4.3: Section deleted |
| | | | Section 4.10.2.1: changed ALG.A821.15 |
| | | | Section 4.10.2.1: changed ALG.A821.40.2 |
| | | | Section 5.5: Added handling of case: points on a line |
| | | | Section 5.23.3: Added clarification to equation (286) |

| *Issue/Revision* | *Date* | *DCN No.* | *Changed Pages / Paragraphs* |
|---|---|---|---|
| | | | Section 5.27: Added clarification |
| | | | Added section 5.30.5: Setting of flag FLG_QUAL |
| | | | Added section 5.37 on vertical grids |
| | | | Section 5.19: Correction of equation 248, added clarification on network structure |
| | | | Section 5.21: Added clarification to equation 262 |
| | | | Section 5.4: Typo correction before eq. 10 |
| | | | Section 5.9: Added clarifications and information |
| | | | Section 5.9: Correction of equations 204 to 208 |
| | | | Section 5.9: Changed threshold for eq. 231 |
| | | | Section 5.4: Correction of equations 5, 6, 8 |
| | | | Section 5.15: Added clarification |
| | | | Added section 5.30.6: Setting of flag FLG_INITIA |
| | | | Section 4.10.7.5.2.3: Deleted requirements ALG.A87533.80.2, ALG.A87533.80.3 Changed ALG.A87533.50.3 |
| | | | Section 5.23.1: Removed redundant method for emissivity calculation over water |
| | | | Section 5.23: Added information |
| | | | Section 5.15: Removed requirement to iterate parameters not chosen for iterative retrieval |
| | | | Section 4.2.1: Added further data sets to ALG.A0.110 |
| | | | Section 5.23.1: Added clarification how to treat incomplete profiles at low pressure values |
| | | | Section 4.10.3.1.5, ALG.A8315.10: Removed reference to IASI_L2_PGS_THR_FRTCLR |
| | | | Section 4.10.3.1.5, ALG.A8315.25: Replaced reference to IASI_L2_PGS_THR_FRTCLR by IASI_L2_PGS_THR_CLDDET |
| | | | Annex B: Removed reference to IASI_L2_PGS_THR_FRTCLR |
| | | | Section 4.10.3.1.5, ALG.A8315.20: Replaced reference to IASI_L2_PGS_SEL_WINTST by IASI_L2_PGS_THR_CLDDET |
| | | | Annex B: Removed reference to IASI_L2_PGS_SEL_WINTST |
| | | | Section 5.18: Clarified use of data set IASI_L2_PGS_COF_ANN and changed the table to give meaning of identifiers |
| | | | Section 5.9: Added clarification on number of surface |

| Issue/Revision | Date | DCN No. | Changed Pages / Paragraphs |
|---|---|---|---|
| | | | conditions for test B |
| | | | Section 5.9: Added clarification on number of surface conditions for test C |
| | | | Section 5.23: Clarification of data set IASI_L2_PGS_COF_SCAL with respect to surface temperatures |
| | | | Section 5.23.1: Clarified handling of incomplete profiles for initialisation |
| Issue 5, revision 6 | 17/05/2004 | EUM.EPS. SYS.DCR. 04.044 | Section 5.29: Waiving implementation of method 4 |
| Issue 6, Revision | 08/08/2007 | | Section 5.7: Removed description of fast radiative transfer model, added reference to RTIASI-4 and PCRTM |
| | | | Section 5.7.3 removed – obsolete |
| | | | Section 5.10: included corrections, added tests/ selections for correct functionality, and added clarifications |
| | | | Section 5.11: included correction and added clarification |
| Issue 5, revision 6 | 17/05/2004 | EUM.EPS. SYS.DCR. 04.044 | Section 5.29: Waiving implementation of method 4 |
| Issue 6, Revision | 08/08/2007 | | Section 5.7: Removed description of fast radiative transfer model, added reference to RTIASI-4 and PCRTM |
| | | | Section 5.7.3 removed – obsolete |
| | | | Section 5.10: included corrections, added tests/ selections for correct functionality, and added clarifications |
| | | | Section 5.11: included correction and added clarification |
| | | | Section 5.7.3 removed – obsolete |
| | | | Section 5.10: included corrections, added tests/ selections for correct functionality, and added clarifications |
| | | | Section 5.11: included correction and added clarification |
| | | | Section 4.10.2.1: Updated ALG.A821.07 in line with changes in Section 5.7 |
| v5G | 20/03/2009 | ODT_DCR_23 | Annex B: Auxiliary datasets listing is now replaced by reference to document RD-501 which includes same tables (thus avoiding duplication of editing effort and possible inconsistencies creeping in). |
| V6 | 17/08/2010 | | Merging of v. 6.0 and v. 5G. Also some cosmetic updates (formatting, and to page header/footer). |
| V7 | 10/09/2010 | ODT_DCR_209 | Section 4.10.3.1.5: Deletion or replacement of several test functions.<br>Chapter 5: Extensive updates, especially to following sections: |

| *Issue/Revision* | *Date* | *DCN No.* | *Changed Pages / Paragraphs* |
|---|---|---|---|
| | | | Sec. 5.9 Cloud detection tests: Several tests removed or replaced with new tests.<br>Sec. 5.10 CO2 slicing method: Various text clarifications; finer search of the pressure domain for the mode of CTP estimates from single channels; dynamic assessment of the upper bound of the pressure domain, based on forecasts.<br>Sec. 5.17 EOF regression retrieval: Addition of an alternative regression scheme description for parameters other than SST.<br>Sec. 5.19 ANN retrieval of trace gases: Scientific algorithm improvements to fix the scan angle dependency and failures over ice/desert surfaces and elevated terrains.<br>Sec 5.23: New section inserted “Noise filtering of radiances”.<br>Annex E: Updates to FLG_CLDTST &FLG_IASICLD (deletion of unwanted bit descriptions).Reference RD-501 replaced by new document (same information but in spreadsheet format).Typo corrections, and editorial updates throughout document layout/formatting, sequential renumbering of equations. (Note: only significant corrections have been marked with change bars.) |
| v 7A | 03/02/2014 | | DocX version created to replace Framemaker version. Subversion used for new Word document Dotx version. No changes to text in body of document. Annexes changed to name Appendix to match technical document template. No change to contents. |